# Seismic Hazards Report for the Exelon Generation Company, LLC Early Site Permit

# Site Safety Analysis Report Appendix B

# Contents

**Attachments**

# Tables

# Figures

# Plates

# Acronyms and Abbreviations

| | |
|---|---|
| AD | anno domini (after Christ)-used to denote specified calendar date |
| ASCE | American Society of Civil Engineers |
| BA | Blytheville arch |
| BAF | Blytheville arch fault |
| BC | before Christ-used to denote specified calendar date |
| BFZ | Blytheville fault zone |
| BL | Bootheel lineament |
| BP | Before present |
| CERI | Center for Earthquake Research and Information |
| CEUS | Central and Eastern United States |
| CFZ | Commerce fault zone |
| CGL | Commerce geophysical lineament |
| CNSS | Council of the National Seismic System |
| CPS | Clinton Power Station |
| DEH | deaggregation earthquake high magnitude |
| DEL | deaggregation earthquake low magnitude |
| DEM | deaggregation earthquake middle magnitude |
| DF | design factor |
| DRS | design response spectrum |
| EGC | Exelon Generation Company |
| EPRI | Electric Power Research Institute |
| ESP | Early Site Permit |
| FAFC | Fluorspar area fault complex |
| fps | feet per second |
| Ga | billion years before present |
| GPS | Global Positioning System |
| HF | high-frequency |
| ka | thousand years before present |
| LF | low-frequency |
| LLC | Limited Liability Corporation |
| **M** | Moment magnitude |
| Ma | million years before present |

| | |
|---|---|
| $m_b$ | Body-wave magnitude |
| $m_{bLg}$ | Lg magnitude |
| $M_{max}$ | Maximum magnitude |
| MMI | Modified Mercalli Intensity |
| $M_O$ | Moment |
| NCEER | National Center for Earthquake Engineering Research |
| Nd | neodymium |
| NEHRP | National Earthquake Hazard Reduction Program |
| NMSZ | New Madrid seismic zone |
| NN | New Madrid North fault |
| NNE | New Madrid North Extension |
| NS | New Madrid South fault |
| NW | New Madrid West fault |
| PGA | Peak ground acceleration |
| PSHA | Probabilistic Seismic Hazard Analysis |
| RE | reference earthquake |
| RF | Reelfoot fault |
| RS | Reelfoot south |
| SCL | St. Charles lineament |
| SCR | Stable continental region |
| SDC | Seismic Design Category |
| SF | scale factor |
| SGFZ | Ste. Genevieve fault zone |
| $SH_{max}$ | Maximum horizontal stress direction |
| SOG | Seismicity Owners' Group |
| SPT | Standard Penetration Test |
| SSC | structures, systems, and components |
| SSE | Safe Shutdown Earthquake |
| SSHAC | Senior Seismic Hazard Analysis Committee |
| SV | Spectral velocity |
| UHRS | Uniform Hazard Response Spectrum |
| UHS | Uniform hazard spectra |
| USAR | Updated Safety Analysis Report |
| USGS | United States Geological Survey |
| USNRC | U.S. Nuclear Regulatory Commission |
| WVFS | Wabash Valley fault system |

WVSZ Wabash Valley seismic zone

**Note on units of measure:** The authors of this report have attempted to maintain consistency in the units of measure cited. The report standard is English units. However, in some cases where the standard unit in published literature is metric or results of other studies are referred to, and those results were presented in metric units, metric units are used to facilitate comparison to published data sets (e.g., fault slip rates are given only in mm[yr]).

CHAPTER 1

# Introduction

This appendix describes the seismic studies and investigations conducted as part of the Early Site Permit (ESP) application for the Exelon Generation Corporation (EGC), LLC, ESP Site in central Illinois. This work was completed in accordance with the general guidance provided in U.S. Nuclear Regulatory Commission (USNRC) Regulatory Guide 1.70, *Standard Format and Content of Safety Analysis Reports*, and Regulatory Guide 1.165, *Identification and Characterization of Seismic Sources and Determination of Safety Shutdown Earthquake Ground Motion*.

## Regulatory Guidance

10 CFR 100.23 defines the requirements for addressing geologic and seismic issues in an ESP application. The principal seismic issues to be addressed are to determine: (1) specification of the Safe Shutdown Earthquake (SSE) for the site; (2) the potential for surface tectonic deformation; (3) the design basis for seismically induced floods and water waves; and (4) the effects of vibratory ground motion on the stability of the site. The study presented in this appendix addresses issues (1) and (2), determination of the SSE and of the potential for tectonic deformation.

Regulatory Guide 1.165 (USNRC, 1997) provides the framework for assessing the appropriate SSE ground motion levels for new nuclear power plants. Regulatory Guide 1.165 indicates that an acceptable starting point for this assessment at sites in the central and eastern United States (CEUS) is the probabilistic seismic hazard analysis (PSHA) conducted by the Electric Power Research Institute (EPRI) for the Seismicity Owners Group (SOG) in the 1980s (EPRI, 1991). The EPRI-SOG study involved an extensive evaluation of the scientific knowledge concerning earthquake hazards in the CEUS by multi-discipline teams of experts in geology, seismology, geophysics, and earthquake ground motions. A broad range of interpretations of potential seismic sources in the CEUS was developed. The uncertainty in characterizing the frequency and maximum magnitude of potential future earthquakes associated with these sources and the ground motion that they may produce was quantified in the seismic hazard model.

Regulatory Guide 1.165 further specifies that the adequacy of the EPRI-SOG hazard results must be evaluated in light of more recent data and evolving knowledge pertaining to seismic hazard evaluation in the CEUS. Appendix E, Section E.3, of Regulatory Guide 1.165 outlines a three-step process for this evaluation, as follows.

Step 1: Evaluate whether recent information suggests significant differences from the previous seismic hazard characterization.

Step 2: If potentially significant differences are identified, perform sensitivity analyses to assess whether those differences have a significant impact on site hazard.

Step 3: If Step 2 indicates that there are significant differences in site hazard, then the PSHA for the site is revised by either updating the previous calculations or, if necessary, performing a new PSHA. If not, the previous EPRI-SOG results may be used to assess the appropriate SSE ground motions.

Regulatory Guide 1.165 calls for the SSE ground motions to be based on the site PSHA results for a reference probability of the median $10^{-5}$ hazard level. The basis for the selected reference probability is described in Appendix B of Regulatory Guide 1.165. The reference probability was set equal to the median value of the annual frequency of exceeding the SSE ground motions (based on the median hazard) computed for a specific set of licensed nuclear power plants. These probabilities were computed using ground motion models developed in the mid-to-late 1980's. As discussed in Regulatory Position 3 in Regulatory Guide 1.165, significant changes to the overall database for assessing seismic hazard in the CEUS may warrant a change in the reference probability. The availability of the recently developed EPRI ground motion characterization for the CEUS (EPRI, 2003) represents a significant advancement in the seismic hazard database for the CEUS, thereby requiring reconsideration of the reference probability approach. Appendix B of Regulatory Guide 1.165 also discusses that selection of another reference probability may be appropriate, such as one founded on risk-based considerations. The risk- based approach is the one taken in this application for developing the EGC ESP SSE design ground motions.

The SSE design response spectra (DRS) have been developed using the graded performance-based, risk-consistent method described in ASCE Standard XXX (ASCE, 2003)[1]. The method specifies the level of conservatism and rigor in the seismic design process such that the performance of structures, systems, and components (SSCs) of the plant achieve a uniform seismic safety performance consistent with the USNRC's safety goal policy statement (USNRC, 1986; USNRC, 2001). The ASCE Standard XXX aims to achieve a quantitative safety performance goal, $P_F$, together with qualitative performance limit states such that SSCs are designed depending on their importance to overall seismic safety performance of the plant, to assure that the plant level seismic performance target is met. The method is based on site-specific mean seismic hazard and the seismic design criteria and procedures contained in NUREG-0800.

The USNRC's safety goal policy statement establishes recognition that nuclear plant safety regulation is a societal risk management activity and provides the foundation for equitably managing the nuclear facility risk in the context of other societal risks. Subsequent to adopting the policy statement the USNRC has continued to develop and evolve supporting policies for a comprehensive risk management framework for nuclear regulation together with supporting implementation guidelines (USNRC, 1998; USNRC, 2002). The seismic design methodology provided in ASCE Standard XXX is a further step in the development of a risk-based standard for seismic design and regulation. The graded performance-based

[1] ASCE Standard XXX (2003) provides a detailed methodology and commentary on procedures required to achieve risk-consistent seismic design of SSCs for nuclear facilities. This Standard is a national consensus standard developed by the Dynamic Analysis of Nuclear Structures Subcommittee of the Nuclear Standards Committee of the American Society of Civil Engineers. The Dynamic Analysis Subcommittee comprises a group of leading designers, researchers, owners, and regulatory staff who are involved in the design and operations of nuclear facilities. The Standard has received technical approval by the Subcommittee and is now undergoing administrative review and approval by the Nuclear Standards Committee of the American Society of Civil Engineers. Publication of the document is expected in 2004.

approach is compatible with the direction provided by the USNRC's Risk-informed, Performance-Based Regulation guidance (USNRC, 1998; USNRC, 1999) and with developing USNRC guidance for the determination of DRS (McGuire, et al., 2001; McGuire, et al., 2002).

The ASCE Standard XXX seismic design method and criteria are intended to implement the USNRC's established qualitative safety goals and the companion quantitative implementation objectives. The qualitative safety goals provide that the consequences of nuclear power plant operation should cause no significant additional risk to the life and health of individuals and that the societal risks to life and health from nuclear power plant operation should be comparable to or less than the risks posed by generating electricity by viable competing technologies and should not be a significant addition to other societal risks. The USNRC's quantitative objectives for implementation of the safety goals are stated in terms of risk to individuals and to society. For an average individual in the vicinity of a nuclear power plant the risk that might result from a reactor accident should not exceed one-tenth of one percent (0.1 percent) of the sum of prompt fatality risks resulting from other accidents to which members of the population are generally exposed. The risk to the public of cancer due to nuclear power plant operation should not exceed one-tenth of one percent (0.1 percent) of the sum of cancer fatality risks resulting from all other causes (USNRC, 2001). A target $10^{-4}$ mean annual risk of core damage due to all accident initiators can implement these quantitative safety goals.

The ASCE Standard XXX assumes that seismic initiators contribute about 10 percent of the risk of core damage posed by all accident initiators. Thus the Standard is intended to conservatively achieve a mean $10^{-5}$ per year risk of core damage due to seismic initiators. The USNRC's seismic design criteria contained in NUREG-0800 conservatively assure a risk reduction factor of at least 10, as discussed in the next paragraph. Thus, a mean ground motion hazard of $10^{-4}$ per year is appropriate for determining the site-specific DRS for the EGC ESP site.

The ASCE Standard XXX aims to conservatively assure a seismic safety performance goal, $P_F$, for Category 1 (Design Category 5 in the draft Standard) SSCs of mean $10^{-5}$ per year. This performance goal is the same as established in DOE-STD-1020-94 (USDOE, 1996) for seismic design of PC-4 SSCs in DOE's nuclear facilities, which have comparable radiological safety performance requirements. The target mean annual performance goal for nuclear plants is achieved by coupling site-specific DRS with the deterministic seismic design criteria and procedures specified by NUREG-0800. The ASCE Standard XXX criteria for deriving a site-specific DRS are based on the conservative assumption that the seismic design criteria specified by NUREG-0800 achieve less than a one percent chance of failure for a given DRS. The conservatism of this assumption is demonstrated by analyses described in McGuire, et al. (2002), which show plant level risk reduction factors ranging from about 20 to about 40 are attained by the USNRC's seismic design criteria. The method is based on use of mean hazard results consistent with the recommendation contained in McGuire, et al. (2002) and with the USNRC's general policy on use of seismic hazard in risk-informed regulation.

# Appendix Organization

This appendix is organized following the three steps given at the start of the previous subsection. Chapter 2 presents Step 1, an evaluation of recent information regarding characterization of seismic hazards in the region of the EGC ESP Site. A field reconnaissance was conducted as part of this evaluation to document the presence or absence of paleoliquefaction features in latest Pleistocene-to-early Holocene deposits in the near region (within an approximately 25- to 30-mile radius of the site) that could be used to evaluate the evidence for prehistoric earthquakes in the region. Because potentially significant new information was identified during Step 1, Step 2 was implemented. Chapter 3 presents Step 2, the sensitivity analyses used to evaluate the potential effects of the new information on the site hazard. Chapter 4 presents Step 3, the development of the SSE ground motions for the EGC ESP Site. These ground motions are based on the EPRI-SOG seismic hazard model with updated maximum magnitude assessments for seismic source zones in the EGC ESP site region and inclusion of a characteristic earthquake model for the New Madrid source zone region (Section 4.1). These modifications to the EPRI-SOG interpretations address new information identified as significant in Step 2. Site-specific soil response analyses were conducted to obtain the soil surface ground motion levels (Section 4.2). The SSE ground motions are then developed following the approach outlined in ASCE Standard XXX (Section 4.3). In addition, the potential for surface faulting at the EGC ESP Site is addressed in Chapter 5.

CHAPTER 2

# Compilation of Recent Information

This chapter presents a summary and review of recent information pertinent to characterizing seismic sources and earthquake ground motions in the vicinity of the EGC ESP Site. Section 2.1 presents the recently obtained data and information pertinent to characterizing seismic sources in the site region. Section 2.1 synthesizes recent information with relevant information gathered as part of licensing of the adjacent operating unit to address the following:

- the regional tectonic setting (Section 2.1.1);
- regional tectonic features, including folds, faults, and lineaments (Section 2.1.2);
- earthquake catalog (Section 2.1.3);
- prehistoric earthquakes inferred from evidence for paleoliquefaction (Section 2.1.4); and
- seismic sources (Section 2.1.5).

Section 2.2 describes updates to the understanding of ground motion characteristics in the site region. Previous work on characterizing earthquake ground motions in the CEUS (the EPRI-SOG study of the 1980s) is described in Section 2.2.1; subsequent work is described in Section 2.2.2. Included is a brief summary of the recently completed EPRI study characterizing earthquake ground motions for the CEUS (EPRI, 2003).

## 2.1 Seismic Source Characterization

Regulatory Position 1 in Regulatory Guide 1.165 (USNRC, 1997) describes the regions around the site and the level of investigation needed to confirm the suitability of the site. Many of these investigations were performed as part of the licensing of the existing unit adjacent to the EGC ESP Site. Therefore, the focus of this study was on summarizing more recent data and interpretations, particularly those completed in the time since the EPRI-SOG study. The primary source of this information was the scientific literature and discussions with active researchers in the region. Field reconnaissance was conducted to search for evidence of prehistoric earthquakes within approximately 25 miles of the site. The data and interpretations gathered from the literature and field investigations are combined with information gathered as part of licensing of the CPS facility to provide an evaluation of potential seismic sources in the site region.

The EGC ESP Site is located in central Illinois (Figure 2.1-1). The site is in a region of low seismic activity, as indicated by the historical seismicity shown on Figure 2.1-1. Regulatory Guide 1.165 indicates that investigation of seismic sources should be performed within a 200-mile (320-kilometer) radius of the site. Two major sources of potential earthquakes are located within or just beyond this distance: the New Madrid seismic zone (NMSZ), and the Wabash Valley seismic zone (WVSZ) in southern Illinois and southern Indiana. The New Madrid region was the location of three earthquakes in 1811-1812, which are the largest

earthquakes recorded in the CEUS. The Wabash Valley region is a zone of elevated seismicity relative to central Illinois in which a number of paleoearthquakes have been identified.

Extensive new data sets have been compiled and interpreted for numerous site-specific and regional studies throughout the CEUS in the time since completion of the EPRI-SOG study in the late 1980's. These studies have used a variety of techniques to characterize the location, extent, and activity of tectonic features; the location, magnitude, and rates of seismic activity; and the general characteristics of the continental crust throughout the central United States. Many of these studies, funded under the National Earthquake Hazard Reduction Program (NEHRP), have focused on the New Madrid and Wabash Valley seismic zones. These studies have included extensive paleoliquefaction investigations, acquisition and reprocessing of shallow high resolution and industry seismic reflection data, paleoseismic trenching and mapping investigations, and seismological studies. This new information includes identification of new seismic sources as well as revisions to the characterization of previously identified seismic sources.

In addition to individual articles, reports, and maps published by state and federal agencies and in professional/academic journals, several major compilations of new data have been published in the past few years. These major compilations and significant new analyses include the following.

Geologic and Geophysical Data

- Special Issue: The New Madrid Seismic Zone, *Seismological Research Letters*, Vol. 63, No. 3, 1992 (25 articles).
- Investigations of the New Madrid Seismic Zone, *U.S. Geological Survey Professional Paper 1538*, Vol. A through S, 1994-1995 (16 individual volumes).
- Seismotectonic Maps of the Wabash Valley Seismic Zone, *U.S. Geological Survey Geologic Investigations Maps I-2583A-D* (4 maps), 1996-1997.
- Special Issue on Investigations of the Illinois Basin Earthquake Region, *Seismological Research Letters*, Vol. 68, No. 4, 1997 (14 articles).
- Crone, J., and R.L. Wheeler, "Data for Quaternary Faults, Liquefaction Features, and Possible Tectonic Features in the Central and Eastern United States, East of the Rocky Mountain Front." *U.S. Geological Survey Open-File Report 00-0260*. 2000.
- Earthquake Hazard Evaluation in the Central United States, Special Issue, *Engineering Geology*, Vol. 62, Nos. 1-3, 2001 (16 articles).
- Special Issue on the Illinois Basin: Seismicity, Faulting, and Seismic Hazard, *Seismological Research Letters*, Vol. 73, No. 5, 2002 (13 articles).
- Estimation of the magnitude of the 1811-1812 New Madrid earthquakes from intensity data (Johnston, 1996; Hough et al., 2000; Bakun and Hopper, 2003, in press).

Seismicity Catalogs

- Seeber, L., and J.G. Armbruster, The NCEER-91 Earthquake Catalog: Improved Intensity-Based Magnitudes and Recurrence Relations for U.S. Earthquakes East of New Madrid, Technical Report NCEER-91-0021, National Center for Earthquake Engineering Research, Buffalo, New York. 1991. (Covers the period 1627 to 1985.)
- Johnston, A.C., K.J. Coppersmith, L.R. Kanter, and C.A. Cornell, The Earthquakes of Stable Continental Regions, Volume 1: Assessment of Large Earthquake Potential. Final Report Submitted to Electric Power Research Institute (EPRI), TR-102261-V1. 1994. (Includes extensive data for worldwide earthquakes occurring in stable continental regions and adjoining areas.)
- Mueller, C., M. Hopper, and A. Frankel, Preparation of Earthquake Catalogs for the National Seismic-Hazard Maps—Contiguous 48 States, U.S. Geological Survey Open-File Report 97-464. 1997. (Body-wave magnitude catalog [$m_b \geq 3.0$] that covers the period 1700 to 1995.)
- Preliminary Determinations of Epicenters, U.S. Geological Survey (USGS), National Earthquake Information Center. Post-1973.
- Center for Earthquake Research and Information (CERI), New Madrid Catalog. (Catalog of instrumental locations for earthquakes in the New Madrid seismic zone and surrounding regions, 1974 to present.)

### 2.1.1 Regional Tectonic Setting

The site is located within the Illinois basin in the stable continental region of the North American craton, which is characterized by low rates of historical seismicity (Figure 2.1-1). The Illinois basin is a spoon-shaped depression covering parts of Illinois, Indiana, and Kentucky. The Illinois basin is bounded on the north by the Wisconsin arch, on the east by the Kankakee and Cincinnati arches, on the south by the Mississippi embayment, and on the west by the Ozark dome and Mississippi River arch (Nelson, 1995) (Figure 2.1-2). The east-west-trending Rough Creek-Shawneetown fault system divides the Illinois basin into two unequal parts (Figure 2.1-3). The large northern part includes the Fairfield basin, which contains approximately 15,000 ft of Paleozoic sedimentary strata overlying basement rocks of the Proterozoic-age Eastern Granite-Rhyolite Province (Figure 2.1-4). The Moorman syncline, south of the Rough Creek-Shawneetown fault system, is smaller, but considerably deeper (as deep as 23,000 ft).

Two major structural elements characterize the basin: a cratonic depression and a rift system. The broad southwestward-plunging cratonic depression extends across central Illinois and southwestern Indiana. Basement elevation ranges from approximately –2950 ft in the northern part of the basin to –14,100 ft in southeastern Indiana (Kolata and Hildenbrand, 1997). Major structures in this depression include wrench-fault assemblages, basement-block faulting, detached normal faults, forced folds, décollement thrust folds, reef-drape structures, and structures produced by igneous intrusion (Nelson, 1995). The southernmost part of the basin is underlain by portions of the Reelfoot rift and Rough Creek graben, a rift system that formed during late Precambrian to Middle Cambrian time. Recent publications (e.g., Nelson, 1995; Kolata and Hildenbrand, 1997; McBride and Kolata, 1999;

Harrison and Schultz, 2002) provide an overview of the tectonic history and crustal architecture of the southern part of the Illinois basin as they relate to neotectonic activity in the region. These are discussed in the following section.

The EGC ESP Site lies within a compressive midplate stress province characterized by a relatively uniform compressive stress field with an $SH_{max}$ oriented NE to ENE (Zoback and Zoback, 1989). Contemporary stress indicators (focal plane solutions, hydrofractures, *in situ* stress measurements, and ground failures in mines, joint patterns, and north-trending thrust faults) show a geographic shift from an east-west maximum horizontal compressive stress at the latitude of the NMSZ to stress that trends just north of east in southern Illinois and Indiana (Nelson and Lumm, 1987; Nelson and Bauer, 1987; Ellis, 1994; Rhea and Wheeler, 1996). Preliminary results from a global positioning system (GPS) network in southern Illinois basin provide evidence for present-day tectonic strain in the WVSZ. Hamburger et al. (2002) note that individual site velocities, as well as formal inversion for tectonic strain, suggest a systematic pattern of shear strain that may be interpreted as either sinistral shear along the north-northeast-trending Wabash Valley fault system, or as dextral shear along the northeast-trending Commerce geophysical lineament. They note, however, that given the current level of error in individual campaign-based GPS observations, an extended period of time will be required before these observations can fully characterize the strain field and confirm these postulated tectonic motions.

Recent geodetic measurements in the NMSZ indicate that the rate of strain accumulation is below the current detection threshold (Newman et al., 1999). These observations are not inconsistent with a model of seismicity in intraplate regions as a transient phenomenon localized along weak zones in the crust (Kenner and Segall, 2000) (see discussion in Section 2.1.5.2.1).

## 2.1.2 Regional Tectonic Features

This section summarizes new information regarding structural features (folds and faults) within the site region based on a review of available published and unpublished reports that post date the EPRI-SOG PSHA study. The Updated Safety Analysis Report (USAR) for the Clinton Power Station (CPS) describes the regional structural geology and important structures (folds and faults) within a 200-mile radius of the site. Nelson (1995) provides a good overview and compilation of new information regarding structures within Illinois and surrounding regions. The structural picture remains the same, but new information is available regarding the style and timing of most recent deformation. Additional information regarding the seismogenic potential of specific features is provided in the following section only for those features for which evidence of neotectonic activity has been reported, or for which new data have implications for seismic source characterization and models relevant to seismic hazard analysis for the project site region. A map showing dominant structural features in the site region is shown on Plate 1. Updated summary lists of folds and faults in the region are given in Tables 2.1-1 and 2.1-2.

### 2.1.2.1 Folds

#### 2.1.2.1.1 La Salle Anticlinorium

Nelson (1995) introduced the name La Salle anticlinorium for the feature that previously had been referred to as the La Salle anticlinal belt. The feature trends north-northwest and

extends for more than 200 miles from Lee County in the northwest to Lawrence County in the southeast. Its closest approach is 15 to 20 miles east of the site. It comprises numerous subparallel anticlines, domes, monoclines, and synclines, several dozen of which are individually named. The pattern of the individual structures comprising the feature has previously been described as en echelon. Nelson (1995), however, reports that this term is misleading, that in a true en echelon fold belt the structures are aligned at an angle to the overall trend of the system, reflecting strike-slip deformation. Nelson (1995) reports that in La Salle anticlinorium individual folds are oriented predominantly parallel to the trend of the larger system. He also reports that individual folds are offset from one another and partially overlap; toward the north individual folds generally step to the west. Nelson (1995) also describes the La Salle anticlinorium as locally exhibiting a branching pattern.

Nelson (1995) reports that the primary uplift of the La Salle anticlinorium occurred in the late Paleozoic. An angular unconformity at the base of Pennsylvanian-age strata is observed along the entire length of the structure. Seismic-reflection profiles across the Charleston monocline indicate that the entire Paleozoic sedimentary column (pre-Pennsylvanian) is folded, and the amount of structural relief does not change significantly with depth.

High-angle reverse faults are documented at depth in several places along the southern part of the La Salle anticlinorium. Nelson (1995) reports that proprietary seismic-reflection profiles reveal faults on the west flank of the Lawrenceville dome, the east flank of the Bridgeport anticline, and the southwest flank of the Hardinville anticline. These faults displace the top of Precambrian basement and overlying Cambrian strata, dying out at or below the Ordovician Knox Group. About 500 ft of displacement occurs on the basement surface of the Bridgeport anticline, and the largest fault on the Hardinville anticline has about 300 to 400 ft of throw. Based on borehole data in Cambrian sandstone at the northern part of the anticlinorium, several east-west-trending faults, defining a graben, are shown on the west side of the dome east of the Peru monocline. As reported by Nelson (1995), borehole data in Coles County also indicate faulting in Mississippian strata near the west flank of Ashmore dome (a small dome near the southern end of the Murdock syncline). No orientations of these faults are reported.

Nelson (1995) and McBride and Nelson (1999) interpret the La Salle anticlinorium as the product of Late Paleozoic displacements on high-angle reverse faults in crystalline basement that propagated upward to monoclines and asymmetrical anticlines in Paleozoic sedimentary cover. The faults could be classified as drape folds or fault-propagation folds. The complex arrangement of folds in the La Salle anticlinorium suggests a mosaic of faults in the basement of eastern Illinois (Nelson, 1995). Marshak and Paulsen (1997) interpret the La Salle deformation belt as consisting of three segments composed of north-trending fault arrays. Each segment terminates at a northwest-trending discontinuity. They note that this geometry resembles the pattern of rift segments linked at accommodation zones, typical of low-strain rifts. McBride and Nelson (1999) state that reflection profiles in the Fairfield basin do not support this hypothesis.

#### 2.1.2.1.2 Peru Monocline

The Peru monocline, which lies within the northern La Salle deformation belt, is a 65-mile long, northwest-southeast-trending fold belt in which the rocks dip steeply to the southwest into the Illinois basin (Nelson, 1995). Its closest approach is 50 to 55 miles north of the EGC

ESP Site. The structure is most prominent in La Salle County, where the relief on the southwest limb is as much as 1,300 ft. In some area coal mines, the coal beds dip 45° on the steep flank of the monocline (Nelson, 1995). The Peru monocline is less pronounced to the northwest, where the relief decreases and the dip becomes very gentle as the structure merges with the Ashton anticline. Two recent earthquakes have been associated with this structure, a magnitude $m_b$ 4.6 in September 1972, and a magnitude $m_b$ 3.5 earthquake in September 1999. Within the precision of the seismographic data, the 1999 and 1972 earthquakes were located 5 and 13 km (3 and 8 miles), respectively, below the Peru monocline (Larson, 2001). The 1972 event occurred about 10 miles southeast of the 1999 event. A focal mechanism solution from the 1972 earthquake indicates movement on a high-angle, strike-slip fault, with either right-lateral to the north-northwest or left-lateral to the east-northeast (Herrmann, 1979). Noting the proximity of this earthquake to the Peru monocline, Heigold (1972) suggests that the earthquake was the result of faulting related to a zone of weakness near the region where the monocline merges with the Ashton anticline. A third earthquake, which occurred on May 27, 1881, also might be related to the Peru monocline based on damage reports from La Salle, which sits directly on the Peru monocline, but an exact location for this event is not known (Larson, 2001). Larson (2002) concludes that the spatial association of recent seismicity may suggest the Peru monocline is a reactivated Paleozoic structure.

#### 2.1.2.1.3 Du Quoin Monocline

The Du Quoin monocline of southern Illinois trends north-south and warps Paleozoic strata down to the east. Marshak and Paulsen (1997) include this structure within the broad southern La Salle deformation belt. Normal faults of the Dowell and Centralia fault zones are coincident with the dipping flank of the fold, and displace strata down to the west. Su and McBride (1999) report that low-resolution seismic-reflection data reveal a west-dipping reverse fault in the Precambrian basement beneath the monocline that cuts the top of the basement-cover contact. Nelson (1995) reports that several high-resolution seismic lines across the Centralia fault zone indicate a normal fault dipping 70° to 75° toward the west, affecting all reflectors down to Ordovician strata. (Su and McBride interpret the same seismic data as affecting upper Mississippian to Ordovician strata). Su and McBride (1999) suggest that the Centralia fault zone represents extensional reactivation of the basement structure beneath the Du Quoin monocline, and that these structures likely connect at depth. Nelson (1995) and Su and McBride (1999) infer that the fault has undergone two episodes of movement. The greatest displacements on the structures took place during early to mid-Pennsylvanian, with intermittent and lesser movements continuing into late Pennsylvanian and possibly Permian time. Post-Pennsylvanian extension and normal faulting occurred along the Centralia fault.

Tuttle et al. (1999a) and Su and McBride (1999) consider the Du Quoin monocline and related Centralia fault as a potential source for an earthquake that could have produced middle Holocene paleoliquefaction features in southwestern Illinois and possibly southeastern Missouri.

#### 2.1.2.1.4 Louden Anticline

Su and McBride (1999) report that recent digital vibroseis data over this feature, which is located directly northeast of the Du Quoin monocline, reveals a major, deep basement fault

that projects to a depth of about 12 km (7.5 miles) from the forward hinge point of the east-facing flexure of the dipping limb. Su and McBride (1999) report a surface area of 97 $mi^2$ for the fault, based on the axial length of the anticline (18 miles) and the vertical length of the basement fault (5.4 miles). This associated basement fault may be a source structure for paleoliquefaction events (Su and McBride, 1999).

#### 2.1.2.1.5 Waterloo-Dupo Anticline

The Waterloo-Dupo anticline is a north-northwest-trending, asymmetrical anticline that has been interpreted to be a southern continuation of the Cap au Gres structures (Harrison and Schultz, 2002). The Waterloo-Dupo anticline has a steep western limb, >45° in places, and a gentle east limb (Nelson, 1995). Similar to the Cap au Gres structure, it experienced at least two periods of deformation: moderate folding in the Late Devonian and a major episode of folding during Late Mississippian to Early Pennsylvanian. Slight post-Pennsylvanian folding also may have occurred on the structure (Nelson, 1995).

Apparent offset of the Waterloo-Dupo anticline suggests right-lateral slip on the St. Louis fault (Harrison and Schultz, 2002). These authors conclude that this offset of the Waterloo-Dupo anticline is consistent with Late Mississippian to Early Pennsylvanian northeast-southwest compression.

Based on the spatial distribution of prehistoric liquefaction features, Tuttle et al. (1999a) indicated that the Waterloo-Dupo anticline, the Valmeyer anticline, and the St. Louis fault are possible sources for paleoearthquake features observed in eastern Missouri, but they also emphasize that other scenarios relying on sources farther east are equally possible (see Attachment 1 to this Appendix).

#### 2.1.2.1.6 Farmington Anticline-Avon Block

The Farmington anticline-Avon block is a broad, as much as 12-mile-wide, northwest-trending, low-relief structural feature that lies between the Ste. Genevieve and Simms Mountain faults (Harrison and Schultz, 2002). Weak to moderate seismicity is clustered around this structure, which has been interpreted to occur above buried faults cutting Middle Proterozoic basement rock. A zone of northwest-trending horsts and grabens with subsidiary and contemporaneous northeast-striking oblique-slip faults coincides with the axis of the fold (Harrison and Schultz, 2002).

#### 2.1.2.1.7 Peoria Folds

Nelson (1995) includes a series of subtle anticlines and synclines originally identified in 1957, which he designates as the Peoria folds. Individual folds named are the Astoria, Farmington, Littleton, Bardolph, Brereton, St. David, Sciota, Seville, and Versailles anticlines and the Bryant, Bushnell, Canton, Elmwood, Fairview, Ripley, and Table Grove synclines. They were mapped from surface and subsurface data on various Pennsylvanian and Mississippian horizons. Nearly all strike slightly north of east. They are linear to slightly arcuate, with the convex side to the north. The folds plunge eastward, as does the regional dip. Most have less than 100 ft of structural relief.

Nelson (1995) notes the correspondence of these minor folds with topography, in particular the east-northeast alignment of small streams. He also notes this is the only region in Illinois where topography appears to be so strongly influenced by bedrock structure

through glacial drift. According to Nelson, the source of the horizontal compression that may have formed these folds is unknown.

#### 2.1.2.2 Faults

##### 2.1.2.2.1 Sandwich Fault Zone

The northwest-trending Sandwich fault zone (Kolata et al., 1978; Nelson, 1995), which also lies within the northern La Salle deformation belt in northeastern Illinois, has a maximum vertical displacement of about 800 ft (Kolata et al., 1978). Movement along the Sandwich fault zone may have been contemporaneous with formation of the Peru monocline (Nelson, 1995). Larson (2002) notes that two historical earthquakes (in 1909 and 1912) may be associated with the Sandwich fault zone, and that these two events may indicate reactivation of a fault within the Precambrian basement associated with the Sandwich fault zone.

##### 2.1.2.2.2 Plum River Fault Zone

The Plum River fault zone strikes east-west across northwest Illinois and into northeast Iowa. Nelson (1995) reports that primary movements on the Plum River faults were post-Devonian and pre-Pennsylvanian. Structural relationships between Pennsylvanian strata and the Plum River fault zone preclude more than about 30 ft of post-Pennsylvanian movement. Bunker et al. (1985) note northward dips of late Quaternary, loess-covered terraces along an ancient, south-flowing channel of the Mississippi River where the terraces cross the Plum River fault zone. Although the northward dips could be interpreted as evidence of Quaternary slip on the fault zone, they could also be explained by terrace erosion and subsequent burial beneath a blanket of loess (Bunker et al., 1985). Geologic evidence is insufficient to demonstrate Quaternary slip or deformation associated with the feature and the fault, therefore, is characterized as a non-Quaternary fault (Crone and Wheeler, 2000; Wheeler and Crone, 2001).

##### 2.1.2.2.3 Centralia Fault Zone

Normal faults of the Centralia fault zone are coincident with the dipping flank of the Du Quoin monocline and displace Paleozoic strata down to the west. Nelson (1995) reports that several high-resolution seismic lines across the Centralia fault zone indicate a normal fault dipping 70° to 75° toward the west, affecting all reflectors down to Ordovician strata. Su and McBride (1999) observe similar displacement of 100 to 160 ft for all levels imaged (upper Mississippian to Ordovician). Su and McBride (1999) suggest that the Centralia fault zone represents extensional reactivation of the basement structure beneath the Du Quoin monocline, and that these structures likely connect at depth. Nelson (1995) and Su and McBride (1999) infer that the fault has undergone two episodes of movement: reverse (west side up) during the Pennsylvanian to form the Du Quoin monocline, and normal (west side down) after the Pennsylvanian. Su and McBride (1999) note the possible association of earthquakes located near the structural axis of the Centralia fault and Du Quoin monocline with focal mechanisms consistent with strike slip along north-trending structures. Tuttle et al. (1999a) and Su and McBride (1999) suggest that the Centralia fault may be the source of earthquakes that produced paleoliquefaction features in the region.

#### 2.1.2.2.4 Rend Lake Fault Zone

The Rend Lake fault zone parallels the west flank of the Benton anticline (Nelson, 1995), which is located directly east of the Du Quoin monocline. Su and McBride (1999) report that seismic-reflection data indicate a pattern of basement-penetrating faulting in and near the Rend Lake fault zone that probably is a product of the same post-Pennsylvanian, east-west extensional stress regime that created the Centralia fault zone.

#### 2.1.2.2.5 Cap au Gres Faulted Flexure

The Cap au Gres is a faulted monocline that exhibits an overall west-northwest trend in Missouri and an east-west trend in Illinois. Strikes of the axial surface of the fold and related faults range from N 5°W to N 85°W (Harrison and Shultz, 2002). The north side has been raised as much as 1,200 ft relative to the south side (Nelson, 1995). Geophysical surveys (gravity) along the structure indicate that the faults are nearly vertical and extend at least several kilometers into the crust (Mateker and Segar, 1965). Various workers have concluded that this structure corresponds to a high-angle, north-dipping reverse fault in Precambrian basement rocks and the associated locally fractured fold near the surface (Nelson, 1995). Harrison and Schultz (2002) conclude that the Cap au Gres structure, the north-striking Florissant dome, the Waterloo-Dupo anticline, and the Lincoln fold are parts of the same deformational system.

Although the feature has undergone recurrent movement, initial uplift occurred in Devonian and early Mississippian time. Harrison and Schultz (2002) summarize studies related to the early deformational events on this structure. Based on kinematic indicators on faults and layer-parallel shortening associated with folding, they conclude that two episodes of deformation occurred along the Cap au Gres structure during the Late Mississippian-earliest Pennsylvanian. The initial episode, which was relatively minor, resulted from north-south compression and produced extension along north-south segments of the structure. The next phase was a major episode of northeast-southwest compression that produced most of the deformational features along the structure (Rubey, 1952). Following this period of deformation, some northwest-striking segments of the structure were reactivated as high-angle normal faults (Harrison and Shultz, 2002). This deformation, which probably was of Early Pennsylvanian age, appears to be the product of northwest-southeast maximum horizontal stress (Harrison and Schultz, 2002).

Nelson (1995) reports that apparent displacement of the Plio-Pleistocene Grover Gravel and its underlying peneplain indicates possible Tertiary tectonic activity on this structure. The gravel and underlying erosional surface on the south side of the flexure lie about 150 ft lower than on the north. Harrison and Schultz (2002) note that this interpretation is tentative because of uncertainties in correlating individual erosional surfaces that may not represent contiguous or equivalent contacts, and the fact that the Grover Gravel occurs at various elevations.

#### 2.1.2.2.6 St. Louis Fault

The St. Louis fault is a northeast-trending fault recognized along the border between Missouri and Illinois. Harrison and Schultz (2002) note that the fault appears to offset the Waterloo-Dupo anticline in a right-lateral sense, a displacement consistent with Late Mississippian to Early Pennsylvanian northeast-southwest compression. Tuttle et al. (1999a)

consider this fault a possible candidate for paleoearthquake features found in eastern Missouri, but emphasize that other structures to the east are equally possible.

#### 2.1.2.2.7 Eureka-House Springs Structure

The complex northwest-striking Eureka-House Springs structure in eastern Missouri has been described in various ways, as summarized by Harrison and Schultz (2002). The structure has been described as a doubly plunging anticline and associated faults, or alternatively as three right-stepping en echelon fault segments. In addition, the Valmeyer anticline in Illinois may be an en echelon segment of the Eureka-House Springs structure. Clendenin et al. (1993) interpret Middle and Late Ordovician, Middle Devonian, and post-Mississippian episodes of deformation on the Eureka-House Springs structure, suggesting that it experienced a minimum of 6 miles of left-lateral strike-slip motion. This estimate is considered tentative given the lack of piercing points and insufficient strike length for that displacement (Tuttle et al., 1999a). Harrison and Schultz (2002) suggest that the zone may have originated as a Proterozoic structure and may extend north of the St. Charles lineament, but that only those segments south of this lineament were reactivated at various times in the Phanerozoic. Tuttle et al. (1999a) observed no clear evidence of recent fault activity associated with the Eureka fault system, but note that proximity to their Meremec River liquefaction site and the uncertainties regarding the exact nature of this structure may warrant additional study.

#### 2.1.2.2.8 Ste. Genevieve Fault Zone

The Ste. Genevieve fault zone (SGFZ) is mapped for approximately 120 miles along strike from southeast Missouri into southwest Illinois (Nelson, 1995). The fault may have originated as a crustal plate boundary or suture zone during the Proterozoic (Heigold and Kolata, 1993). It consists of numerous, en echelon strands and braided segments having variable deformation styles and a complex history of reactivation (Nelson et al., 1997). Displacement across the zone ranges from less than 650 feet to as much as 3,900 feet. Harrison and Schultz (2002) note that the zone dies out near both the St. Charles and Commerce lineaments (see Section 2.1.2.3), suggesting a genetic link and demonstrating the influence of these structural features on tectonism in the region. Detailed studies of this fault zone document contractional, extensional, and strike-slip movement along high-angle faults as well as multiple periods of movement (Nelson et al., 1997; Harrison and Schultz, 2002). In Illinois, compressional deformation is documented along the Ste. Genevieve fault in Early Pennsylvanian rocks (Nelson, 1995). This deformation is correlative to the Late Mississippian to Middle Pennsylvanian tectonic episode identified elsewhere in the Midcontinent (Harrison and Schultz, 2002). Harrison and Shultz (2002) describe evidence for a period of extension probably of Late Pennsylvanian to Permian age.

Harrison and Schultz (2002) states that detailed and reconnaissance mapping along the Ste. Genevieve fault zone for more than 75 years has revealed no evidence for Tertiary or Quaternary faulting. Nelson et al. (1997), however, report that some faults along the southeast part of the Ste. Genevieve fault zone in Illinois displace Cretaceous and Tertiary sediments, but Quaternary deposits are not faulted. Tuttle et al. (1999a) found soft-sediment deformation that could be related to low levels of ground shaking at one location along a strand of the fault. Diffuse seismicity occurs in the block between the Ste. Genevieve fault zone and Simms Mountain fault system. However, no evidence has been documented of

any tectonic deformation of Quaternary deposits, nor has convincing evidence for paleoliquefaction been observed in this area (Tuttle et al., 1999a).

#### 2.1.2.2.9 Simms Mountain Fault System

The Simms Mountain fault system in southeast Missouri consists of numerous braided and en echelon fault strands that are continuous southward into the Cape Giradeau fault system. Together these fault systems extend more than 66 miles and in places reach as much as 24 miles wide. Faults along the entire system were active in the Late Cambrian as transfer faults related to Reelfoot rift extension (Clendenin et al., 1993). Left-lateral strike-slip movement occurred on the fault system, primarily before formation of Mississippi Valley-type ore deposits of Permian age, but some are post-ore and of unknown age (Harrison and Schultz, 2002).

#### 2.1.2.2.10 Bodenschatz-Lick Fault System

The Bodenshatz-Lick fault system is a complex, northeast-striking zone that has been mapped for approximately 25 miles in southeast Missouri and southern Illinois (Harrison and Schultz, 2002). Similarities in strike, dip, and early Paleozoic history suggest that this fault system may be related to the Greenville fault that has been interpreted as a major early Paleozoic extensional fault associated with the Reelfoot rift (Clendenin et al., 1993).

Two clusters of low-magnitude seismicity have been recorded by the New Madrid network near the southwest part of the Bodenschatz-Lick fault system near its intersection with the Simms Mountain-Cape Girardeau fault systems (Tuttle et al., 1999a). Field investigations by Tuttle et al. (1999a) in the areas of seismicity found no evidence of earthquake-induced paleoliquefaction in Holocene deposits.

#### 2.1.2.2.11 Cape Girardeau Fault System

The Cape Girardeau fault system, which is a continuation of the Simms Mountain fault system (Harrison and Schultz, 2002), consists of numerous branching and anastomosing, dominantly northwest-striking, near-vertical faults. Although northeast- and north-northwest-striking faults are less common, they appear to show evidence for the most recent deformation (Harrison and Schultz, 2002). There are rhomb-shaped pull-apart graben related to strike-slip faulting that can be divided into three groups: (1) those that contain only Paleozoic rocks; (2) those that contain Upper Cretaceous and lower Tertiary formations; and (3) those that contain Quaternary strata.

Unequivocal evidence of faulting of Quaternary gravel has been observed in a quarry and roadcut at the southeast end of the fault system near its intersection with the Commerce geophysical lineament. Harrison and Schultz (2002) report results of recent trenching that show evidence for Quaternary faulting, possibly post-Sangamon in age. Unfaulted Peoria Loess (late Wisconsinan in age) and possibly Roxana Silt overlie the fault and graben fill. These authors interpret the Quaternary deformation to have formed under east-northeast horizontal maximum principal stress. A site of possible faulting in Quaternary gravel was discovered by Tuttle et al. (1999a) on part of the Cape Girardeau fault system approximately 9 miles to the northwest, but they suggest that erosion and fill was an alternative and favored possible source.

#### 2.1.2.2.12 Wabash Valley Fault System

The Wabash Valley fault system (WVFS) is a major zone of northeast-trending, high-angle, normal and strike-slip faulting along the border area of Illinois, Kentucky, and Indiana (Nelson, 1995) (Plate 1). These faults lie within and form the borders of the northeast-trending Grayville graben. The Grayville graben and WVFS are bounded to the south by the Rough Creek-Shawneetown fault system (Plate 1). The WVFS is about 55 to 60 miles long and as much as 30 miles wide (Bristol and Treworgy, 1979; Nelson and Lumm, 1987). At the closest distance, these faults lie approximately 130 miles from the site. The faults of the WVFS outline elongated, gently tilted or arched horsts and grabens, with the axial part of the system down-faulted relative to the margins. Drillhole data indicate predominantly normal movement with vertical offset of as much as 480 ft along the faults that is post-Late Pennsylvanian (Bristol and Treworgy, 1979; Nelson and Lumm, 1987; Nelson, 1995). Nelson and Lumm (1987) suggest that the WVFS most likely developed in the early Permian, the same age as the Cottage Grove fault system. Individual faults within the zone are characterized by slightly arcuate segments that overlap. The faults die out downward; some may reach basement, but do not necessarily penetrate it (Bristol and Treworgy, 1979).

Major structures within the zone identified from interpretation of drillhole and downhole geophysical logs (Bristol and Treworgy, 1979) and recent seismic-reflection studies (Sexton et al., 1986; Bear et al., 1997) include the Albion-Ridgeway, Cottonwood, Herald-Phillipstown, Inman, Inman West, Inman East, Junction, Maunie, Mt. Carmel-New Harmony, North Fork, Pitcher Lake, and Ribeyre Island faults (see Figure 2.1-5 for locations of the larger faults within this zone).

Sexton et al. (1986) argue that the faults of the WVFS developed by reactivation of a Precambrian rift zone (Grayville graben) that was the northern extension of the Reelfoot-Rough Creek system. Bear et al. (1997), however, conclude that the fault system is not a northward continuation of the Reelfoot rift, because fault displacements of the WVFS decrease southward in the direction of the rift complex. Nelson and Lumm (1987) also conclude that the WVFS does not cross the Rough Creek-Shawneetown fault zone.

Based on previous interpretations of WVFS structures as primarily normal faults (Bristol and Treworgy, 1979), Nelson and Lumm (1987) conclude that the WVFS developed in response to west-northwest and east-southeast extension. Nelson (1995) proposes that the faults originated from a deformation episode that initially produced doming along a north-northeast-trending axis. Recent analysis of industry reflection data across the fault system (Bear et al., 1997) indicates Cambrian fault movements as well as early Paleozoic dextral strike slip along some of the faults.

Wheeler et al. (1997) show two possible neotectonic points in the lower Wabash Valley, one of which is associated with the WVFS (Point 4, Plate 1). At this locality Heigold and Larson (1994) investigated two sites where suspected neotectonism and ground deformation were associated with historical seismicity. One of the sites experienced liquefaction during the 1811 New Madrid earthquake. The second was an escarpment (referred to as the Meadow Bank) along projection of the Herald-Phillipstown fault zone. Vertical electrical soundings, seismic refraction profiling, resistivity profiling, and boreholes were used to evaluate the depth to Pennsylvanian bedrock across the escarpment. It was concluded that the escarpment probably formed as a result of erosion, possibly along the fault zone. The study

found no evidence to support recent movement along preexisting or newly formed faults. In the restraining bend region along the western edge of the Commerce deformation zone (see discussion of Commerce geophysical Lineament, Section 2.1.2.3.1), morphometric analysis of the land surface, detailed geologic mapping, and structural analysis of bedrock indicate westward-dipping surfaces in the Wabash Valley (between Points 3, Plate 1) (Fraser et al., 1997).

#### 2.1.2.2.13 Fluorspar Area Fault Complex

Faults that bound horsts and grabens within the fluorspar mining district of Illinois and Kentucky are included in the Fluorspar area fault complex (FAFC). FAFC faults exposed in the Paleozoic bedrock uplands that border the Mississippi embayment to the north strike northeast and dip steeply into Precambrian basement (Kolata and Nelson, 1991). At the nearest distance, these faults lie 175 miles from the EGC ESP Site. The structural style of the FAFC consists mostly of normal faults, with dip-slip offsets of as much as 2,460 ft, that define horsts and grabens, although high-angle reverse and oblique-slip faults also have been recognized (Kolata and Nelson, 1991). Nelson et al. (1997, 1999) interpret the FAFC as a series of strike-slip pull-apart grabens bounded by N20°E- to N40°E-striking normal and reverse faults. The faults probably originated as normal faults during an episode of crustal rifting of latest Proterozoic to early Cambrian time that formed the Reelfoot rift (locally, the Lusk Creek fault zone). Evidence for episodic reactivation of these faults in post-Pennsylvanian, pre-Cretaceous, and again in late Neogene to Quaternary time is reported by Nelson et al. (1999).

Results of shallow drilling, trenching, outcrop mapping, and seismic reflection acquisition in southern Illinois just north of the New Madrid zone show evidence for Quaternary-age faulting on the FAFC in the northern Mississippi embayment (Nelson et al., 1997, 1999: McBride et al., 2002b) (see neotectonic Points 5 and 6 on Plate 1). In the adjoining region south of the Ohio River, Woolery and Street (2002) interpret clear evidence of fault and apparent fold propagation into the near-surface Quaternary sediments along the southwestern projection of the FAFC in an area referred to as the Jackson Purchase. In Illinois, northeast-trending faults in the Fluorspar area fault complex down-drop Mounds Gravel of late Miocene to early Pleistocene age (11 to 1 Ma[2])) approximately 490 ft in the deepest graben and locally displace Metropolis terrace gravel that is believed to be Illinoian or older (~185 to 128 ka[3]) (Nelson et al., 1997; McBride et al., 2002b). Definitive faulting of Wisconsinan loess or Holocene alluvium, however, is not observed, which suggests that the faults have been inactive for at least 55 ka (basal loess ages) to 128 ka (youngest Illinoian age) (McBride et al., 2002b). Average vertical slip rates are estimated to be 0.01 to 0.03 mm/year, and recurrence intervals for earthquakes of magnitude 6 to 7 are on the order of 10,000's of years for any given fault (Nelson et al., 1999). McBride et al. (2002b) propose a dynamic structural model that suggests a mechanism by which seismicity and active (Holocene) faulting have shifted within the central Mississippi Valley (away from the Fluorspar area fault complex) over the past several 10,000s of years.

[2] Ma – million years before present

[3] ka – thousand years before present

#### 2.1.2.2.14 Rough Creek Graben Faults

The Rough Creek graben is an eastward extension or branch of the Reelfoot rift. The Rough Creek graben is bounded by large faults that are known from geologic mapping and from well and seismic-reflection data (Wheeler et al., 1997, and references cited therein). Its north boundary is marked by the subsurface section of the Rough Creek-Shawneetown fault system. The south border is along the parallel Pennyrile fault system of southwest Kentucky. Displacements reach 8,000 ft on the Rough Creek-Shawneetown fault system. Wheeler (1997) defines the approximate location of the boundary between the Reelfoot and the Rough Creek graben according to geologic criteria that might limit the ability of large seismic ruptures to propagate from the seismically active Reelfoot rift into the less-active Rough Creek graben.

Nelson (1995) summarizes evidence for the tectonic evolution of the Rough Creek-Shawneetown fault system. The major period of graben faulting apparently ended by the Late Cambrian. Post-Pennsylvanian stresses reactivated faults in the Rough Creek graben, creating the surficial Rough Creek-Shawneetown, Pennyrile, and related fault systems. The Rough Creek-Shawneetown fault system was reactivated as a reverse fault at that time. Nelson (1995) cites evidence to discount significant post-Pennsylvanian horizontal displacement along this fault system, as several researchers had suggested. Normal displacement occurred along this fault in a subsequent episode of extension during early Mesozoic. It is uncertain when faulting died out, but the area is seismically quiet today. Wheeler et al. (1997) show locations where strands of the Rough Creek fault system in Kentucky might offset Pliocene (?) to Holocene alluvium (see neotectonic points 1 and 7 on Plate 1). At these locations shallow geophysical methods and auger-hole data suggest offsets in the bedrock surface that may be tectonic or post-Miocene burial of older fault scarps or fault-line scarps, rather than recent faulting (Stickney, 1985; Chadwick, 1989).

#### 2.1.2.2.15 Cottage Grove Fault System

Heyl (1972) includes the Cottage Grove in his 38$^{th}$ Parallel lineament, which also contains the Rough Creek-Shawneetown fault system and Ste. Genevieve fault zone. He proposes that the lineament represents a Precambrian suture or shear zone of continental proportions, and that it may have undergone several tens of miles of right-lateral strike-slip displacement in Precambrian time. The Cottage Grove fault system is known from mapping of extensive exposures in underground coal mines as well as from coal and oil test borings and seismic profiles (Nelson, 1995). The Cottage Grove fault system is a right-lateral, strike-slip fault system consisting of: (1) a master fault zone, (2) a series of en echelon extensional faults flanking both sides of the master fault zone, and (3) a belt of anticlines along the master fault (Nelson, 1995). The master fault zone trends slightly north of west and is approximately 70 miles long. Post-Pennsylvanian horizontal displacement probably is on the order of several hundred to a few thousand ft; maximum post-Pennsylvanian horizontal offset is less than 1 mile, and maximum dip-slip displacements are about 200 ft in Pennsylvanian and Chesterian strata (Nelson, 1995). Most faulting probably was post-Missourian, pre-Early Permian, with only minor displacement occurring later (Nelson, 1995).

### 2.1.2.3 Regional Lineaments

Analyses of gravity and magnetic data have been used to evaluate the geologic framework of the northern Mississippi embayment and Illinois basin regions (e.g., Hildenbrand and

Ravat, 1997; Hildenbrand et al., 2002; Kane et al., 1981; Hildenbrand and Hendricks, 1995; Braile et al., 1997). Harrison and Schultz (2002) propose that along the southwest margin of the Illinois basin, the Commerce geophysical lineament to the south and the St. Charles lineament to the north divide the region into three distinct tectonic domains. They suggest that these lineaments represent ancient shear zones, or accommodation zones, that juxtapose different-aged Proterozoic crustal blocks, and that these accommodation zones have partitioned strain throughout the Phanerozoic, which is reflected in the northward decrease of seismic activity in the region. Harrison and Schultz (2002) report that structural features within each of the three tectonic domains vary in deformational styles and orientations, reflecting decoupling of deformation across the two lineaments.

#### 2.1.2.3.1 Commerce Geophysical Lineament

The Commerce geophysical lineament (CGL) is a northeast-trending feature that extends from northeast Arkansas to at least Vincennes, Indiana. This lineament comprises a series of linear, northeast-trending magnetic and gravity anomalies traceable for more than 240 miles (Hildenbrand and Hendricks, 1995; Langenheim and Hildenbrand, 1997). This feature has been interpreted to consist of en echelon faults and igneous intrusions in the basement that are related to the Neoproterozoic to early Paleozoic Reelfoot rift. It is postulated, however, to have an even older ancestry.

New inversions of existing magnetic and gravity data provide additional information on upper crustal structures in the central Illinois basin (Hildenbrand et al., 2002). Results of 2-D and 3-D inversion techniques suggest that the source of the CGL follows the southeast boundary of a dense and magnetic, northeast-trending igneous center named the Vincennes igneous center (Figure 2.1-6). The CGL that is defined in this region by a 3- to 6-mile wide deformation zone appears to have influenced the structural development of the Vincennes igneous center. Overlying this igneous center is the Centralia seismic-reflection sequence, expressed as highly coherent reflectors (McBride and Kolata, 1999) (Figures 2.1-7, 2.1-8, and 2.1-9). Hildenbrand et al. (2002) suggest that the buried Vincennes igneous center is the source of inferred volcanic units of the Centralia sequence and is related to a rifted margin or a Proterozoic plate boundary. Comparing gravity and magnetic fields of the Vincennes igneous center with those of the St. Francois Mountains igneous center in southeast Missouri suggests that the associated sources in each region are similar in composition and perhaps origin. Hildenbrand et al. (2002) conclude that the Commerce deformation zone evolved in the Mesoproterozoic (1.1 to 1.5 Ga[4]) as a major cratonic rheological boundary and has been the focus of episodic reactivation related to varying stress regimes throughout its history.

Quaternary deformation has been associated with this feature at several sites. The CGL coincides with the surficial trace of the Commerce fault in Missouri, a structure that recently has been shown to have Quaternary displacement (Harrison et al., 1995; Palmer et al., 1997a and b). Paleoliquefaction features and Tertiary-age faults have been mapped at other locations along the CGL (Vaughn, 1994; Nelson et al., 1997). In the Thebes Gap of Missouri and Illinois, a well-developed system of northeast- to north-northeast-trending, strike-slip faults occur directly over the CGL (Harrison and Schultz, 1994; Nelson et al., 1997). These faults cut Paleozoic, Mesozoic, and Cenozoic formations and have had a long-lived and

[4] Ga – billion years before present

episodic tectonic history, including Pleistocene and Holocene activity (Harrison et al., 1999; Harrison and Schultz, 2002). Odum et al. (2002) identify near-surface faulting and deformation overlying the CGL in southern Illinois that may be Quaternary in age in at least one locality. High-resolution seismic-reflection data acquired at three sites along the surface projection of the CGL in southeast Missouri show a complex history of post-Cretaceous faulting that has continued into the Quaternary (Stephenson et al., 1999). Langenheim and Hildenbrand (1997) list 16 earthquakes on or near the CGL; these events have body-wave magnitudes of $m_b$ 3.0 to 5.5, with a median of $m_b$ 3.9.

#### 2.1.2.3.2 St. Charles Lineament

The St. Charles lineament (SCL) is the informal name given to an alignment of geochemical and geophysical features that extends from southwest Ontario to southeast Oklahoma (Harrison and Schultz, 2002) (Plate 1). This lineament is defined by a regional, neodymium (Nd) isotopic boundary (Van Schmus et al., 1996) that coincides with linear geophysical trends along most of its length (Hildenbrand and Kucks, 1992; Hildenbrand and Hendricks, 1995). Van Schmus et al. (1996) interpret the Nd isotopic boundary as a Paleoproterozoic crustal margin that separates late Paleoproterozoic lower crustal rocks to the northwest from early Mesoproterozoic lower crustal rocks to the southeast. Sims (1990) and Sims and Peterman (1986) mapped a boundary between Paleoproterozoic metamorphic/granitoid rocks and Mesoproterozoic rhyolitic/granitic rocks along the St. Charles lineament, which they interpret as the margin of a Paleoproterozoic Central Plains orogen. Sims et al. (1987) suggest that this margin is an ancient suture zone.

A paleotectonic history of the SCL is difficult to decipher, because much of the structural features related to the lineament lie beneath the alluvial plain of the Missouri River. There is no apparent stratigraphic offset of Paleozoic strata across the SCL, but a zone of conjugate strike-slip faults of probable Late Mississippian to Early Pennsylvanian age is exposed along the SCL near Acton, Illinois (Harrison and Schultz, 2002). These faults do not displace overlying Pleistocene loess (Harrison and Schultz, 2002).

Harrison and Schultz postulate two lines of weak and non-definitive evidence for neotectonic activity along the SCL. The first is that the Missouri River bends to a northeast course upon encountering the SCL, suggesting a tectonic control on the river, which alternatively could reflect the influence of an older deformational fabric. The second line of evidence is that the post-depositional tilting of Miocene (?) Grover Gravel, which Rubey (1952) attributes to movement on the Cap au Gres structure (see above), may instead be due to faulting along the SCL. Mateker et al. (1966) note that the SCL is parallel to the Reelfoot rift and the New Madrid seismic zone, as well as to a trend of minor earthquake activity in the St. Louis-St. Charles area.

#### 2.1.2.3.3 South-Central Magnetic Lineament

A regional west-northwest-trending lineament characterized by a band of steep magnetic gradients coincides with a prominent Bouguer anomaly and the general position of the Cottage Grove fault system, Ste. Genevieve fault zone, and Hicks dome. This lineament is referred to as the South-Central magnetic lineament by Hildenbrand et al. (1983). Seismic-reflection profiles show that a layered Precambrian sequence in the upper crust in the southern Illinois basin terminates abruptly at this boundary (Kolata and Hildenbrand, 1997).

### 2.1.3 Earthquake Catalog

The earthquake catalog developed as part of the EPRI-SOG study covered the period from 1568 to the beginning of 1985. Within the region pertaining to the EGC ESP Site, the earliest event occurred in 1777. This earthquake catalog is plotted on Figure 2.1-1.

For this study, the earthquake catalog was updated using information from the following sources.

- The NCEER-91 Earthquake Catalog (Seeber and Armbruster, 1991),
- USGS National Hazard Mapping Catalog (Mueller et al., 1997),
- Center for Earthquake Research and Information (CERI), New Madrid Catalog (1974 - 8/1/2002)
- Council of the National Seismic System (CNSS) composite catalog (1985 - 8/1/2002)

When developing the NCEER-91 catalog, Seeber and Armbruster evaluated the EPRI-SOG catalog and produced revised estimates of the uniform magnitudes for the earthquakes. Figure 2.1-10 presents a comparison of the EPRI-SOG and NCEER catalog magnitudes for earthquakes in the study region. The comparison suggests that the NCEER magnitudes are, on average, about 0.1 unit lower than the EPRI-SOG magnitudes for earthquakes in the study region. Also shown on Figure 2.1-10 is a linear fit to the data for earthquakes of magnitude $m_b \geq 3.3$ (the minimum magnitude used to define recurrence rates in the EPRI-SOG study). The slope of the fitted line is $0.96 \pm 0.04$. Based on this comparison, it is judged that use of the NCEER magnitudes would have little effect on source zone recurrence rates.

An updated earthquake catalog for the region was created by adding post-1984 data to the EPRI-SOG catalog. Two principal catalog sources were used for this update. The first was the USGS National Hazard Mapping Catalog produced by Mueller et al. (1997). Data for the period 1985 through June 1995 were used. The data in the USGS catalog are declustered (foreshocks and aftershocks were removed). For this period, the magnitudes are instrumentally recorded. For the period July 1995 through June 2002, 31 earthquakes of magnitude $m_b \geq 3.3$ were taken from the CNSS catalog for the region. These data were visually inspected for obvious dependent earthquakes and then added to the catalog. Figure 2.1-11 compares the map distribution of earthquakes in the EPRI-SOG catalog to the distribution of earthquakes recorded since 1984. The spatial distribution of earthquakes is similar for the two time periods.

Another important catalog source is that of the Center for Earthquake Research and Information (CERI). Figure 2.1-12 compares map distributions of earthquakes in the EPRI-SOG catalog to that in the CERI New Madrid catalog for the period 1974 to August 2002. The CERI New Madrid catalog, which focuses on the New Madrid region, contains many more small-magnitude earthquakes ($m_b < 3$). However, it does not provide additional information for earthquakes of $m_b \geq 3.3$ for the study region.

Since 1985, two earthquakes larger than magnitude 4.0 have occurred in the study region (Figure 2.1-13). On June 10, 1987, a $m_{bLg} = 5.2$ earthquake occurred east of Olney, Richland County, Illinois (Taylor et al., 1989; Langer and Bollinger, 1991). Based on Johnston (1996), Rhea and Wheeler (1996) assign a magnitude of **M** 5.0 to this event. Source parameters for

the main shock were estimated by Taylor et al. (1989) from an analysis of surface-wave amplitude spectra. The source that best fit the observed data has a focal depth of 10 ± 1 km (6 ± 0.6 miles); mechanism with strike = 40.6° ± 5.9°, dip = 76.2° ± 5.6°; slip = 159.7° ± 6.0°; tension and pressure axes of (T) trend = 357°, plunge = 24°, (P) trend = 89°, plunge = 4°; and a seismic moment of 3.1 $*10^{23}$ dyne-cm. The distribution of well-located aftershocks indicates that the rupture was confined to a pencil-like zone within the Precambrian basement, extending from 7 to 11 km (4.2 to 6.6 miles) in depth (Taylor et al., 1989) or from 9 to 12 km (5.4 to 7.2 miles) in depth (Langer and Bollinger, 1991). The northeast-trending aftershock zone, coupled with the preponderance of northeast-striking nodal planes of the aftershock focal mechanism solutions, indicates that the preferred nodal plane for the main shock focal mechanism solution strikes northeast (Langer and Bollinger, 1991). The preferred mechanism (right-lateral strike-slip) is similar to one reported for an April 3, 1974, **M** 4.3 event located 9.6 miles to the southwest (Figure 2.1-13) (Herrmann, 1979; Taylor et al., 1989).

An **M**.4.45 earthquake occurred at 17:37 UT on June 18, 2002, in southern Indiana near Evansville. Analysis of regional waveforms of this earthquake yield a depth of 19 km (11.4 miles), a strike of 120°, dip of 80°, and rake of 10° (Herrmann et al., 2002). The focal mechanism and depth are similar to those of two other earthquakes (the 1974 and 1987 events) in the region during the past 28 years.

### 2.1.4 Prehistoric Earthquakes Inferred from Paleoliquefaction Studies

The region of the southern Illinois basin is characterized by persistent, scattered seismicity that includes several moderate historical earthquakes. Investigation of liquefaction features at several sites indicates that multiple paleoearthquakes having magnitudes significantly larger than historical events have occurred in the region (Figure 2.1-14).

Mapping and dating of liquefaction features throughout most of the southern Illinois basin and in parts of Indiana, Illinois, and Missouri have identified energy centers for at least eight Holocene and latest Pleistocene earthquakes having estimated moment magnitudes of **M** 6 to ~7.8 (Figure 2.1-15) (Obermeier et al., 1991; Munson et al., 1997; Pond and Martin, 1997; Tuttle et al., 1999b; Obermeier, 1998; McNulty and Obermeier, 1999). Except for the youngest features observed in Cache Valley in extreme southern Illinois, which probably were induced by the great New Madrid, Missouri, earthquakes of 1811-1812, the energy sources (and inferred epicenters) for the paleoliquefaction are all inferred to have occurred within Indiana and Illinois (Obermeier, 1998). Evidence for the location, size, and timing of these events is summarized in Attachment 1 to this Appendix.

Field reconnaissance conducted for this study provides additional information regarding the prehistoric record of earthquakes within the near region (approximately 25- to 30-mile radius) of the EGC ESP Site. These studies are described in Attachment 1. The primary results of these investigations are summarized below.

1. No evidence for a post-hypsithermic (post-mid-Holocene) earthquake comparable to the postulated Springfield event (McNulty and Obermeier, 1999) was observed in the study area. Sufficient exposures of pre-hypsithermic (> 6 to 7 ka) deposits were observed to demonstrate the absence of paleoliquefaction features indicative of an energy source for a comparable event (estimated to be **M** 6.2 to 6.8) in the EGC ESP Site vicinity.

2. Isolated features of mid-Holocene and latest Pleistocene/early Holocene age were observed in the study area that may be interpreted as evidence of seismically induced paleoliquefaction. Features of probable mid- to early Holocene age were observed at two localities (SC 16 and SC 19/18) along Salt Creek approximately 11.5 to 13 miles from the EGC ESP Site (Attachment 1, Figure B-1-6). Characteristics of dikes exposed at these locations are consistent with seismic liquefaction features. Assuming that these features are seismically induced, their small scale and the lack of evidence for similar features elsewhere in the area suggest they resulted from either a more distant source (possibly related to one of the previously reported events) or a low-magnitude event (at or close to threshold of paleoliquefaction, estimated to be Modified Mercalli Intensity (MMI) VI or VII). Radiocarbon ages for samples from Station SC 19 indicate these features formed after 9550 ± 40 yr BP (Cal BC 9,150 to 8,750).

3. Older features, clastic dikes that cut the post-glacial silt cap (probably early post-glacial loess deposits), were observed at Locality SC 25, approximately 17 miles from the EGC ESP Site (Attachment 1, Figure B-1-6). The features post-date the loess deposits, which are estimated to be ~16 to 17 ka. Based on weathering and soil development of the clastic dikes and silt cap and the height of the water table at the time of formation (~ 3 ft higher than at present), the dike injection features are inferred to be latest Pleistocene to early Holocene in age (<17 to 10 ka). Sedimentary and stratigraphic characteristics of host deposits and material source, as well as conduit morphology, are consistent with a seismic origin for these features. It is estimated that, if they were seismically triggered, the observed clastic dikes would imply MMI values of at least VII -VIII at that location.

4. Clastic dikes observed in till deposits at Locality M 6, approximately 29 miles north-northeast of the EGC ESP Site, appear to have formed during the latest glacial advance in that region (~ 17.7 ± 1 ka). The event that triggered the injection of the clastic dikes at this location is uncertain. Both dewatering related to glacial processes and seismic shaking are viable mechanisms.

5. No evidence for paleoliquefaction of an age similar to that observed at SC 25 has been identified at any other locality, although the possibility that clastic dikes at M 6 formed contemporaneously with the SC 25 features cannot be precluded at this time because of uncertainties in the age estimates. The limited amount of exposure of older deposits makes it difficult to document the well-defined regional pattern needed to estimate a magnitude and location for this event. Susceptible deposits of estimated latest Pleistocene age at Stations M 2, S 6, S 14, and NSC 1 show no evidence of liquefaction (Attachment 1, Figure B-1-6). These localities should have been favorable sites for liquefaction throughout much of the latest Pleistocene and Holocene, with the possible exception of NSC 1, where it is less certain that the fluvial deposits have been below the water table for most of the Holocene. Deposits at these sites thereby provide reasonable evidence for the absence of significant ground shaking since latest Pleistocene/early Holocene time, and may limit the geographic extent of liquefaction that can be correlated with that observed at Station SC 25. The extensive Mahomet gravel pit exposures (S 14) (Attachment 1, Figure B-1-6), in particular, provide strong evidence for the absence of strong ground motion that would produce significant liquefaction since deposition of the upper silt approximately 17 to 18 ka.

## 2.1.5 Seismic Sources

### 2.1.5.1 EPRI Source Evaluations

Figures 2.1-16 through 2.1-18 show the seismic sources defined by the six expert teams in the EPRI-SOG study for sources within the region pertaining to the EGC ESP Site application. In general, the geometries of these source zones are similar across the six teams. A localized zone typically is used to represent the region of the epicenters of the 1811-1812 earthquakes and the concentration of recorded seismicity near New Madrid, Missouri. A variety of source zones are used to represent the region of southern Illinois and southwestern Indiana. Sources typically include a northeast-trending Wabash Valley arm and a northwest-trending St. Louis arm. The earthquake potential in central Illinois is characterized either by a local Illinois basin source region (e.g., the Dames and Moore and Law teams), or as part of a large, regional background source.

The rate of earthquake activity within the sources was characterized using the recorded earthquake catalog for the CEUS for the time period covered by the earthquake catalog. Earthquake size was defined in terms of body-wave magnitude, $m_b$ or $m_{bLg}$. Earthquake rates were characterized using a truncated exponential (truncated Gutenburg-Richter) recurrence model. Seismicity parameters were allowed to vary spatially within each source zone over a grid size defined by one-degree longitude by one-degree latitude. The catalog of earthquakes used for assessing the seismicity parameters in the EPRI-SOG study is shown on Figure 2.1-1.

The maximum magnitude earthquake within each source was defined by a distribution of weighted values defined by each expert team. Figure 2.1-19 shows the composite distribution of these assessments for three source regions. The distributions for the New Madrid sources were based primarily on estimates of the size of the 1811-1812 earthquakes. Broad maximum magnitude distributions were assessed for sources in the Wabash Valley and southern Illinois sources reflecting the uncertainty at that time with regard to the earthquake potential of the region north of the New Madrid seismic zone. The EPRI-SOG expert teams typically assessed lower maximum magnitude values for the stable North America craton region of the CEUS relative to the Wabash Valley source, as reflected by the composite distribution for central Illinois shown on Figure 2.1-19.

### 2.1.5.2 New Data Relative to Seismic Source Evaluation

The EPRI-SOG evaluation indicated that the most significant contributors to hazard at the EGC ESP Site are the New Madrid seismic zone, the Wabash Valley seismic zone, and the random background event in the local source zone. The following sections summarize new information regarding the characterization of these seismic sources.

#### 2.1.5.2.1 Seismic Sources in the New Madrid Region

The New Madrid region is the source of the 1811-1812 New Madrid earthquakes, which include the three largest earthquakes to have occurred in historical time in the CEUS. Extensive geologic, geophysical, and seismologic studies have been conducted to characterize the location and extent of the likely causative faults of each of these earthquakes and to assess the maximum magnitude and recurrence of earthquakes in this region. Table 2.1-3 provides a summary of recent publications pertinent to the identification

and characterization of seismic sources in this region. These data have been incorporated into recent source characterizations performed for seismic hazard analyses (e.g., Cramer, 2001; Toro and Silva, 2001; Atkinson and Beresnev, 2002).

Kenner and Segall (2000) present a time-dependent model for the generation of repeated intraplate earthquakes that incorporates a weak lower crustal zone within an elastic lithosphere. Relaxation of this weak zone after tectonic perturbations transfers stress to the overlying crust, generating a sequence of earthquakes that continues until the zone relaxes fully. Model predictions mostly are consistent with earthquake magnitude, coseismic slip, recurrence intervals, cumulative offset, and surface deformation rates in the NMSZ. In particular, the computed interseismic strain rates may be undetectable with available geodetic data, implying that low observed rates of strain accumulation cannot rule out future large-magnitude earthquakes. Modeling studies by Grollimund and Zoback (2001) show that the removal of the Laurentide ice sheet approximately 20 ka changed the stress field in the vicinity of New Madrid, causing seismic strain rates to increase by about three orders of magnitude. Their modeling predicts that the high rate of seismic energy release observed during late Holocene time is likely to continue for the next few thousand years.

Alternative source models for the NMSZ presented in recent seismic hazard analyses have used actual fault segments as identified by seismicity, by geophysical and geologic data, and by historical accounts of deformation that occurred during the 1811-1812 sequence as well as modeled fictional faults and areal source zones. Data supporting alternative source geometries, particularly related to the northern extent, assessments of maximum magnitude, and recurrence parameters for the NMSZ are described below. Of significance to the EGC ESP Site are the seismic sources within the central NMSZ that generate the more frequent, large-magnitude earthquakes.

The northern boundary of the source region for New Madrid earthquakes is generally considered to lie at or just beyond the 200-mile radius of the EGC ESP Site. In contrast to earlier work that suggested there may be a through-going crustal structural link between the NMSZ and an arm of the rift that extends northeast into southwestern Indiana (e.g., Braile et al., 1982 and 1986), recent geologic and geophysical information suggests that the cause of earthquakes in the NMSZ is unrelated to that in the north (Pratt et al., 1989; Heigold and Kolata, 1993; Hildenbrand and Hendricks, 1995; Bear et al., 1997; Hildenbrand and Ravat, 1997; Kolata and Hildenbrand, 1997; Wheeler, 1997) (see Table 2.1-3).

Van Arsdale and Johnston (1999) summarize the major structures within the Mississippi embayment that show evidence for Quaternary activity. The principal seismic activity within the upper Mississippi embayment is interior to the Reelfoot rift along the NMSZ. The NMSZ consists of three principal trends of seismicity; two northeast-trending arms with a connecting northwest-trending arm. This seismicity pattern has been interpreted as a northeast-trending, right-lateral strike-slip fault system with a compressional left-stepover zone (Russ, 1982; Schweig and Ellis, 1994). The southern arm is coincident with the subcrop Blytheville arch; the central arm is coincident with the subcrop Pascola arch and surface Lake Country uplift; and the northern arm trends at a low angle to the western margin of the Reelfoot rift (Figure 2.1-20; Figure 2.1-21). Johnston and Schweig (1996) identify the following fault segments within the central fault system of the NMSZ: Blytheville arch (BA); Blytheville fault zone (BFZ); Bootheel lineament (BL); New Madrid west (NW); New Madrid north (NN); Reelfoot fault (RF); Reelfoot south (RS) (Figure 2.1-22(a)). They outline three

rupture scenarios associating each of the three 1811-1812 earthquakes with fault segments (individually or in various combinations) using historical accounts and geologic evidence (Figure 2.1-22(b)). Their interpretation is consistent with the spatial distribution and source characteristics of contemporary NMSZ seismicity (Figure 2.1-23).

The December 16, 1811, earthquake (referred to by different authors as either the D1 or NM1 earthquake), is believed to have occurred on the southern arm of seismicity (possibly the Cottonwood Grove-Ridgley fault system) associated with the Blytheville arch, a major crustal transpressional fault structure identified from seismic-reflection data. Two alternative geometries for the main fault rupture are outlined by Johnston and Schweig (1996): BA/BL (preferred) or BA/BFZ (Figure 2.1-22(b)).

The causative fault for the January 23, 1812, earthquake (referred to by different authors as either the J1 or NM2 earthquake) is generally inferred to be the northern seismicity arm of the NMSZ (segment NN) (Figure 2.1-22(a)). Toro and Silva (2001) following Van Arsdale and Johnston (1999) refer to this fault as the East Prairie fault. Baldwin et al. (2002) suggest that the North Farrenburg lineament may be associated with the New Madrid North fault and may represent the surface expression of coseismic rupture from the January 23, 1812, earthquake. Johnston and Schweig (1996) also consider an alternative scenario (S#3, Figure 2.1-22(b)) in which the source for the January 23 event is fault NW (the west-trending zone of seismicity that lies along trend of the Reelfoot fault) (Figure 2.1-22(b)). In this alternative model, both the NN and Reelfoot faults ruptured in the February 7, 1812 event.

A possible northward continuation of the New Madrid North (NN) fault is suggested by a second-order seismicity pattern that is emerging slowly from the regional seismic network data. Braile et al. (1997) have identified two parallel trends of concentrated seismicity ~ 60 miles long that extend north-northeast from the central NMSZ to within 9 miles of the Illinois/Kentucky border (Wheeler, 1997; Woolery and Street, 2002) (Figure 2.1-24).

The February 7, 1812, earthquake occurred on the Reelfoot fault, which connects the two other fault zones through the stepover region (Johnston and Schweig, 1996). The Reelfoot scarp is the surface expression of a west-dipping reverse fault that lies within the left-stepping restraining bend between two dextral strike-slip arms of the NMSZ (Russ, 1982; Sexton and Jones, 1986; Kelson et al., 1992, 1996; Schweig and Ellis, 1994). The fault and associated fold are defined by microearthquakes (Pujol et al., 1997); seismic-reflection profiles (e.g., Sexton and Jones, 1986; Odum et al., 1998; Van Arsdale et al., 1999); surface topography; shallow trench excavations (Russ, 1982; Kelson et al., 1992, 1996; Mueller et al., 1999); and borehole data (e.g., Milhills and Van Arsdale, 1999; Champion et al., 2001). Using the constraints on fault geometry derived from interpretation of microearthquakes and seismic-reflection profiles and given the amounts of surface deformation based on geomorphic and trenching investigations, the slip rate for the Reelfoot fault is estimated (Mueller et al., 1999; Van Arsdale, 2000; Champion et al., 2001) (see Table 2.1-3). Mueller and Pujol (2001) use these constraints on geometry, slip rate, and displacement during historical and prehistoric events to estimate the rate of late Holocene moment release and the magnitudes of earthquakes for the two most recent strain cycles.

Maximum magnitudes in the New Madrid region are based largely on the analysis of intensity data from the 1811-1812 earthquake sequence (Johnston, 1996; Johnston and Schweig, 1996; Hough et al., 2000; Bakun and Hopper, 2003 in press) and to a lesser degree

on magnitude assessments inferred from paleoliquefaction features (Tuttle et al., 2001, 2002) (Table 2.1-3). Cramer (2001) calculates the range of characteristic magnitudes for fault segments that capture the range of uncertainty in the dimensions of the segment rupture (length and width of the seismogenic crust) and choice of magnitude/area relationship (Table 2.1-4). Mueller and Pujol (2001) provide an additional assessment of past earthquake magnitudes through detailed mapping of the geometry and area of the Reelfoot fault, combined with estimates of fault slip rate, recurrence, and displacement in individual events to estimate the rate of late Holocene moment release. In general, more recent analyses (Hough et al., 2000, Mueller and Pujol, 2001; and Bakun and Hopper, 2003 in press) favor lower magnitude values, suggesting that site effects and population distribution biased earlier interpretations. Bakun and Hopper (2003 in press) use a new method for evaluating magnitude by directly inverting observations of intensities. They suggest that MMI attenuation is less in Eastern North America than in other stable continental regions (SCRs), and that **M** estimated for earthquakes in Eastern North America using a common SCR attenuation model (such as used by Johnston, 1996, and Hough et al., 2000) will be too high.

Constraints on the recurrence of large-magnitude earthquakes in the NMSZ come from paleoliquefaction studies (Saucier, 1991; Tuttle, 1993, 1999, 2001; Tuttle and Schweig, 2001; Craven, 1995; Li et al., 1998; Tuttle and Schweig, 1996, 2000; Tuttle et al., 1998, 1999b, 2000, 2002; and Tuttle and Wolf, 2003) and from evaluation of fault-related deformation along the Reelfoot scarp (Kelson et al., 1992, 1996). The age constraints for these events are summarized in Table 2.1-5. Findings from these studies indicate that major earthquakes occurred in the New Madrid region in AD 1450 ± 150 yr and AD 900 ± 100 yr (Figures 2.1-25 and 2.1-26*)* (Tuttle and Schweig, 2001; Tuttle et al., 2002). Saucier (1991) presents evidence for a significant earthquake in the northern part of the region in about AD 490 ± 50 yr. Tuttle and Schweig (2001) document evidence for two major earthquakes in the same area, about AD 300 ± 200 yr and BC 1370 ± 970 yr. Given uncertainties in dating liquefaction events, Tuttle et al. (2002) note that the time between any pair of the past three New Madrid events may have been as short as 200 years or as long as 800, with an average of 500 years (Figure 2.1-27). Tuttle (2001) notes that similarities in the size and spatial distributions of historical (1811-1812) and paleoliquefaction features indicate the NMSZ was the likely source of the two paleoearthquakes that are recognized regionally. Tuttle et al. (2002) document evidence that prehistoric sand blows, like those formed during the 1811-1812 earthquakes, probably are compound structures resulting from multiple earthquakes closely clustered in time (earthquake sequences).

The assumption that a large seismic-moment release in the New Madrid region involves events on all three NMSZ faults occurring within months or a few years of each other (more precisely, within an interval shorter than the temporal resolution of the paleoearthquake chronology) is adopted in the Toro and Silva (2001) seismic hazard analysis. As discussed by Van Arsdale and Johnston (1999), this assumption is supported by the 1811-1812 events, by the observation that the history of displacement on the Reelfoot fault is consistent with the paleoliquefaction history (even though the paleoliquefaction features at the northern and southern extremes of the NMSZ could not have been caused by events on the Reelfoot fault), and by the observation that the Reelfoot and Ridgely faults demonstrate similar displacement histories since the Late Cretaceous. The evidence for compound

paleoliquefaction features forming during prehistoric earthquakes (as described above) provides additional support for this hypothesis.

Other faults, including the SE Flank fault (Van Arsdale and Johnston, 1999), also referred to as the Crittenden County fault zone (Figure 2.1-21) and the Commerce/Benton Hills fault, which are located at or near the southeast and northwest margins of the Reelfoot rift, are thought to be rift-bounding normal faults that have been reactivated as oblique thrusts or transpressional strike-slip faults in the current stress regime. These fault sources are included in the seismic source model of Toro and Silva (2001) and are considered in alternative fault rupture scenarios by Cramer (2001). Van Arsdale and Johnston (1999) assign a very low weight to the possibility that coseismic rupture could extend for lengths greater than 18 miles along either the northwest or southeast margins of the Reelfoot rift. They consider two alternatives for the maximum magnitude for the SE Flank fault. The first alternative is that SE Flank segmentation is limited to Crittendenden-type fault lengths of approximately 19 miles, yielding $M_{max}$ ~ 7.2; the second is that the maximum magnitude could approach the magnitude of primary NMSZ faulting. They estimate long recurrence intervals (~10,000 yr) for earthquakes characteristic of the rift margin, based on evidence for only two Holocene occurrences. Toro and Silva (2001) use historical seismicity as observed by Chiu et al. (1997) to define the exponential portion of the magnitude-recurrence model for the SE Flank fault. They use the rate of characteristic events and the associated maximum magnitudes defined by Van Arsdale and Johnston (1999) to characterize this fault. They assign the same parameters to the Commerce/Benton Hills fault.

#### 2.1.5.2.2 Wabash Valley/Southern Illinois Seismic Zone

Table 2.1-6 provides a summary of recent publications pertinent to the identification and characterization of seismic sources in the WVSZ. These data have been incorporated into recent source characterizations for seismic hazard analyses (e.g., Frankel et al., 1996, 2002; Toro and Silva, 2001; Wheeler and Cramer, 2002).

Within the source region for the earthquake that paleoliquefaction studies indicate occurred 6,100 yr BP, candidate thrust faults have been identified at depth (McBride et al., 2002a). It has been postulated that a broad flexure (restraining bend or kink) in bedrock structure results in a concentration of stress in this region (Hildenbrand and Ravat, 1997) (Figures 2.1-6 and 2.1-28). This kink lies near the northern terminus of a 360 mile-long magnetic and gravity lineament, referred to as the Commerce geophysical lineament (CGL), that extends from Vincennes, Indiana, far into Arkansas (see Section 2.1.2.3.1). Late Quaternary faulting that displays major offsets recently has been identified near this lineament, close to the Missouri-Illinois border (Langenheim and Hildenbrand, 1997). The new paleoliquefaction data suggests the existence of a source of repeated large-magnitude (~**M** = 7.0-7.8) earthquakes in the Wabash Valley region (Attachment 1 to this Appendix). McBride and Kolata (1999) also note a possible relationship between the most deformed region of the Precambrian basement yet to be identified beneath the Illinois basin (the anomalous Enterprise subsequence) and some of the largest twentieth-century earthquakes in the central Midcontinent (Figure 2.1-7). This region roughly coincides with the area of the broad flexure (kink) in the CGL. Morphometric analysis of the land surface, detailed geologic mapping, and structural analysis of bedrock also indicate westward-dipping surfaces in the Wabash Valley region along the western edge of the CGL in the restraining bend region (Fraser et al., 1997) (Figure 2.1-28).

Evaluation of recently acquired industry seismic-reflection profile data from southern Illinois provides additional insights regarding the causative structures for recent earthquakes. McBride et al. (1997, 2002a) reprocessed industry seismic-reflection profiles, integrating the results with those from potential field analysis to evaluate structural features in southern Illinois basin (Figures 2.1-5 and 2.1-8). They report a northeast-trending zone of dipping reflectors and diffractions that they interpret as a zone of intrusions, a zone of deformation, or both. This zone lies along the CGL. McBride et al. (2002b) suggest that the zone may represent thrust faults deep within crystalline basement, faults that may be subject to reactivation. The largest instrumentally recorded earthquake in the Illinois basin, which occurred in 1968, had a moment magnitude of **M** 5.4 (Johnston, 1996) ($m_{bLg}$ *5.5*, McBride et al., 2002a). Its focal mechanism has a nodal plane that is subparallel to the zone of dipping reflections, a mid-crustal hypocenter that is located within the zone, and a seismic moment that corresponds to a rupture zone approximately the same size as one of the reflectors (Figure 2.1-9). McBride et al. (1997 and 2002a) note that earthquakes may be nucleating along compressional structures in crystalline basement and thus may occur in parts of the basin where there are no obvious surface faults or folds. McBride et al. (2002a) note that dipping reflector patterns in the Precambrian crust are not collinear, in that fault surfaces are updip in the Paleozoic sedimentary section. They conclude that shallow Paleozoic structures are "decoupled" from deeper, possibly seismogenic, structures. The results of their study suggest that the seismogenic source just north of the New Madrid seismic zone consists, in part, of a pre-existing fabric of thrusts in the basement localized along pre-existing igneous intrusions that are locally coincident with the CGL.

Maximum-magnitude distribution for the Wabash Valley-southern Illinois source zones are based on recent analysis of paleoliquefaction features in the vicinity of the lower Wabash Valley of southern Illinois and Indiana (see Attachment 1 to this Appendix). The magnitude of the largest paleoearthquake, which occurred 6,011 ± 200 yr BP, was estimated to be ≥ **M** 7.5 using the magnitude-bound method (Obermeier, 1998). The magnitude estimate for this event would be **M** 7.3 if the largest estimate for New Madrid magnitude used to calculate this value was reduced from **M** 8 to **M** 7.6 (S. Obermeier, electronic communication to Kathryn Hanson, November 7, 2002). Estimates based on a suite of approaches (magnitude–bound, cyclic stress, and energy-stress methods) range from **M** 7.5 to 7.8 (summarized in Obermeier et al., 2001). The highest value of **M** 7.8 is based on geotechnical studies using the energy-acceleration method (Pond and Martin, 1997). The magnitude of this earthquake was recently re-assessed by R. Green, S. Olson, and S. Obermeier using (1) the more recent attenuation relations of peak ground acceleration (PGA) for the central United States CEUS (Somerville et al., 2001; Campbell, 2001; Atkinson and Boore, 1995; and Toro et al., 1997); (2) review of approximately 50 boring logs presented by Pond to select appropriate Standard Penetration Test (SPT) values for the reanalysis; and (3) the most recent magnitude-scaling factors, suggested by Youd and Idriss (S. Obermeier, electronic communication to Kathryn Hanson, January 10, 2003). They conclude that the input values and energy stress method that give the highest magnitude estimates of **M** 7.7-7.8 likely are too conservative (S. Obermeier, electronic communication to Kathryn Hanson, 13 May, 2003). Using the cyclic stress method, the best estimate of the magnitude for the Vincennes earthquake based on all these solutions ranges from **M** 7+ to 7.5. The energy-based solution developed by Green (2001) circumvents the use of magnitude-scaling factor, which is a large uncertainty in

applying the cyclic stress method in the CEUS. Green's solution gives a value of **M** ~7.5 for each of the four newer attenuation relations.

The next-largest earthquake occurred 12,000 ± 1000 yr BP (Munson et al., 1997 and Obermeier, 1998). This earthquake size is estimated to be **M** 7.1 to 7.2 by Munson et al. (1997) and **M** 7.3 by Pond and Martin (1997). Both these earthquakes occurred close to one another, in the general vicinity of the most numerous and strongest historical earthquakes (**M** 4 to 5.5) in the lower Wabash Valley of Indiana-Illinois (Obermeier, 1998).

Su and McBride (1999) suggest that all paleoliquefaction features in south-central Illinois and southeastern Missouri may have been induced by the paleoearthquakes that occurred near the potential seismogenic sources identified by the re-analysis of industry seismic-reflection data (i.e., the Louden anticline, Centralia fault zone, and Du Quoin monocline). Based on the dimensions of basement-involved faults that may be associated with these structures, they estimate the maximum possible moment magnitude for an earthquake nucleating in the basement in this region to be between 6 to a little more than 7.

The WVFS is a zone of northeast-trending, high-angle, normal and strike-slip faulting that occurs within the WVSZ (Plate 1). As described in more detail above (Section 2.1.2.2.12), faults within this system lie within and form the borders of the northeast-trending Grayville graben. Recent analysis of industry reflection data across the fault system (Bear et al., 1997) indicates Cambrian fault movements as well as early Paleozoic dextral strike slip along some of the faults. The age of faulting in Paleozoic rocks is post-Pennsylvanian and pre-Pleistocene (Bristol and Treworgy, 1979; Nelson and Lumm, 1987). There is no indication of any recent faulting (Heigold and Larson, 1994).

#### 2.1.5.2.3 Central Illinois Basin/Background Source

Evidence from recent paleoliquefaction studies and seismic-reflection data suggests that moderate magnitude earthquakes may occur in parts of the Illinois basin where there are no obvious surface faults or folds. One or two prehistoric earthquakes may have occurred near Springfield, Illinois, approximately 30 miles southwest of the EGC ESP Site (see Figure 2.1-14). The earthquakes were of sufficient size to generate liquefaction features. The largest is estimated to have been in the range of moment magnitude **M** 6.2 to 6.8. At present, these events cannot be associated clearly with any known geologic structure, and no seismicity trends are observed in this area (Figure 2.1-14). As described in Attachment 1 to this Appendix, paleoliquefaction evidence suggests there may have been additional moderate-magnitude events in central and southern Illinois (e.g., the Shoal Creek earthquake) that are larger than the largest instrumentally recorded earthquake in the Illinois basin (the 1968 **M** 5.4 earthquake, Johnston, 1996) (Table B-1-1 in Attachment 1 to this Appendix). The location, size, and recurrence of such events are not well constrained by available data. Although the pattern of liquefaction features suggests local sources (Obermeier, 1998; McNulty and Obermeier, 1999), these features could also be related to more distant sources, such as basement thrust faults associated with fold structures in southern Illinois (e.g., Du Quoin Monocline/Louden Anticline or Centralia fault) or the Wabash Valley or New Madrid seismic source regions (Su and McBride, 1999; Martitia Tuttle, M. Tuttle & Associates, Personal Communication, September 3, 2002; R. Bauer, Illinois Geological Survey, Letter to K. Hanson, November 21, 2002). The non-uniform nature and distribution of liquefiable deposits and the possible influence of directivity

effects suggest that uncertainties of a few tens of kilometers should be acknowledged in the location of earthquakes epicenters from paleoliquefaction data (Wheeler and Cramer, 2002). Given the low rate of historical seismicity in this region, the apparent long recurrence between events suggested by the paleoliquefaction data, and the lack of clearly defined seismogenic structures close to the inferred energy centers, it is unlikely that distinct seismic sources can be defined for these paleoliquefaction events.

Field reconnaissance conducted as part of this study found evidence of possible older prehistoric earthquakes north and east of the EGC ESP Site, but the data are too limited to provide a basis for estimating the size or location of the event or events (Attachment 1 to this Appendix). The results of these paleoliquefaction investigations suggest that there have not been repeated moderate to large events (comparable to the postulated **M** 6.2 to 6.8 Springfield event) in the vicinity of the EGC ESP Site in latest Pleistocene to Holocene time. The late Holocene record in particular is sufficient to demonstrate the absence of such events in the past approximately 6 to 7 ka. The significance of the latest Pleistocene/early Holocene features recorded at location SC 25, approximately 17 miles east-northeast of the site, is less certain. There is insufficient information to accurately estimate a location or magnitude for a postulated seismic source. The presence of these features, however, suggests that the range in maximum magnitude assigned to a random background earthquake for the PSHA for the EGC ESP Site should include events comparable to that estimated for the postulated Springfield earthquake.

# 2.2 Ground Motion Characterization

The review of existing information for the EGC ESP Site determined that new ground motion attenuation relationships exist for characterizing the level of ground motion resulting from seismic events in CEUS. This section provides a review of the methods used to characterize ground motions within the original EPRI-SOG work, and then summarizes recent ground motion characterization work that was completed as part of an EPRI project (EPRI, 2003) and that served as the basis for updating the PSHA at the EGC ESP Site.

## 2.2.1 EPRI-SOG Characterization

The PSHA conducted in the EPRI-SOG study characterized epistemic uncertainty in earthquake ground motions using three strong-motion attenuation relationships. These were the relationships developed by McGuire et al. (1988), Boore and Atkinson (1987), and Nuttli (1986) combined with the response spectral relationships of Newmark and Hall (1982). These relationships were based to a large extent on modeling earthquake ground motions using simplified physical models of earthquake sources and wave propagation. The McGuire et al. (1988) and Boore and Atkinson (1987) models use random vibration theory to produce estimates of peak motion based on the predicted Fourier spectrum of motions.

Figure 2.2-1 compares the median ground motion levels predicted by these three attenuation relationships for peak acceleration and response spectral acceleration at a frequency of 1 Hz. The motions are plotted against the horizontal distance from the source assuming a hypocentral depth of 10 km (6 miles). The weights assigned to the three sets of attenuation relationships in the EPRI-SOG study are a weight of 0.5 for the McGuire et al.

(1988) relationships, a weight of 0.25 for the Boore and Atkinson (1987) relationships, and a weight of 0.25 for the Nuttli (1986)-Newmark and Hall (1982) relationships. The random (aleatory) variability about the three sets of median attenuation relationships was modeled as a lognormal distribution with a standard deviation of 0.5 in units of the natural log of peak motion amplitude.

### 2.2.2 Recent Assessments of CEUS Ground Motions

Estimating earthquake ground motions in the CEUS has been the focus of considerable research since completion of the EPRI-SOG studies. The research has produced a number of ground motion attenuation relationships, many of which are based on the approach used by McGuire et al. (1988) and Boore and Atkinson (1987), but incorporating more recent information on the characteristics of the propagation of earthquake source and waves in the CEUS. A study, conducted by EPRI (1993), involved extensive evaluations of the characteristics of wave propagation, specifically incorporating epistemic and aleatory uncertainty in the CEUS. This study resulted in development of an attenuation model (published by Toro et al., 1997) that has been used widely for ground motion assessments.

The Toro et al. (1997) model is based on the Brune (1972) representation of the Fourier spectrum of ground motions at an earthquake source, the so called "single-corner" source spectrum. In the mid-1990s, an alternative representation was developed, the so-called "double-corner" source spectrum. Atkinson and Boore (1995) developed a ground motion model based on the double-corner source spectrum. The Toro et al. (1997) and Atkinson and Boore (1995) ground motion models are compared to the EPRI-SOG set on Figure 2.2-2.

The Toro et al. (1997) and Atkinson and Boore (1995) models produce similar estimates of high frequency motion but differ significantly in the prediction of low frequency ground motion (frequencies of about 1 Hz or less). The difference is due primarily to the difference in the source spectrum. The Toro et al. (1997) and Atkinson and Boore (1995) models also produce median ground motion levels or high frequency motions that are similar to those obtained by the two spectral models used in the EPRI-SOG study (McGuire et al., 1988; Boore and Atkinson, 1987). The low-frequency motions predicted by the Toro et al. (1997) model are similar to those obtained from the McGuire et al., (1988) and Boore and Atkinson (1987) models. All three of these models are based on a single-corner source spectrum.

All of these models predict lower levels of low-frequency ground motion than does the Nuttli (1986)-Newmark and Hall (1982) model, based on an improved understanding of the effects of crustal properties on ground motion amplitudes. The Newmark and Hall (1982) spectral shapes were based primarily on recordings of ground motions in western North America. Recent studies have shown that significant differences in the crustal properties between western and eastern North America lead to significant differences in the relative frequency content of ground motions in the two regions. One would no longer expect the Newmark and Hall (1982) western North America spectral shape to be appropriate for ground motions on hard rock in the CEUS.

The spectral models of Toro et al. (1997) and Atkinson and Boore (1995) also provide updated estimates of the aleatory variability of ground motions. These values are frequency-dependent and, for Toro et al. (1997), also magnitude-dependent. In general the

revised estimates are larger than the value of 0.5 natural log unit used in the EPRI-SOG study.

Other investigators have developed ground motion models using the spectral approach, incorporating various alternatives for characterization of the source and path. Such models include those developed by Hwang and Huo (1997), Frankel et al. (1996), and several developed by Silva et al. (2002).

In addition to spectral models, other approaches have been applied to estimating CEUS ground motions. Since the mid-1980s, investigators have been developing numerical models for predicting strong ground motion that use a more complete model of the physics of earthquake rupture on a fault plane and wave propagation through a layered crust. These models are shown increasingly to provide reasonable estimates of ground motions in the frequency range of engineering interest and have been applied to the assessment of seismic hazards at nuclear facilities. Using these techniques, Somerville et al. (2001) developed ground motion attenuation relationships for the CEUS. Taking an alternative approach, Campbell (2003) develop a "hybrid" attenuation model by using spectral ground motion models to adjust empirical western North America attenuation relationships to conditions in the CEUS. The models developed by Somerville et al. (2001) and Campbell (2003), along with several spectral models, were used by the USGS to develop the current generation of national seismic hazard maps (Frankel et al., 2002).

EPRI has completed a study to characterize the distribution of strong ground motion prediction in the CEUS (EPRI, 2003). This study was conducted following the SSHAC (1997) guidelines for a Level III analysis. SSHAC (1997) provided guidance on the appropriate methods to use for quantifying uncertainty in evaluations of seismic hazard. In a SSHAC Level III analysis, the responsibility for developing the quantitative description of the uncertainty distribution for the quantity of interest lies with an individual or team designated the Technical Integrator. The Technical Integrator is guided by a panel of experts (referred to as the Experts), whose role is to provide information, advice, and review.

For the EPRI (2003) study, a panel of six ground motion Experts was assembled. During a series of workshops, the Experts provided advice on the available CEUS ground motion attenuation relationships that they considered appropriate for estimating strong ground motion in the CEUS. The Experts also provided information on the appropriate criteria for evaluating the available ground motion models. The Technical Integrator then used this information to develop a composite representation of the current scientific understanding of ground motion attenuation in the CEUS.

The product of the EPRI (2003) study is a suite of ground motion relationships and associated relative weights that represent the uncertainty in predicting the median level of ground motion. The EPRI (2003) relationships are defined in terms of moment magnitude, **M**, while the EPRI-SOG attenuation relationships were defined in terms of body wave magnitude, $m_b$. Thus, direct comparison of the two sets requires a relationship between $m_b$ and **M**. (Note that Atkinson and Boore, 1995, and Toro et al., 1997, relationships discussed above provided ground motion estimates in terms of both $m_b$ and **M**.) The relationship between $m_b$ and **M** magnitudes is discussed in Section 4.1.4 and is evaluated using relationships published by EPRI (1993), Atkinson and Boore (1995), and Johnston (1996).

(The EPRI, 1993, and Atkinson and Boore, 1995, $m_b$ - **M** relationships were used by Toro et al., 1997 and by Atkinson and Boore, 1995, respectively, to develop their attenuation relationships in terms of both $m_b$ and **M**.) For purposes of comparing the EPRI-SOG and the EPRI (2003) median ground motion models, the three $m_b$ - **M** relationships were used to estimate values of **M** for $m_b$ values of 5, 6, and 7, and the results averaged, as indicated in the following table.

| Body Wave Magnitude, $m_b$ | Moment Magnitude, **M** | | | |
|---|---|---|---|---|
| | EPRI (1993) | Atkinson and Boore (1995) | Johnston (1996) | Average |
| 5 | 4.6 | 4.5 | 4.7 | 4.6 |
| 6 | 5.5 | 5.6 | 5.9 | 5.7 |
| 7 | 7.2 | 7.0 | 7.4 | 7.2 |

Figure 2.2-3 compares the EPRI (2003) median attenuation relationships to those used in the EPRI-SOG study. EPRI (2003) defined the uncertainty in the median ground motions in terms of four ground motion "cluster" models. Each cluster represented a group of models based on a similar approach for ground motion modeling. The relationships shown on Figure 2.2-3 represent the median estimates of ground motions produced by the models within each cluster. The EPRI (2003) median models are generally consistent with the two spectral models used in the EPRI-SOG study (McGuire et al., 1988; Boore and Atkinson, 1987). All of the EPRI (2003) median models predict lower levels of motion than obtained using the Nuttli (1986)-Newmark and Hall (1982) model.

EPRI (2003) provided guidance on the use of the models for various types of seismic sources. In particular, the Cluster 4 model, which is based on the Somerville et al. (2001) ground motion relationships, is not considered applicable to seismic sources where a significant portion of the hazard is due to earthquakes below magnitude **M** 6.0. This is because Somerville et al. (2001) did not include earthquake magnitudes below **M** 6 in their numerical simulations when developing their model. In general, the types of seismic source for which the Cluster 4 model would not be used are general area sources in the vicinity of the site (such as the central Illinois sources in the EPRI-SOG model for the EGC ESP Site). The Cluster 4 model is applicable for computing hazard from large magnitude earthquakes.

In the EPRI (2003) representation of the uncertainty in ground motion attenuation, the uncertainty in the median model for each ground motion cluster is defined by two addition models, one representing the 5$^{th}$- percentile of the uncertainty distribution for the median and one representing the 95$^{th}$- percentile. The range in these models defines the uncertainty range in the median ground motions. Figure 2.2-4 compares the composite range in median ground motions across all clusters for the EPRI (2003) grounds motion models with the EPRI-SOG attenuation relationships. For $m_b$ 5 and 6, only models for Clusters 1, 2, and 3 are included in defining the range; Cluster 4 models are included in the range for $m_b$ 7. The uncertainty range for the EPRI (2003) peak acceleration relationships generally encompasses the three EPRI-SOG median relationships. However, for 1-Hz spectral acceleration, the

Nuttli (1986)-Newmark and Hall (1982) model lies outside of the uncertainty band for the EPRI (2003) ground motion models.

The EPRI (2003) study also developed an assessment of the aleatory variability about the median attenuation relationships. Figure 2.2-5 compares the EPRI (2003) assessments of aleatory variability (defined in terms of the standard deviation of ln[spectral acceleration]) to the value used in the EPRI-SOG study. The EPRI (2003) assessments are significantly larger than those used in the EPRI-SOG study.

## TABLE 2.1-1

## SUMMARY OF FOLDS

Seismic Hazards Report for EGC ESP Site

| NAME | MEANS OF IDENTIFICATION [1] | MAJOR MOVEMENT/RECENCY | |
|---|---|---|---|
| | | CPS USAR [2] | THIS STUDY [3] |
| **Illinois** | | | |
| Ashton Arch | B, S | Late Paleozoic (Templeton and Willman, 1952) | Renamed Ashton Anticline (Nelson, 1995) |
| Benton Anticline | S, G | | Late Mississippian and early Pennsylvanian (Nelson, 1995; Su and McBride, 1999) |
| Cap au Gres Faulted Flexure | S, B | Post-Middle Mississippian, Pre-Pennsylvanian (Rubey, 1952) | Late Pennsylvanian/Permian, possible Post-Miocene (Harrison and Schultz, 2002) |
| Clay City Anticline | B | Pre-Pennsylvanian, Pennsylvanian, and/or Post-Pennsylvanian (DuBois and Siever, 1955) | Principal deformation in early Pennsylvanian time (Nelson, 1995) |
| Downs Anticline | B, G | Mississippian through Pennsylvanian (Clegg, 1972) | Same[4]; probably a basement structure (Nelson, 1995) |
| Dupo-Waterloo Anticline | B,S | Late Missisippian, Pre-Pennsylvanian (Buschbach, written communication, 1973) | Late Mississippian to Early Pennsylvanian (Nelson and Lumm, 1987, slight post-Pennsylvanian (Nelson, 1995); possible tectonic source for paleoliquefaction (Tuttle et al., 1999a) |
| Du Quoin Monocline | B, G | Pennsylvanian or earlier (Buschbach, written Communication, 1973) | Early to mid-Pennsylvanian. Associated faults-<br>Two episodes of movement: reverse (west side up) during the Pennsylvanian, and normal (west side down) after the Pennsylvanian (Nelson, 1995; and Su and McBride, 1999); possible tectonic source for paleoliquefaction (Tuttle et al., 1999a) |
| Illinois Basin | S, B, G | Early to Late Paleozoic (Willman et al., 1975) | Same; see Figure 2.1-2 |
| Kankakee Arch | S, B, G | Ordovician to Pennsylvanian (Eardley, 1951) | Same; see Figure 2.1-2 |

## TABLE 2.1-1

## SUMMARY OF FOLDS

Seismic Hazards Report for EGC ESP Site

| NAME | MEANS OF IDENTIFICATION [1] | MAJOR MOVEMENT/RECENCY | |
|---|---|---|---|
| | | CPS USAR [2] | THIS STUDY [3] |
| **Illinois** | | | |
| La Salle Anticlinal Belt | S, B, G | Post-Mississippian to Permian (Buschbach, written communication, 1973) | Renamed La Salle Anticlinorium (Nelson, 1995); post-Mississippian (late Paleozoic); associated reverse faults in basement |
| Louden Anticline | S,G | Pennsylvanian to Post-Pennsylvanian (Buschbach, written communication, 1973) | Fold developed in early to mid-Pennsylvanian; associated with major deep basement fault; possible source structure for paleoliquefaction events (Su and McBride, 1999) |
| Peoria Folds | S,B | Not recognized as significant structure | Mississippian and Pennsylvanian; correspondence with topography as imaged in aerial photographs and satellite imagery (Nelson, 1995) |
| Peru Monocline (Part of La Salle Anticliorium) | S | Included as part of La Salle Anticlinorium | Upper Pennsylvanian (Nelson, 1995); possible association of seismicity (Larson, 2002) |
| Lincoln Anticline | S,B | Late-Mississippian to Early Pennsylvanian (McQueen et al., 1961) | Additional uplift occurred after Pennsylvanian sedimentation. A final episode of uplift along the eastern part of the fold may have occurred late in the Tertiary Period (Rubey, 1952) |
| Marshall Syncline | B | Late or Post-Pennsylvanian (Clegg, 1965) | Same[4] |
| Mattoon Anticline | B | Late Paleozoic (Clegg, 1965) | Same[4] |
| Mississippi River Arch | S, B, G | Late Paleozoic (Buschbach, written communication, 1973) | Post-Early Pennsylvanian (Bunker et al., 1985) |
| Moorman Syncline | S, B | Post-Pennsylvanian (Bell et al., 1964) | Mesozoic Era (Nelson and Lumm, 1987) |
| Murdock Syncline | B | Late or Post-Pennsylvanian (Clegg, 1965) | Same[4] |

## TABLE 2.1-1

## SUMMARY OF FOLDS

Seismic Hazards Report for EGC ESP Site

| NAME | MEANS OF IDENTIFICATION [1] | MAJOR MOVEMENT/RECENCY | |
|---|---|---|---|
| | | CPS USAR [2] | THIS STUDY [3] |
| **Illinois** | | | |
| Pittsfield-Hadley Anticline | B | Post Pennsylvanian anticline (Buschbach, written communication, 1973) | Reactivation of basement faults (Nelson, 1995) |
| Salem Anticline | B | Pennsylvanian and Post-Pennsylvanian anticlines (Buschbach, written communication, 1973) | Major folding in early Pennsylvanian; additional deformation during and after middle Pennsylvanian (Nelson, 1995) |
| Sangamon Arch | B, G | Devonian to Early Mississippian (Buschbach, written communication, 1973) | Short-lived structural high in the Middle Devonian Epoch (Nelson, 1995); see Figure 2.1-2 |
| Structures associated with the Plum River Fault Zone | S, B, G | Pennsylvanian, Post-Pennsylvanian, Pre-Middle Illinoian (Pleistocene) fault zone (Kolata and Buschbach, 1976) | See CPS USAR for discussion and map showing location |
| Tuscola Anticline | B | Pennsylvanian and Post-Pennsylvanian (Bristol and Prescott, 1968) | Same[4] |
| **Iowa** | | | |
| Bentonsport | B | Mississippian (Harris and Parker, 1964) | Same[4] |
| Burlington | B | Mississippian (Harris and Parker, 1964) | Same[4] |
| Oquawka | B | Mississippian (Harris and Parker, 1964) | Same[4] |
| Skunk River | B | Mississippian (Harris and Parker, 1964) | Same[4] |
| Sperry | B | Mississippian (Harris and Parker, 1964) | Same[4] |
| **Missouri** | | | |
| Auxvasse Creek Anticline | S | Post-Pennsylvanian (McCracken, 1971) | Same[4] |
| Browns Station Anticline | S | Late Mississippian or Pennsylvanian (CPS USAR) | Same[4] |

## TABLE 2.1-1

## SUMMARY OF FOLDS

Seismic Hazards Report for EGC ESP Site

| NAME | MEANS OF IDENTIFICATION [1] | MAJOR MOVEMENT/RECENCY | |
|---|---|---|---|
| | | CPS USAR [2] | THIS STUDY [3] |
| **Missouri** | | | |
| College Mound-Bucklin Anticline | S | Later part or Post-Pennsylvanian (McCracken, 1971) | Same[4] |
| Crystal City Anticline | S | Post-Mississippian (CPS USAR) | Same[4] |
| Cuivre Anticline | S | Post-Mississippian (CPS USAR) | Not identified as a significant structure by Harrison and Schultz (2002) |
| Davis Creek Anticline | B | Post-Mississippian (CPS USAR) | Same[4] |
| Eureka-House Springs | S, B | Post-Mississippian anticline (McCracken, 1971) | No clear evidence of recent fault activity, but close to paleoliquefaction site (Tuttle et al., 1999a) |
| Farmington Anticline | S, B | No older than Devonian (McCracken, 1971) | Microseismicity and magnetic data suggest this structure is underlain by buried faults in basement that may be seismogenic (Harrison and Schultz, 2002; Tuttle et al., 1999a) |
| Kruegers Ford Anticline | S, B | Post-Ordovician (CPS USAR) | Same[4] |
| Mexico Anticline | S, B | Late or Post-Pennsylvanian (CPS USAR) | Same[4] |
| Mineola Structure | S | Pennsylvanian, Post-Pennsylvanian (CPS USAR) | Same[4] |
| Ozark Uplift | S, B, G | Paleozoic, Mesozoic, Tertiary (McCracken, 1971) | Same[4]; see Figure 2.1-2 |
| Pershing-Bay -Gerald Anticline | S | Post-Mississippian, Early Pennsylvanian (CPS USAR) | Same[4] |
| Plattin Creek Anticline | S | Post-Mississippian ( CPS USAR) | Same[4] |
| Troy Brussels Syncline | S, B | Late Mississippian or Early Pennsylvanian (Rubey, 1952) | Same[4] |

## TABLE 2.1-1

## SUMMARY OF FOLDS

Seismic Hazards Report for EGC ESP Site

| NAME | MEANS OF IDENTIFICATION [1] | MAJOR MOVEMENT/RECENCY | |
|---|---|---|---|
| | | CPS USAR [2] | THIS STUDY [3] |
| **Wisconsin** | | | |
| Meekers Grove Anticline | B, S | Late Paleozoic (Heyl et al., 1959) | Same[4] |
| Mineral Point Anticline | B, S | Late Paleozoic (Heyl et al., 1959) | Same[4] |
| Wisconsin Arch | S, B, G | Early to Late Paleozoic (Eardley, 1951) | Same[4]; see Figure 2.1-2 |

**NOTES:**

1 S = surface mapping, B = borehole, G = geophysical data

2 The absence of sediments representing the interval from Pennsylvanian to Cretaceous or Pleistocene time makes it impossible to precisely date the age of the most recent movement on these structures. Based on stratigraphic relationships and geologic history outside of the regional area, however, final movement on the structures is considered to have occurred prior to Pleistocene time, and possibly before the end of the Paleozoic.

3 Locations of folds are shown on Plate 1, except where noted.

4 No new information regarding recency is available. The assessment for the timing of major movement/recency as outlined in the CPS USAR is the same.

## TABLE 2.1-2

## SUMMARY OF FAULTS

Seismic Hazards Report for the EGC ESP Site

| FAULT NAME | MEANS OF IDENTIFICATION [1] | FAULT DISPLACEMENT | LAST MOVEMENT/RECENCY | |
|---|---|---|---|---|
| | | | CPS USAR | THIS STUDY |
| Cap au Gres Faulted Flexure | S, B, G | Maximum structural relief of 1,200 feet (Rubey, 1952) | Late Pliocene- Pre-Pleistocene (Buschbach, written communication, 1973) | Apparent displacement of Plio-Pleistocene Grover Gravel may indicate possible Tertiary activity (Nelson, 1995), or alternatively may be due to miscorrelation of individual erosion surfaces (Harrison and Schultz, 2002). |
| Centralia Fault | S (in mines), B, G | Downthrown as much as 200 feet on west side (Buschbach, written communication, 1973) Dip of fault plane is 70° to 75°; throw is 100 to 160 feet (Su and McBride, 1999) | Post-Pennsylvanian, Pre-Pleistocene (Buschbach, written communication, 1973) | Likely connects with a basement fault at depth. Two episodes of movement: reverse (west side up) during Pennsylvanian, and normal (west side down) after Pennsylvanian. Possible association of seismicity (focal mechanisms consistent with strike slip along N-trending structures) and paleoliquefaction features (Su and McBride, 1999; Tuttle et al., 1999a). |
| Chicago Area Basement Fault (Inferred) | G, B | Downthrown 900 feet on southwest side (McGinnis, 1966) | Pre-Middle Ordovician (McGinnis, 1996) | Referred to as unnamed fault zone; new well and seismic data indicate no offset of the Precambrian surface (Nelson, 1995). |

## TABLE 2.1-2

## SUMMARY OF FAULTS

Seismic Hazards Report for the EGC ESP Site

| FAULT NAME | MEANS OF IDENTIFICATION [1] | FAULT DISPLACEMENT | LAST MOVEMENT/RECENCY | |
|---|---|---|---|---|
| | | | CPS USAR | THIS STUDY |
| Chicago Area Minor Faults (Inferred) | G, S | North or south side of faults downthrown, 55 feet maximum displacement (Buschbach and Heim, 1972) | Post-Ordovician or Post-Silurian, Pre-Pleistocene (Buschbach and Heim, 1972) | Referred to as Cook County faults. Some faults interpreted from seismic data are questionable or have been shown based on tunnel exposures to be folds. Trend of faults is NW to WNW, similar to trend of Sandwich fault zone (Nelson, 1995). |
| Chicago Area Minor Faults | S | Few inches to few feet (Buschbach and Heim, 1972) | Post-Silurian, Pre-Pleistocene (Gray, written communication, 1974) | |
| Fluorspar Area Fault Complex | S, B, G | Graben structures present; northwest or southeast walls of faults downthrown. Displacements variable, may reach 2,460 feet. (Baxter and Desborough, 1965; Kolata and Nelson, 1991)<br><br>Possible pull-apart structure related to strike-slip faulting (Nelson et al., 1997, 1999) | Tertiary, possibly Pre-Cretaceous (Becker and Head, 1975) | The faults probably originated as normal faults during an episode of crustal rifting of latest Proterozoic to early Cambrian time that formed the Reelfoot rift. Evidence for episodic reactivation of these faults in post-Pennsylvanian, pre-Cretaceous time and subsequently in late Neogene to Quaternary time, is reported by Nelson et al. (1997, 1999); McBride et al. (2002 b); and Woolery and Street (2002). Possible association with seismicity (Wheeler, 1997). Most recent activity older than 55 to 128 ka (McBride et al., 2002b). |

## TABLE 2.1-2

## SUMMARY OF FAULTS

Seismic Hazards Report for the EGC ESP Site

| FAULT NAME | MEANS OF IDENTIFICATION [1] | FAULT DISPLACEMENT | LAST MOVEMENT/RECENCY | |
|---|---|---|---|---|
| | | | CPS USAR | THIS STUDY |
| Fortville Fault | B | Downthrown 60 feet on southeast side (Becker, written communication, 1975) | Post-Devonian, Pre-Pleistocene (Gray, written communication, 1974) | Same[2] |
| Janesville Fault (also referred to as the Evansville fault) | B | Downthrown 70 feet on north side (R. M. Peters, Wisconsin Geological and Natural History Survey, written communication, 2 May 2003) | Phanerozoic, but, Pre-Pleistocene possible Pre-Cretaceous (Ostrom, written communication, 1975, Thwaites, 1957) | No evidence of Pleistocene or post-Pleistocene activity observed (R. M. Peters, Wisconsin Geological and Natural History Survey, electronic communication to Kathryn Hanson, 14 May 2003) |
| Madison Fault (also referred to as the west-east fault system) | B | Northern trace- north side downthrown 40 to 75 feet; Southern trace- south side downthrown 85 to 125 feet (Brown et al., in preparation, 2003) | Phanerozoic, but, Pre-Pleistocene possible Pre-Cretaceous (Ostrom, written communication,1975, and Thwaites, 1957) | No evidence of Pleistocene or post-Pleistocene activity observed (R. M. Peters, Wisconsin Geological and Natural History Survey, electronic communication to Kathryn Hanson, 14 May 2003) |
| Mt. Carmel Fault | S, B | Downthrown in excess of 200 feet on west side (Melhorn and Smith, 1959) | Early Pennsylvanian (Melhorn and Smith, 1959) | Same[2] |
| Northeast-Trending Faults South of the Rough Creek Fault Zone (See Fluorspar Area Fault Complex) | | | | |
| Oglesby Fault (Inferred) | B | Downthrown 1,200 feet on west side (Green, 1957) | Pre-Cretaceous (CPS USAR) | Discarded; available data do not permit interpretation of a continuous fault in this area (Nelson, 1995) |

## TABLE 2.1-2

## SUMMARY OF FAULTS

Seismic Hazards Report for the EGC ESP Site

| FAULT NAME | MEANS OF IDENTIFICATION [1] | FAULT DISPLACEMENT | LAST MOVEMENT/RECENCY | |
|---|---|---|---|---|
| | | | CPS USAR | THIS STUDY |
| Plum River Fault Zone | S, B, G | Downthrown up to 400 feet on north side (Kolata and Buschbach, 1976) | Post-Silurian, Pre-Middle Illinoian (Kolata and Buschbach, 1976) | No evidence of Quaternary activity identified in recent studies (Crone and Wheeler, 2000;Wheeler and Crone, 2001). |
| Rend Lake Fault Zone | S, G | High-angle normal faults; displacement ranges from less than 1 inch to about 55 feet (Nelson, 1995) | Not identified as a significant fault | Basement-penetrating faults associated with fold (Benton Anticline) primarily active during late Mississippian and early Pennsylvanian time; reactivated normal faulting late- or post-Pennsylvanian (Nelson, 1995; Su and McBride, 1999). |
| Rough Creek Fault Zone | S, B, G | North side downthrown; maximum reported displacement of 3,400 feet along the fault zone. (Buschbach, written communication,1973) | Post-Pennsylvanian Pre-Late Cretaceous (Buschbach, written communication, 1973) | Possible post-Pliocene (?) and Holocene offsets (Stickney, 1985; Chadwick, 1989). |
| Royal Center Fault | B | Downthrown 100 feet on southeast side (Becker and Head, 1975) | Post-Middle Devonia, Pre-Pleistocene (Gray, written communication, 1974) | Same[2] |

## TABLE 2.1-2

## SUMMARY OF FAULTS

Seismic Hazards Report for the EGC ESP Site

| FAULT NAME | MEANS OF IDENTIFICATION [1] | FAULT DISPLACEMENT | LAST MOVEMENT/RECENCY | |
|---|---|---|---|---|
| | | | CPS USAR | THIS STUDY |
| Ste. Genevieve Fault Zone | S, B, G | Net displacement along the fault zone is down to the north and east; maximum displacement exceeds 1,000 feet, possibly as much as 3,900 feet (Buschbach, written communication, 1973; Harrison and Schultz, 2002) | Post-Pennsylvania, Pre-Pleistocene (Bell et al., 1964, and Willman et al., 1975) | No evidence for Tertiary or Quaternary faulting (Harrison and Schultz, 2002). Nelson et al. (1997) report evidence for displacement of Tertiary units. Tuttle et al. (1999a) found soft-sediment deformation that could be related to low levels of ground shaking at one location along a strand of the fault. |
| Sandwich Fault Zone | S, B, G | Downthrown as much as 800 feet on northeast side (Bell et al., 1964) | Post-Pennsylvanian, Pre-Pleistocene (Kolata et al., 1978) | Larson (2002) notes that two historical earthquakes (in 1909 and 1912) may be associated with the Sandwich fault zone, and that these two events may indicate reactivation of a fault within the Precambrian basement associated with the Sandwich fault zone. |
| St. Louis Fault | S | Down-to-the-west and down-to-the-east displacements | | Late Mississippian-Early Pennsylvanian right-lateral offset (Harrison and Schultz, 2002). Possible Possible source for Holocene paleoliquefaction (Tuttle et al., 1999a). |

## TABLE 2.1-2

## SUMMARY OF FAULTS

Seismic Hazards Report for the EGC ESP Site

| FAULT NAME | MEANS OF IDENTIFICATION [1] | FAULT DISPLACEMENT | LAST MOVEMENT/RECENCY | |
|---|---|---|---|---|
| | | | CPS USAR | THIS STUDY |
| Tuscola Fault (Inferred) | B | Downthrown 2,000 feet on west side (Green, 1957) | Pre-Cretaceous (CPS USAR) | Discarded. Seismic profile shows no indication of faulting at Trenton (Ordovician) level or higher; data do not rule out basement faults along parts of La Salle Anticlinorium, but presence of fault is not documented (Nelson, 1995). |
| Wabash Valley Fault Zone | B, G, S | Graben structures present; northwest or southeast sides of faults downthrown; maximum displacement 480 feet (Buschbach, written communication, 1973; Bristol and Treworgy, 1979; Nelson and Lumm, 1987; Nelson, 1995) | Post-Pennsylvanian, Pre-Pleistocene (Buschbach, written communication, 1973) | Pliocene-early Pleistocene (New Columbia/Lusk Creek); Pleistocene (Barnes Creek A/Barnes Creek and Midway/Barnes Creek) (Nelson et al., 1997; Wheeler et al., 1997). |
| Waukesha Fault | S, B | Downthrown 1,500+ feet on southeast side (Thwaites, 1957) | Phanerozoic, but Pre-Pleistocene, possibly Pre-Cretaceous (Ostrom, written communication, 1975, and Thwaites, 1957) | Location revised based on Evans et al. (2003, in preparation). No evidence of Pleistocene or post-Pleistocene activity observed (R. M. Peters, Wisconsin Geological and Natural History Survey, electronic communication to Kathryn Hanson, 14 May 2003) |

## TABLE 2.1-2

## SUMMARY OF FAULTS

Seismic Hazards Report for the EGC ESP Site

| FAULT NAME | MEANS OF IDENTIFICATION [1] | FAULT DISPLACEMENT | LAST MOVEMENT/RECENCY | |
|---|---|---|---|---|
| | | | CPS USAR | THIS STUDY |
| Wisconsin Minor Faults: Dane County (Yahara Hills complex) | S, B | Downthrown as much as 400 feet on the northwest side (Ostrom, 1971; Brown et al., in preparation, 2003)) | Post-Ordovician, Pre-Pleistocene, possibly Pre-Cretaceous (Ostrom, written communication, 1975, and Ostrom, 1971) | No evidence of Pleistocene or post-Pleistocene activity observed (R. M. Peters, Wisconsin Geological and Natural History Survey, electronic communication to Kathryn Hanson, 14 May 2003) |
| Wisconsin Minor Faults: Waukesha | S | Downthrown 27 feet on the southeast side (Ostrom, written communication, 1975) | Post-Silurian, Pre-Pleistocene; possibly Pre-Cretaceous (Ostrom, written communication, 1975) | No evidence of Pleistocene or post-Pleistocene activity observed (R. M. Peters, Wisconsin Geological and Natural History Survey, electronic communication to Kathryn Hanson, 14 May 2003) |

Notes:

1 S = surface, B = borehole, G = geophysical data

2 Characterization of fault follows CPS USAR.

## TABLE 2.1-3

## SUMMARY OF NEW INFORMATION FOR NEW MADRID SEISMIC ZONE

Seismic Hazards Report for the EGC ESP Site

| AUTHOR(S) (YEAR) | TITLE | SIGNIFICANCE |
|---|---|---|
| | | |
| **GEOLOGIC STRUCTURES INTERPRETED FROM GRAVITY, MAGNETIC, AND SEISMIC-PROFILE DATA** | | |
| McKeown et al. (1990) | ”Diapiric origin of the Blytheville and Pascola arches in the Reelfoot rift, east-central United States: Relation to New Madrid seismicity” | Earthquakes in the NMSZ correlate spatially with the Blytheville arch and part of the Pascola arch, which are interpreted to be the same structure. Both arches were formed by diapirism. The rocks in the arch are more highly deformed, and therefore weaker, than adjacent rocks. Seismicity is hypothesized to be localized in these weaker rocks. |
| Nelson and Zhang (1991) | “A COCORP deep reflection profile across the buried Reelfoot rift, south-central United States” | Deep reflection profile line reveals features of the late Precambrian (?)/early Paleozoic Reelfoot rift. The Blytheville arch, an axial antiformal feature, as well as lesser structures indicative of multiple episodes of fault reactivation, are evident on profile. |
| Hildenbrand and Hendricks (1995) | “Geophysical setting of the Reelfoot rift and relations between rift structures and the New Madrid seismic zone” | Provides discussion of several potential-field features inferred from magnetic and gravity data that may focus earthquake activity in the northern Mississippi embayment and surrounding region. Summarizes complex tectonic and magmatic history of the rift. |
| Braile et al. (1997) | “New Madrid seismicity, gravity anomalies, and interpreted ancient rift structures” | Epicentral patterns, correlative geophysical data, and historical seismic energy release indicate the significance of New Madrid area seismicity, both within the Reelfoot segment of the rift structures and in areas outside of this segment, particularly to the north. Deep structure of the crust, including thickness variations in the upper crust and the presence of a high-density lower crustal layer, is a controlling factor in New Madrid seismicity. |
| Hildenbrand et al. (2001) | “Geologic structures related to New Madrid earthquakes near Memphis, Tennessee, based on gravity and magnetic interpretations” | Defines boundaries of regional structures and igneous complexes in the region north of Memphis, Tennessee, and south of latitude 36° that may localize seismicity. |

## TABLE 2.1-3

## SUMMARY OF NEW INFORMATION FOR NEW MADRID SEISMIC ZONE

Seismic Hazards Report for the EGC ESP Site

| AUTHOR(S) (YEAR) | TITLE | SIGNIFICANCE |
|---|---|---|
| **NORTHERN TERMINUS OF REELFOOT RIFT** | | |
| Pratt et al. (1989) | "Major Proterozoic basement features of the eastern Midcontinent of North America revealed by recent COCORP profiling" | Interpretation of deep seismic reflection data from southern Illinois and southern Indiana indicates an absence of a thick section of rift-related sedimentary rocks. |
| Heigold and Kolata (1993) | "Proterozoic crustal boundary in the southern part of the Illinois basin" | Conclude that structures associated with the NMFZ may be distinct from structures to the northeast (in the Wabash Valley zone), as evidenced by the east-southeast-trending geophysical anomaly that separates two areas of distinctly different crust. |
| Hildenbrand and Hendricks (1995) | "Geophysical setting of the Reelfoot rift and relations between rift structures and the New Madrid seismic zone" | Inspection of regional magnetic and gravity anomaly maps suggests that the northwest margin does not continue northeastward into southern Indiana. A preferred geometry is that both the northwest and southeast margins bend to the east and merge with the Rough Creek graben. |
| Bear et al. (1997) | "Seismic interpretation of the deep structure of the Wabash Valley fault system" | Interpretation of recently compiled seismic reflection data suggests that structures associated with the Wabash Valley fault system may not be directly linked to northeast-trending structures in the New Madrid area.<br>The authors note that a graben may exist within the southern Indiana arm (Braile et al., 1982), but it is limited in geographic extent and is not structurally continuous with the Reelfoot rift-Rough Creek graben. |
| Hildenbrand and Ravat (1997) | "Geophysical setting of the Wabash Valley fault system" | Concludes from high-resolution aeromagnetic data and the lack of regional potential-field features extending south from the Wabash Valley that the Wabash Valley fault system apparently is not structurally connected to the faults related to the NMSZ |
| Kolata and Hildenbrand (1997) | "Structural underpinnings and neotectonics of the southern Illinois basin: An overview" | Summarizes geologic and geophysical information suggesting that the cause of earthquakes in the NMSZ is unrelated to that in the region north of the Reelfoot rift system. |

## TABLE 2.1-3

## SUMMARY OF NEW INFORMATION FOR NEW MADRID SEISMIC ZONE

Seismic Hazards Report for the EGC ESP Site

| AUTHOR(S) (YEAR) | TITLE | SIGNIFICANCE |
|---|---|---|
| | | |
| **NORTHERN TERMINUS OF REELFOOT RIFT** | | |
| Wheeler (1997) | "Boundary separating the seismically active Reelfoot rift from the sparsely seismic Rough Creek graben" | Concludes that the structural boundary between the relatively high hazard of the Reelfoot rift and low hazard of the Rough Creek graben is marked by bends and ends of large faults, a Cambrian transfer zone, and the geographic extent of alkaline igneous rocks. |
| **SEISMOGENIC FAULTS** | | |
| Sexton and Jones (1986) | "Evidence for recurrent faulting in the New Madrid seismic zone from mini-sosie high-resolution reflection data" | Interpretation and integration of three seismic reflection data sets provides evidence for recurrent movement along the Reelfoot fault, the major reverse fault associated with the Reelfoot scarp. Estimated displacements vary from 200 feet (60 ms) for late Paleozoic rocks to 50 feet (20 ms) for late Eocene sedimentary units. A graben structure is interpreted to be caused by tensional stresses resulting from uplift and folding of the sediments. The location of the graben coincides with normal faults in Holocene sediments observed in trenches. These features are interpreted to be related and caused by reactivation of the Reelfoot fault. |
| Harrison and Schultz (1994) | "Strike-slip faulting at Thebes Gap, Missouri and Illinois: Implications for New Madrid tectonism" | Documents evidence for Quaternary faulting in trenches in the Benton Hills of southeast Missouri. |
| Pujol et al. (1997) | "Refinement of thrust faulting models for the central New Madrid seismic zone" | Seismicity cross sections define the downdip geometry of the Reelfoot thrust |
| Johnston and Schweig (1996) | "The Enigma of the New Madrid earthquakes of 1811-1812" | Associated each of three 1811-1812 earthquakes with a specific fault by using historical accounts and geologic evidence:<br>Event D1—Blytheville arch/CDF or Bootheel lineament<br>Event J1—East Prairie fault<br>Event F1—Reelfoot fault |

## TABLE 2.1-3

## SUMMARY OF NEW INFORMATION FOR NEW MADRID SEISMIC ZONE

Seismic Hazards Report for the EGC ESP Site

| AUTHOR(S) (YEAR) | TITLE | SIGNIFICANCE |
|---|---|---|
| | | |
| **SEISMOGENIC FAULTS** | | |
| Schweig and Van Arsdale (1996) | "Neotectonics of the upper Mississippi embayment" | Summarizes geologic and geophysical evidence of neotectonic activity, including faulting in Benton Hills and Thebes Gap, paleoliquefaction in Western Lowlands, subsurface faulting beneath and tilting of Crowley's Ridge, subsurface faulting along the Crittenden County fault zone, and numerous indicators of historical and prehistoric large earthquakes in New Madrid seismic zone. |
| Palmer et al. (1997b) | "Seismic evidence of Quaternary faulting in the Benton Hills area, southeast Missouri" | Seismic profiles show the English Hill area to be tectonic in origin. Individual faults have near-vertical displacements with maximum offsets on the order of 50 feet. Faults are interpreted as flower structures with NNE-striking, vertically dipping, right-lateral oblique-slip faults. These data suggest previously mapped faults at English Hill are deep-seated and tectonic in origin. |
| Odum et al. (1998) | "Near-surface structural model for deformation associated with the February 7, 1812, New Madrid, Missouri, earthquake" | Integrates geomorphic data and documentation of differential surficial deformation (supplemented by historical accounts) with interpretation of seismic reflection data to develop a tectonic model of the near-surface structures in the New Madrid area. Model consists of two primary components: a north-northwest-trending thrust fault (Reelfoot fault), and a series of northeast-trending, strike-slip tear faults.<br><br>The authors estimate an overall length of at least 30 km (18 miles) and a dip of ~ 31° for the Reelfoot fault. |
| Crone (1998) | "Defining the southwestern end of the Blytheville arch, northeastern Arkansas: Delimiting a seismic source zone in the New Madrid region" | Interprets viboseis seismic-reflection profiles to document the southwesterly extent of the Blytheville arch and the length (134 km [80 miles]) of a fault zone that coincides with the arch. |

## TABLE 2.1-3

## SUMMARY OF NEW INFORMATION FOR NEW MADRID SEISMIC ZONE

Seismic Hazards Report for the EGC ESP Site

| AUTHOR(S) (YEAR) | TITLE | SIGNIFICANCE |
|---|---|---|
| | | |
| **SEISMOGENIC FAULTS** | | |
| Harrison et al. (1999) | "An example of neotectonism in a continental interior—Thebes Gap, midcontinent, United States" | Documents evidence for four episodes of Quaternary faulting, two of which occurred during the Holocene. The overall style of neotectonic deformation is interpreted as right-lateral strike-slip faulting. |
| Mihills and Van Arsdale (1999) | "Late Wisconsin to Holocene deformation in the New Madrid seismic zone" | Interprets a structure contour map of the unconformity between the Eocene strata and overlying Quaternary Mississippi River alluvium as representing the Late Wisconsin to present strain field of the NMSZ. Areas of Holocene uplift include the Lake County uplift, Blytheville arch, and Crittenden fault. Areas of Holocene subsidence include Reelfoot Lake, historical Lake Obion, the Sunklands of northeast Arkansas, and possibly areas east and west of the Crittenden County fault. |
| Mueller et al. (1999) | "Fault slip rates in the modern New Madrid seismic zone" | Based on structural and geomorphic analysis of late Holocene sediments deformed by fault-related folding above the blind Reelfoot thrust fault, a slip rate of 6.1 ± 0.7 mm/yr is estimated for the past 2,300 ± 100 years. Using an alternative method based on the structural relief across the scarp and the estimated dip of the underlying blind thrust, a slip rate of 4.8 ± 0.2 mm/yr is calculated. Geometric relations suggest that the right-lateral slip rate on the New Madrid seismic zone is 1.8 to 2.0 mm/yr.<br>The onset of shortening across the Lake County uplift is estimated to be between 9.3 ka and 16.4 ka, with a preference for the younger age. |
| Van Arsdale et al. (1999) | "Southeastern extension of the Reelfoot fault" | This evaluation of microseismicity, seismic-reflection profile data, and geomorphic anomalies indicates that prehistoric and 1811-1812 coseismic uplift in the hanging wall of the Reelfoot fault has produced subtle surface warping that extends from Reelfoot Lake to Dyersburg, a total distance of 70 km (42 miles). |

## TABLE 2.1-3

## SUMMARY OF NEW INFORMATION FOR NEW MADRID SEISMIC ZONE

Seismic Hazards Report for the EGC ESP Site

| AUTHOR(S) (YEAR) | TITLE | SIGNIFICANCE |
|---|---|---|
| | | |
| **SEISMOGENIC FAULTS** | | |
| Van Arsdale (2000) | "Displacement history and slip rate on the Reelfoot fault of the New Madrid seismic zone" | Develops a displacement history and slip rates for the Reelfoot fault in the NMSZ from a seismic-reflection profile and trench data.<br>▪ Average slip rate estimates—seismic profile:<br>0.0009 mm/yr (past 80 Ma)<br>0.0007 mm/yr (Late Cretaceous)<br>0.002 mm/yr (Paleocene Midway Group)<br>0.001 mm/yr (Paleocene-Eocene Wilcox Form.)<br>0.0003 mm/yr (post-Wilcox/pre-Holocene)<br>1.8 mm/yr (Holocene )<br>▪ Average slip rate estimates—trench data<br>4.4 mm/yr (past 2,400 years based on 10 m of topographic relief and a fault dip of 73°)<br>6.2 mm/yr (maximum; estimated 5.4 m cumulative displacement for two events between AD 900 and AD 1812). |
| Champion et al. (2001) | 'Geometry, numerical models, and revised slip rate for the Reelfoot fault and trishear fault-propagation fold, New Madrid seismic zone" | Analysis of trench excavations, shallow borings, a digital elevation model of topography, and bathymetry shows that Reelfoot monocline is a forelimb on a fault-propagation fold that has accommodated relatively little shortening. Reelfoot fault is a reactivated Paleozoic structure. A late Holocene fault slip rate of 3.9 ± 0.1 mm/yr is based on 9 m of structural relief, the 2,290 ± 60 years BP age of folded sediment, and a 75° dip for the fault. The fault tip is 1,016 m beneath the surface. The thrust is flatter at deeper levels (5 to 14 km) based on the location of earthquake hypocenters (~ 40°SW for northern segment, ~ 35°W for central segment, ~ 45°SW for southern segment). |

## TABLE 2.1-3

## SUMMARY OF NEW INFORMATION FOR NEW MADRID SEISMIC ZONE

Seismic Hazards Report for the EGC ESP Site

| AUTHOR(S) (YEAR) | TITLE | SIGNIFICANCE |
|---|---|---|
| | | |
| **SEISMOGENIC FAULTS** | | |
| Mueller and Pujol (2001) | "Three-dimensional geometry of the Reelfoot blind thrust: Implications for moment release and earthquake magnitude in the New Madrid seismic zone" | Based on seismicity data and structural analysis, the Reelfoot blind thrust is a complex fault that changes in geometry along strike. The thrust is bound to the north by an east-trending strike-slip fault. The south end is defined by seismicity; it is not truncated by a known transverse fault. The north part of the thrust steepens to 75° to 80° at shallow depths (within the upper 4 km), forming a listric shape. The center of the central part of this thrust segment strikes N-S; the north and south segments strike between N10°W and N22°W, respectively. This segment dips between 31° and 35° W. The southeast fault segment is oriented N28°W and dips 48-51° SW. Available data suggest that the thrust flattens to <35° between about 2- and 4-km depth (possibly at the Precambrian basement-Paleozoic cover contact at about 3-km depth). (Magnitude estimates are discussed below in this table.) |
| Cox et al. (2001) | "Neotectonics of the southeastern Reelfoot rift zone margin, central United States, and implications for regional strain accommodation" | Suggests that the 90-miles (150-km)-long southeastern Reelfoot rift margin fault system may be accommodating significant northeastward transport as a right-lateral fault that is capable of producing earthquakes of $M \geq 7$. |
| Baldwin et al. (2002) | "Preliminary paleoseismic and geophysical investigation of the North Farrenburg lineament: Primary tectonic deformation associated with the New Madrid north fault?" | Presents geomorphic, geologic, seismic-reflection, trench, and microtextural data that strongly suggest that the North Farrenburg lineament, as well as the South Farrenburg lineament, may be the surface expression of an underlying tectonic fault that ruptured in the January 23, 1812, earthquake. Northeast-trending contemporary microseismicity beneath Sikeston Ridge and previously inferred New Madrid North fault locations aligns partly with the lineaments. |

## TABLE 2.1-3

## SUMMARY OF NEW INFORMATION FOR NEW MADRID SEISMIC ZONE

Seismic Hazards Report for the EGC ESP Site

| AUTHOR(S) (YEAR) | TITLE | SIGNIFICANCE |
|---|---|---|
| | | |
| **MAGNITUDE ESTIMATES** | | |
| Atkinson and Hanks (1995) | "A high-frequency magnitude scale" | Based on a high-frequency magnitude scale (m), the magnitude of the 1812 New Madrid event is estimated to be m 7.7 ± 0.3. |
| Johnston (1996) | "Seismic moment assessment of earthquakes in stable continental regions—III. New Madrid 1811-1812, Charleston 1886, and Lisbon 1755" | Estimates magnitudes for the 1811-1812 earthquake sequence based on intensity data. Estimated magnitudes for the three largest events are:<br>D1 (December 16, 1811): **M** 8.1 ± 0.3<br>J1 (January 23, 1812): **M** 7.8 ± 0.3<br>F1 (February 7, 1812): **M** 8.0 ± 0.3 |
| Johnston and Schweig (1996) | "The enigma of the New Madrid earthquakes of 1811-1812" | This review paper focuses on the 1811-1812 earthquakes, their geophysical setting, fault rupture scenarios, and magnitude estimates based on intensity data. Using historical accounts and geologic evidence, the three main 1811-1812 earthquakes are associated with specific structures. |
| Hough et al. (2000) | "On the Modified Mercalli intensities and magnitudes of the 1811-1812 New Madrid, central United States, earthquakes" | Re-interprets intensity data, obtaining maximum magnitude estimates from 7.0 to 7.5 for the main three events in the 1811-1812 earthquake sequence:<br>December 16, 1811: M 7.2-7.3<br>January 23, 1812: M 7.0<br>February 7, 1812: M 7.4-7.5 (thrust event) |
| Tuttle (2001a) | "The use of liquefaction features in paleoseismology: Lessons learned in the New Madrid seismic zone, central United States" | Uses two approaches:<br>Magnitude-bound—estimates minimum magnitude for AD 1450 and AD 900 events of M 6.7 and M 6.9, respectively, based on Ambraseys' (1988) relationship between M and epicentral distance to surface manifestations of liquefaction.<br>Energy stress—estimates M 7.5 to 8.3 from in situ geotechnical properties similar to M ≥7.6 from Ambraseys' relation for the largest 1811-1812 earthquakes. |

## TABLE 2.1-3

## SUMMARY OF NEW INFORMATION FOR NEW MADRID SEISMIC ZONE

Seismic Hazards Report for the EGC ESP Site

| AUTHOR(S) (YEAR) | TITLE | SIGNIFICANCE |
|---|---|---|
| | | |
| **MAGNITUDE ESTIMATES** | | |
| Mueller and Pujol (2001) | "Three-dimensional geometry of the Reelfoot blind thrust: implications for moment release and earthquake magnitude in the New Madrid seismic zone" | The area of the blind thrust (1,301 $km^2$), coupled with estimates of displacement in the February 7, 1812, event, is used to estimate values of $M_O$ from 6.8 x $10^{26}$ to 1.4 x $10^{27}$ dyne-cm, with preferred values between 6.8 x $10^{26}$ and 8.7 x $10^{26}$ dyne-cm. Computed $M_W$ for this event ranges from $M_W$ 7.2 to 7.4, with preferred values between $M_W$ 7.2 and 7.3. The moment magnitude for the AD 1450 event is computed as $M_W$ 7.3. |
| Tuttle et al. (2002) | "The earthquake potential of the New Madrid seismic zone" | The size, internal stratigraphy, and spatial distributions of prehistoric sand blows indicate that the AD 900 and AD 1450 earthquakes had source zones and magnitudes similar to those of the three largest shocks in the 1811-1812 sequence. |
| Bakun and Hooper (2003, in press) | "The 1811-12 New Madrid, Missouri, and the 1886 Charleston, South Carolina, earthquakes" | Using a new method for evaluating magnitude by directly inverting observations of intensities, the authors determine the following $M_I$ (intensity magnitudes):<br>$M_I$ 7.2 (**M** 6.8 to 7.5 at the 95% confidence level) for the December 16, 1811, event (NM1) that occurred in the NMSZ on the Bootheel lineament or on the Blytheville seismic zone<br>$M_I$ 7.1 (**M** 6.7 to 7.4 at the 95% confidence level) for the January 23, 1812, event (NM2) for a location on the New Madrid north zone of the NMSZ.<br>$M_I$ 7.4 (**M** 7.0 to 7.7 at the 95% confidence level) for the February 7, 1812, event (NM3) that occurred on the Reelfoot blind thrust of the NMSZ. |
| **RECURRENCE** | | |
| See Table 2.1-5 for a summary of age constraints on the timing of NMSZ earthquakes. | | |

## TABLE 2.1-3

## SUMMARY OF NEW INFORMATION FOR NEW MADRID SEISMIC ZONE

Seismic Hazards Report for the EGC ESP Site

| AUTHOR(S); YEAR | TITLE | SIGNIFICANCE |
|---|---|---|
| | | |
| **RECURRENCE** | | |
| Tuttle (2001a) | "The use of liquefaction features in paleoseismology: Lessons learned in the New Madrid seismic zone, central United States" | Major earthquakes occurred in the New Madrid region in:<br>AD 1450 ± 150 years<br>AD 900 ± 100 years<br>Consistent with other paleoliquefaction studies in the region and with studies of fault-related deformation along Reelfoot scarp (Kelson et al., 1996).<br>Evidence for earlier events, but age estimates and areas affected are poorly constrained.<br>Based on similarities in size and spatial distribution of paleoliquefaction features from these events and close spatial correlation to historical features, NMSZ was probable source of two earlier events. |
| Cramer (2001) | "A seismic hazard uncertainty analysis for the New Madrid seismic zone" | A 498-year mean recurrence interval is obtained based on a Monte Carlo sampling of 1,000 recurrence intervals and using the Tuttle and Schweig (2000) uncertainties as a range of permissible dates (± two standard deviations). From these results, the 68% confidence limits range from 267 to 725 years; the 95 % confidence limits range from 162 to 1,196 years (one and two standard deviation ranges, respectively). |
| Tuttle et al. (2002) | "The earthquake potential of the New Madrid seismic zone" | Recurrence—Based on studies of hundreds of earthquake-induced paleoliquefaction features at more than 250 sites, the fault system responsible for New Madrid seismicity generated very large earthquakes temporally clustered in AD 900±100 and AD 1450±150, years as well as 1811-1812. Given uncertainties in dating liquefaction features, the time between the past three events may be as short as 200 years or as long as 800 years, with an average of 500 years. Evidence suggests that prehistoric sand blows probably are compound structures, resulting from multiple earthquakes closely clustered in time, or earthquake sequences. |

## TABLE 2.1-3

## SUMMARY OF NEW INFORMATION FOR NEW MADRID SEISMIC ZONE

Seismic Hazards Report for the EGC ESP Site

| AUTHOR(S); YEAR | TITLE | SIGNIFICANCE |
|---|---|---|
| | | |
| **GEODETIC AND MODELING STUDIES** | | |
| Newman et al. (1999) | "Slow deformation and lower seismic hazard at the New Madrid seismic zone" | Recent geodetic measurements indicate that the rate of strain accumulation is less than the current detection threshold. Global positioning system (GPS) data show no significant differences in velocities on either side of the southern arm of the NMSZ. Near-field and intermediate-field (primarily hard-rock sites) yield measurements of 0.6 ± 3.2 and –0.9 ± 2.2 mm/yr, respectively. They are consistent with both 0 and 2 mm/yr at 2-sigma.<br>GPS data for the upper Mississippi embayment show that the interior of the Reelfoot rift is moving northeast relative to the North American plate. Modeling stable North America as a single rigid plate fits the site velocities, with a mean residual of 1.0 mm/yr.<br>The authors conclude that the present GPS data imply that 1811-1812-size earthquakes are either much smaller or far less frequent than previously assumed (i.e., smaller than M 8 [5 to 10 m slip/event], or longer than a recurrence interval of 400 to 600 years). |
| Kenner and Segall (2000) | "A mechanical model for intraplate earthquakes: Application to the New Madrid seismic zone" | Postulates a time-dependent model for the generation of repeated intraplate earthquakes in which seismic activity is driven by localized transfer of stress from a relaxing lower crustal weak body. Given transient perturbation to the stress field, the seismicity is also transient, but can have a significantly longer duration. This model suggests that interseismic strain rates computed between damaging slip events would not be geodetically detectable. |
| Grollimund and Zoback (2001) | "Did deglaciation trigger intraplate seismicity in the New Madrid seismic zone?" | Modeling of the removal of the Laurentide ice sheet ca. 20 ka changed the stress field in the vicinity of New Madrid and caused seismic strain to increase by about three orders of magnitude. The high rate of seismic energy release observed during late Holocene is likely to remain essentially unchanged for the next few thousand years. |

## TABLE 2.1-3

## SUMMARY OF NEW INFORMATION FOR NEW MADRID SEISMIC ZONE

Seismic Hazards Report for the EGC ESP Site

| AUTHOR(S); YEAR | TITLE | SIGNIFICANCE |
|---|---|---|
| | | |
| **SEISMIC SOURCE CHARACTERIZATION MODELS** | | |
| Cramer (2001) | "A seismic hazard uncertainty analysis for the New Madrid seismic zone" | Develops a logic tree of possible alternative parameters to characterize earthquake sources in the NMSZ. Source model alternatives include "fictional" faults from Frankel et al. (1996), actual faults (Bootheel lineament, eastern rift boundary, northeast arm, southwest arm, Reelfoot fault, west arm, and western rift boundary). |
| Frankel et al. (2002) | "Documentation for the 2002 update of the national seismic hazard maps" | Identifies three alternative fault sources: a fault trace matching recent microearthquake activity, and two adjacent sources situated near borders of the Reelfoot rift. The center fault is given twice the weight of the other two. Mean recurrence interval = 500 years:<br>**M** 7.3: (0.15 wt)<br>**M** 7.5: (0.20 wt)<br>**M** 7.7: (0.50 wt)<br>**M** 7.9: (0.15 wt) |
| Toro and Silva (2001) | "Scenario earthquakes for Saint Louis, MO, and Memphis, TN, and seismic hazard maps for the Central United States region including the effect of site conditions". | Develops alternative geometries for NMSZ. Uses fault sources identified by Johnston and Schweig (1996), augmented by alternative fault source model to the north (East Prairie extension), to represent more diffuse patterns of seismicity. Assumes that a large seismic-moment release in the region involves events on all three NMSZ faults occurring within a short interval. Occurrences of large earthquakes in the NMSZ are not independent in time. Uses mean recurrence intervals of 500 to 1,000 years. |

## TABLE 2.1-4

## CHARACTERISTIC MAGNITUDES FROM RUPTURE AREAS FOR FAULT SEGMENTS IN THE NMSZ[1]

Seismic Hazards Report for the EGC ESP Site

| Segment | Length | $W = 10$ | $W = 14$ | $W = 15$ | $W = 19$ | $W = 28$ | $W = 32$ |
|---|---|---|---|---|---|---|---|
| *Wells and Coppersmith (1994) magnitude-area relation (median)*: $M = 4.07 + 0.98 \log(\text{Area})$ | | | | | | | |
| Southwest arm | 117 | 7.1 | 7.2 | 7.3 | 7.4 | 7.5 | 7.6 |
| Reelfoot fault | 60 | 7.0 | 7.1 | 7.2 | 7.3 | 7.4 | 7.5 |
| Bootheel lineament | 70 | 6.9 | 7.0 | 7.0 | 7.1 | 7.3 | 7.4 |
| Northeast arm | 59 | 6.8 | 6.9 | 7.0 | 7.1 | 7.2 | 7.3 |
| West arm | 33 | 6.5 | 6.7 | 6.7 | 6.8 | 7.0 | 7.0 |
| East Rift Boundary | 99 | 7.0 | 7.1 | 7.2 | 7.3 | 7.4 | 7.5 |
| West Rift Boundary | 137 | 7.1 | 7.3 | 7.3 | 7.4 | 7.6 | 7.6 |
| Bootheel + southern SW arm | 133 | 7.1 | 7.3 | 7.3 | 7.4 | 7.6 | 7.6 |
| Remaining (northern) SW arm | 54 | 6.7 | 6.9 | 6.9 | 7.0 | 7.2 | 7.2 |
| Bootheel + NE arm | 129 | 7.1 | 7.3 | 7.3 | 7.4 | 7.6 | 7.6 |
| *Somerville and Saikia (2000) magnitude-area relation (median)*: $M = 4.35 + \log(\text{Area})$ | | | | | | | |
| Southwest arm | 117 | 7.4 | 7.6 | 7.6 | 7.7 | 7.9 | 7.9 |
| Reelfoot fault | 60 | 7.3 | 7.5 | 7.5 | 7.6 | 7.8 | 7.8 |
| Bootheel Lineament | 70 | 7.2 | 7.3 | 7.4 | 7.5 | 7.6 | 7.7 |
| Northeast arm | 59 | 7.1 | 7.3 | 7.3 | 7.4 | 7.6 | 7.6 |
| West arm | 33 | 6.9 | 7.0 | 7.0 | 7.1 | 7.3 | 7.4 |
| East Rift Boundary | 99 | 7.3 | 7.5 | 7.5 | 7.6 | 7.8 | 7.9 |
| West Rift Boundary | 137 | 7.5 | 7.6 | 7.7 | 7.8 | 7.9 | 8.0 |
| Bootheel + southern SW arm | 133 | 7.5 | 7.6 | 7.6 | 7.8 | 7.9 | 8.0 |
| remaining (northern) SW arm | 54 | 7.1 | 7.2 | 7.3 | 7.4 | 7.5 | 7.6 |
| Bootheel + NE arm | 129 | 7.5 | 7.6 | 7.6 | 7.7 | 7.9 | 8.0 |

from Crone et al., 2001.

1 Rupture lengths and widths (W) in kilometers. Length uncertainty not included; weighting on magnitudes used in the uncertainty analysis are evenly distributed among widths and magnitude-area relations.

**TABLE 2.1-5**

**SUMMARY OF AGE CONSTRAINTS FOR NEW MADRID SEISMIC ZONE EARTHQUAKES**

Seismic Hazards Report for the ECG ESP Site

| Name of Site | Lab Sample Number[1] | Material | Time Relationship of Sample to Liquefaction | $^{14}C$ Age, years BP ± 1-sigma | Calibrated Age 2-sigma (95% Probability)[2] | Age Estimate Based on Ceramics and Points | Maximum Age Range (published correlation, comments) | Estimated Event Correlation | Reference |
|---|---|---|---|---|---|---|---|---|---|
| Amanda | Beta-133004 (T1-C2) | Charcoal | Preliquefaction (event 2) | 100 ± 40 | AD 1680 to 1780<br>*AD 1800 to 1940*<br>*AD 1950 to 1955* | NA | Event in trench T2, followed by event in trench T1, occurred during or soon after AD 1000 to 1400 (Middle Mississippian) | Two events:<br>1811-1812<br>and<br>event Y,<br>1450 ± 150 yr. | Tuttle et al. (2000) |
| | Beta-133006 (T2-C14) | Charcoal (top of lower sand blow) | Preliquefaction (event 2)<br>Postliquefaction (event 1) | 240 ± 50 | AD 1520 to 1590<br>AD 1620 to 1690<br>*AD 1740 to 1810*<br>*AD 1930 to 1950* | NA | | | |
| | Beta-133005 (T2-C13) | Charcoal (19 cm below sand blow) | Preliquefaction (event 1) | 920 ± 40 | AD 1020 to 1210 | NA | | | |
| | | Artifacts on surface and within plow zone | Reworked | NA | NA | Presence of Mississippian archeological site | | | |
| | | Artifacts, including diagnostic ceramics | Preliquefaction (event 1) | NA | NA | AD 800 to 1400<br>(Early and Middle Mississippian) | | | |
| | Beta-171216 (FSN27) | Nutshell | Preliquefaction (event 1) | 470 ± 40 | AD 1410 to 1470 | NA | Close maximum age | Confirms correlation of event 1 to event Y:<br>1450 ± 150 yr. | Tuttle and Wolf (2003) |
| | | Ceramics | Preliquefaction (event 1) | NA | NA | AD 800 to 1400 (Early and Middle Mississippian: from 4 to 15 cm below sand blow; depth of artifacts suggests ~ 300 years passed between last occupation and event 1) | | | |
| Archway | Beta-166245 (C1) | Charcoal | Postliquefaction | 200 ± 40 | AD 1640 to 1690<br>AD 1730 to 1810<br>AD 1920 to 1950 | NA | | Event X<br>900 ± 100 yr. | Tuttle and Wolf (2003) |
| | Beta-166246 (C5) | Charcoal | Anomalous result unless root grew into horizon from above | 920 ± 40 | AD 1020 to 1210 | NA | | | |
| | Beta-171219 (FSN6) | Hickory nutshell collected 0-10 cm below sand blow | Preliquefaction | 1310 ± 40 | AD 660 to 780 | NA | Sand blow formed ≤ 200 yr. after this time | | |
| | | Ceramics | Preliquefaction | NA | NA | AD 400 to 800, Middle to Late Woodland | Sand blow directly above cultural horizon | | |
| Brooke | Beta-102497 | Soil | Preliquefaction | 1960 ± 40 | 40 BC to AD 130 | NA | Unweathered sand blow, 15 to 20 cm thick; A horizon developed post-occupation and preliquefaction | AD 1811 to 1812 | Tuttle (1999) |
| | Beta-102498 | Charcoal collected 45 cm below sand blow; artifacts from B horizon more than 15 cm below sand blow | Preliquefaction | 370 ± 50 | AD 144 to 1650 | AD 140 to 1670<br>Late Mississippian | | | |

**TABLE 2.1-5**

**SUMMARY OF AGE CONSTRAINTS FOR NEW MADRID SEISMIC ZONE EARTHQUAKES**

Seismic Hazards Report for the ECG ESP Site

| Name of Site | Lab Sample Number[1] | Material | Time Relationship of Sample to Liquefaction | $^{14}C$ Age, years BP ± 1-sigma | Calibrated Age 2-sigma (95% Probability)[2] | Age Estimate Based on Ceramics and Points | Maximum Age Range (published correlation, comments) | Estimated Event Correlation | Reference |
|---|---|---|---|---|---|---|---|---|---|
| Bugg | Beta-108883 | Charcoal | Postliquefaction | 130 ± 40 | AD 167 to 1950 | AD 80 to 1000<br>Early Mississippian | AD 800 to 1000; sand blow deposited directly on cultural horizon; thickness of plow zone plus remnant A horizon below (50 cm) suggest sand blow formed ~ 1000 yr. ago | Event X<br>900 ± 100 yr. | Tuttle (1999) |
| | NA | Ceramics | Preliquefaction | NA | NA | AD 40 to 1000<br>Late Woodland-Early Mississippian | | | |
| Burkett | Beta-142708<br>(TR6-C100) | Charcoal | Preliquefaction (event 4) | 110 ± 40 | AD 167 to 1780<br>AD 180 to 1955 | NA | Event 4 | 1811-1812 or<br>1895 Charleston | Tuttle (2001)<br><br>Tuttle (M. Tuttle and Associates, electronic commun. to Kathryn Hanson, February 27, 2003). |
| | TR-6 | Artifacts-Burkett phase | Preliquefaction (event 3) | NA | NA | ~ 400 BC to AD 330<br><br>Early-Middle Woodland (radiocarbon dating of horizon by Prentice Thomas) | Event 3 probably occurred at end of Burkett phase (AD 300 ± 200 yr.) | Event W<br>AD 300 ± 200 yr.<br><br>May be same event as older Towosaghy S1 event | |
| | TU-56 | Artifacts—Mississippian and Burkett phase artifacts? | Postliquefaction (event 3) | NA | NA | Woodland-Mississippian | Event 3 probably occurred toward end of Burkett phase (AD 300 ± 200 yr.) | Event W<br>AD 300 ± 200 yr.<br><br>May be same event as older Towosaghy S1 event | |
| | TU-56 | Artifacts—Burkett phase | Preliquefaction (event 3) and postliquefaction (events 1 and 2) | NA | NA | ~400 BC to AD 330<br><br>Early-Middle Woodland (radiocarbon dating of horizon by Prentice Thomas) | TU56-events 1 and 2 occurred after deposition of O'Bryan Ridge-phase artifacts and before deposition of Burkett-phase artifacts | Event U?<br>2350 BC<br>± 200 yr.<br><br>Perhaps same as event 1 at Eaker 2 | |
| | TU-56 | Artifacts—O'Bryan Ridge phase | Preliquefaction (events 1 and 2) | NA | NA | Late Archaic (3000 to 400 BC) | TR5—events 1 and 2 occurred during Late Archaic shortly after BC 2580; event 3 occurred during or soon after Burkett phase<br><br>BL7—event 1 occurred after 2340 to 2190 BC; event 2 occurred after 2570 to 2990 BC. | TR-5: event U?<br>2350 BC<br>± 200 yr.<br><br>Perhaps same as event 1 at Eaker 2<br><br>BL7—event U? included two earthquakes large enough to induce liquefaction;<br>2350 BC<br>± 200 yr.<br><br>Perhaps same as event 1 at Eaker 2 | |
| | Beta-142448<br>(TR5-C9) | Charcoal | Postliquefaction (event 3) | 70 ± 40 | AD 1680 to 1740<br>AD 1810 to 1930<br>AD 1950 to 1955 | NA | | | |
| | TR5 | Artifacts——Burkett phase | Preliquefaction<br>(event 3) | NA | NA | ~400 BC to AD 330<br>Early-Middle Woodland (radiocarbon dating of horizon by Prentice Thomas) | | | |
| | Beta-142447<br>(TR5-C5) | Charcoal and artifacts—O'Bryan Ridge phase | Preliquefaction<br>(events 1 and 2) | 3980 ± 40 | BC 2580 to 2430;<br>close maximum (event 1) | Late Archaic (3000 to 400 BC) | | | |
| | Beta-142445<br>(BW1-C2) | Charcoal from midden adjacent to mound | Reworked by natives; probably preliquefaction (events 1 and 2) | 4090 ± 40 | BC 2870 to 2800<br>BC 2760 to 2560<br>BC 2540 to 2490 | NA | | | |
| | Beta-153985<br>(BW1-C4) | Charcoal from midden adjacent to mound | Reworked by aboriginals; probably preliquefaction (events 1 and 2) | 4090 ± 40 | BC 2870 to 2800<br>BC 2760 to 2560<br>BC 2540 to 2490 | NA | | | |

**TABLE 2.1-5**

**SUMMARY OF AGE CONSTRAINTS FOR NEW MADRID SEISMIC ZONE EARTHQUAKES**

Seismic Hazards Report for the ECG ESP Site

| Name of Site | Lab Sample Number[1] | Material | Time Relationship of Sample to Liquefaction | $^{14}C$ Age, years BP ± 1-sigma | Calibrated Age 2-sigma (95% Probability)[2] | Age Estimate Based on Ceramics and Points | Maximum Age Range (published correlation, comments) | Estimated Event Correlation | Reference |
|---|---|---|---|---|---|---|---|---|---|
| Burkett (continued) | Beta-153985 (BW1-C3) | Charcoal from contact between clay of mound and soil horizon below | Postliquefaction (event 1); preliquefaction (event 2) | 3940 ± 50 | BC 2570 to 2290; Contemporaneous | NA | | | |
| | Beta-142706 (BW1-C6) | Charcoal from soil horizon below sand blows of events 1 and 2 and within graben structure | Preliquefaction (events 1 and 2) | 3970 ± 40 | BC 2580 to 2400<br>BC 2380 to 2360 | NA | | | |
| | Beta-142446 (BW2-C7) | Charcoal from soil horizon below lower sand blow | Preliquefaction (events 1 and 2) | 3820 ± 30 | BC 2340 to 2190<br>BC 2170 to 2150; Close maximum | NA | | | |
| | Beta-142707 (BW2-C8) | Charcoal from clay used to construct base of mound | Probably reworked by aboriginals; preliquefaction (event 1) | 4300 ± 40 | BC 3010 to 2980<br>BC 2940 to 2880 | NA | | | |
| Cagle Lake | Beta-160377 (F101) | Wood from aboriginal post mold in top of sand blow | Postliquefaction | 240 ± 60 | AD 1500 to 1690<br>*AD 1730* to *-1810*<br>*AD 1920* to *1950;* Close minimum | Site occupied by aboriginals following formation of sand blow | AD 1420 to 1690—prehistoric compound sand blow; exclude minimum constraining dates post-AD 1700 | Event Y 1450 ± 150 yr. | Tuttle and Wolf (2003) |
| | Beta-166251 (C106) | Charcoal from aboriginal post mold in top of sand blow | Postliquefaction | 170 ± 40 | AD 1650 to 1890 *AD 1910* to *1950* | Site occupied by aboriginals following formation of sand blow | | | |
| | Beta-171217 (FSN116) | Hickory nutshell collected 0 to 5 cm below sand blow | Preliquefaction | 440 ± 40 | AD 1420 to 1500; Close maximum | NA | | | |
| | Beta-166250 (C104) | Charcoal collected 5 to 15 cm below sand blow | Preliquefaction | 580 ± 40 | AD 1300 to 1420 | NA | | | |
| | Beta-166249 (C100) | Charcoal collected 47 cm below sand blow | Preliquefaction | 460 ± 40 | AD 1410 to 1480 | NA | | | |
| | | | Preliquefaction | NA | NA | ~AD 1400 to 1500<br>Late Mississippian; occupied at time of sand blow | | | |
| Central Ditch 1 | Beta-108869 | Charcoal | Postliquefaction | 70 ± 40 | AD 1690 to 1740<br>AD 1810 to 1930 | NA | AD 800 to 1000<br>Radiocarbon dating—sand blow formed from AD 790 to 1240; Early Mississippian | Event X 900 ± 100 yr. | Tuttle (1999) |

**TABLE 2.1-5**

**SUMMARY OF AGE CONSTRAINTS FOR NEW MADRID SEISMIC ZONE EARTHQUAKES**

Seismic Hazards Report for the ECG ESP Site

| Name of Site | Lab Sample Number[1] | Material | Time Relationship of Sample to Liquefaction | $^{14}$C Age, years BP ± 1-sigma | Calibrated Age 2-sigma (95% Probability)[2] | Age Estimate Based on Ceramics and Points | Maximum Age Range (published correlation, comments) | Estimated Event Correlation | Reference |
|---|---|---|---|---|---|---|---|---|---|
| Central Ditch 1 (continued) | Beta-81308 | Soil (30 cm thick, with few small artifacts possibly reworked) | Postliquefaction | 940 ± 60 | AD 1000 to 1240 | AD 400 to 1000<br>Late Woodland | and Late Woodland artifacts in horizon immediately below—sand blow formed from AD 800 to 1000; A horizon developed in sand blow suggests it formed ≥ 600 yr. ago | | |
| | Beta-81309 | Soil;<br>artifacts | Preliquefaction | 1120 ± 60 | AD 790 to 1020 | AD 400 to 1000<br>Late Woodland-Early Mississippian | | | |
| C1-Cooter | Beta-74678 | Organic material | Postliquefaction | 110 ± 60 | AD 1660 to 1950 | NA | AD 1410-1811;<br>Event pre-dates 1811 based on soil development above sand blow, weathering characteristics of sand blow, and liquefaction of sand blow by subsequent event, probably 1811-1812 | Probably correlates with event Y<br>1450 ± 150 yr. | Craven (1995) |
| | Beta-74099 | Thatch from aboriginal dwelling | Preliquefaction | 440 ± 50 | AD 1410 to 1520<br>AD 1570 to 1630 | NA | AD 1400 to 1650; sand blow deposited directly on occupation horizon; dating of thatch and artifacts provides close maximum | | |
| | | Artifacts—Parkin Punctate | Preliquefaction | NA | NA | AD 1400 to 1670<br>Late Mississippian | | | |
| Current River 2 | Beta-110225 | Charcoal | Postliquefaction | 570 ± 60 | AD 1300 to 1450 | NA | AD 1310 to 1450 | Event Y<br>1450 ± 150 yr. | Tuttle (1999) |
| | Beta-110223 | Cypress knees | Preliquefaction | 510 ± 60 | AD 1310 to 1360<br>AD 1390-1480 | NA | | | |
| | Beta-110224 | Charcoal | Preliquefaction | 640 ± 90 | AD 1240 to 1440 | NA | | | |
| Current River 8 | Beta-110227 | Root | Postliquefaction | Modern | | NA | 2 to 4 earthquakes, 3490 BC to AD 1670; weathering characteristics of upper 30 to 50 cm of dikes suggest that they are prehistoric | | Tuttle (1999) |
| | Beta-110226 | Plant material | Preliquefaction<br>(2 to 4 subsequent events) | 4560 ± 50 | 3490 to 3470 BC<br>3380 to 3090 BC | NA | | | |
| Dillahunty | Beta-166247 (C4) | Charcoal | Postliquefaction | 70 ± 70 | Modern | NA | AD 910 to 1490<br>Compound sand blow (3 major units); events closely spaced in time; prehistoric based on soil development; C5 provides close minimum, whereas FSN4 and artifacts only provide maximum | Event Y<br>(1450 ± 150 yr.) | Tuttle and Wolf (2003) |
| | Beta-166248 (C5) | Charcoal from base of soil developed in sand-blow crater | Postliquefaction | 470 ± 50 | AD 1400 to 1490; close minimum | NA | | | |
| | Beta-171218 (FSN4) | Maize kernel fragment from 0 to 10 cm below sand blow | Preliquefaction | 980 ± 70 | AD 910 to 920<br>AD 960 to 1210 | NA | | | |
| | | Ceramics 10 to 20 cm below sand blow | Preliquefaction | NA | NA | Middle Woodland ~ (200 BC to AD 400); soil development suggests at least 200 years between occupation and deposition of sand blow | | | |

**TABLE 2.1-5**

**SUMMARY OF AGE CONSTRAINTS FOR NEW MADRID SEISMIC ZONE EARTHQUAKES**

Seismic Hazards Report for the ECG ESP Site

| Name of Site | Lab Sample Number[1] | Material | Time Relationship of Sample to Liquefaction | $^{14}C$ Age, years BP ± 1-sigma | Calibrated Age 2-sigma (95% Probability)[2] | Age Estimate Based on Ceramics and Points | Maximum Age Range (published correlation, comments) | Estimated Event Correlation | Reference |
|---|---|---|---|---|---|---|---|---|---|
| Dodd | Beta-102503 | Charcoal | Postliquefaction | 110 ± 50 | AD 1670 to 1950 | 1400 to 1670<br>Late Mississippian—during this period | AD 1290 to 1460 from dating;<br>AD 1400 to 1670 from archeology;<br>AD 1400 to 1460 combining the two | Event Y<br>(1450 ± 150 yr.) | Tuttle (1999)<br>Tuttle et al. (1999b)<br>Tuttle and Schweig (2000) |
| | Beta-119103 | Charcoal; artifacts | Postliquefaction | 120 ± 50 | AD 167 to 1950 | 1400 to 1670<br>Late Mississippian | | | |
| | Beta-142449 | Charred corn kernel from aboriginal wall trench dug into sand blow | Postliquefaction | 490 ± 40 | AD 1410 to 1460;<br>close minimum | | | | |
| | Beta-119102 | Charcoal | Preliquefaction | 630 ± 40 | AD 1290 to 1410;<br>close maximum | 1000 to 1670<br>Middle-Late Mississippian | | | |
| | Beta-102502 | Charcoal | Preliquefaction | 770 ± 40 | AD 1220 to 1300 | 1000 to 1670<br>Middle-Late Mississippian | | | |
| Eaker 1 | Beta-91511 | Charcoal<br>(vertical root) | Postliquefaction | 50 ± 50 | AD 1690 to 1740<br>AD 1810 to 1930 | NA | Either AD 1180 to 1630 or AD 1410 to 1650; soil development (including lamellae) above sand blow suggests it is prehistoric; liquefaction of sand blow suggests subsequent event, probably 1811-1812 | Event Y<br>(1450 ± 150 yr.) | Tuttle (1999) |
| | Beta-75326 | Charcoal | Postliquefaction | 170 ± 60 | AD 1650 to 1950 | NA | | | |
| | Beta-75325 | Plant material<br>(lateral root) | If preliquefaction, close maximum; if postliquefaction, close minimum | 450 ± 60 | AD 1410 to 1530<br>AD 1560 to 1630 | NA | | | |
| | Beta-81313 | Soil; ceramics | Preliquefaction | 740 ± 70 | AD 1180 to 1400 | 400 to 1000<br>Middle-Late Woodland | | | |
| Eaker 2 | NA | Ceramics | Postliquefaction (event IV) | NA | NA | 800 to 1000<br>Late Woodland-Early Mississippian | AD 470 to 1310—event IV;<br>site occupied before and after event | Event X<br>(900 ± 100 yr.) | Tuttle (1999) |
| | Beta-86810 | Charcoal | Postliquefaction (event IV) | 460 ± 60 | AD 1400 to 1520<br>AD 157 to 1630 | NA | | | |
| | Beta-86811 | Charcoal | Postliquefaction (event IV) | 510 ± 60 | AD 1310 to 1360<br>AD 1390 to 1480 | NA | | | |
| | Beta-77450 | Charcoal | Postliquefaction (event IV) | 660 ± 60 | AD 1270 to 1420 | NA | | | |
| | Beta-86190 | Soil | Postliquefaction (event IV) | 770 ± 60 | AD 1180-1310 | NA | | | |
| | Beta-86816 | Soil and ceramics | Preliquefaction (event IV) | 1420 ± 80 | AD 470 to 480<br>AD 520 to 780 | AD 400 to 1000<br>Late Woodland | | | |
| | Beta-86816 | Soil and ceramics | Postliquefaction (event III) | 1420 ± 80 | AD 470 to 480<br>AD 520 to 780 | AD 400 to 1000<br>Late Woodland | 800 BC to AD 780<br>Event III | Event W ?<br>AD 300 ± 200 yr. | Tuttle (1999) |

**TABLE 2.1-5**

**SUMMARY OF AGE CONSTRAINTS FOR NEW MADRID SEISMIC ZONE EARTHQUAKES**

Seismic Hazards Report for the ECG ESP Site

| Name of Site | Lab Sample Number[1] | Material | Time Relationship of Sample to Liquefaction | $^{14}C$ Age, years BP ± 1-sigma | Calibrated Age 2-sigma (95% Probability)[2] | Age Estimate Based on Ceramics and Points | Maximum Age Range (published correlation, comments) | Estimated Event Correlation | Reference |
|---|---|---|---|---|---|---|---|---|---|
| Eaker 2 (Continued) | Beta-86814 | Soil | Preliquefaction (event III) | 2410 ± 90 | 800 to 360 BC<br>290 to 230 BC | NA | | | |
| | Beta-86814 | Soil | Postliquefaction (event II) | 2410 ± 90 | 800 to 360 BC<br>290 to 230 BC | NA | 1430 to 800 BC<br>Event II | Event V? | Tuttle (1999) |
| | Beta-81311 | Soil | Preliquefaction (event II) | 2970 ± 100 | 1430 to 910 BC | NA | | | |
| | Beta-86815 | Soil | Preliquefaction (event II) | 3020 ± 80 | 1430 to 910 BC | NA | | | |
| | Beta-86812 | Soil | Preliquefaction (event II) | 3200 ± 100 | 1690 to 1250 BC | NA | | | |
| | Beta-86812 | Soil | Postliquefaction (event I) | 3200 ± 100 | 1690 to 1250 BC | NA | 3340 to 1250 BC<br>Event 1 | Event U ?<br>May correlate with events 1 and 2 at Burkett site | Tuttle (1999) |
| | Beta-86813 | Soil | Preliquefaction (event I) | 4180 ± 190 | 3340 to 2210 BC | NA | | | |
| Eaker 3 | Beta-69618 | Charcoal and artifacts | Postliquefaction | 300 ± 60 | AD 1460 to 1680<br>AD 1770 to 1800<br>AD 1940 to 1960 | AD 1000 to 1400<br>Middle Mississippian | AD 800 to 1400<br>(Evidence for two events probably during same earthquake sequence) | Event X<br>900 ± 100 yr. | Tuttle (1999) |
| | NA | Ceramics | Preliquefaction | NA | NA | 800 to 1000<br>Late Woodland-Early Mississippian | | | |
| Haynes | G-19080 | Charcoal | Postliquefaction | 455 ± 110 | AD 1300 to 1660 | AD 1000 to 1400<br>Middle Mississippian | AD 800 to 1400 | Event X<br>900 ± 100 yr. | Tuttle (1999)<br>Tuttle et al. (2000) |
| | NA | Ceramics | Preliquefaction | NA | NA | AD 800 to 1000<br>Early Mississippian | | | |
| Hillhouse | Beta-102500 | Charcoal and ceramics | Postliquefaction | 1150 ± 50 | AD 780 to 1000 | AD 400 to 1000<br>Late Woodland | AD 790 to 1000 | Event X<br>900 ± 100 yr. | Tuttle (1999) |
| | Beta-102499 | Charcoal | Preliquefaction | 1140 ± 50 | AD 790 to 1010 | NA | | | |
| | Beta-102501 | Soil | Preliquefaction | 4880 ± 60 | 3780 to 3620 BC<br>3580 to 3530 BC | AD 400 to 1000<br>Late Woodland | | | |
| Hueys | Beta-91642 | Charcoal (hearth) and ceramics | Postliquefaction | 280 ± 60 | AD 1470 to 1680<br>*AD 1750* to *1810*<br>*AD 1940* to *1950* | AD 800 to 1000<br>Late Woodland-Early Mississippian | AD 880 to 1000 | Event X<br>900 ± 100 yr. | Tuttle (1999) |
| | Beta-108939 | Charcoal (maize) | Postliquefaction | 630 ± 50 | AD 1290 to 1420 | AD 800 to 1000<br>Late Woodland-Early Mississippian | | | |
| | Beta-91641 | Charcoal and artifacts | Preliquefaction | 1090 ± 50 | AD 880 to 1030 | AD 800 to 1000<br>Late Woodland-Early Mississippian | | | |
| | Beta-91643 | Charcoal | Preliquefaction | 1280 ± 60 | AD 650 to 890 | NA | | | |

**TABLE 2.1-5**

**SUMMARY OF AGE CONSTRAINTS FOR NEW MADRID SEISMIC ZONE EARTHQUAKES**

Seismic Hazards Report for the ECG ESP Site

| Name of Site | Lab Sample Number[1] | Material | Time Relationship of Sample to Liquefaction | $^{14}C$ Age, years BP ± 1-sigma | Calibrated Age 2-sigma (95% Probability)[2] | Age Estimate Based on Ceramics and Points | Maximum Age Range (published correlation, comments) | Estimated Event Correlation | Reference |
|---|---|---|---|---|---|---|---|---|---|
| Johnson 5 | Beta-102504 | Charcoal | Postliquefaction | 220 ± 50 | AD 1540 to 1550<br>AD 1640 to 1700<br>AD 1720 to 1820<br>AD 1855 to 1860<br>AD 1920 to 1950 | | AD 770 to 1670<br>Minimum age not well constrained; probably formed during Late Woodland-Early Mississippian. Soil development suggests sand blow formed prior to 1811 and was exposed at the surface for at least 670 years | Event X<br>900 ± 100 yr. | Tuttle (1999) |
| | Beta-102505 | Soil | Preliquefaction | 1110 ± 80 | AD 770 to 1040 | AD 800 to 1000<br>Late Woodland-Early Mississippian | | | |
| K1<br>Champey Pocket | | | | | | | Event Z—AD 1812<br>Unweathered liquefaction features | AD 1812 | Kelson et al. (1992 and 1996) |
| | Beta-49608 | Charcoal | Post-monoclinal folding; colluvium | - | AD 1430 to 1650 | NA | Event Y<br>AD 1220 to 1650; ~AD 1400 | Event Y<br>(1450 ± 150 yr.) | |
| | Beta-49609 | Charcoal | Pre-monoclinal folding | - | AD 1220 to 1390 | NA | | | |
| | Beta-48553 | Charcoal; artifacts | Postliquefaction | - | AD 430 to 890 | AD 800 to 1000<br>Close minimum (third most recent event) | Event X<br>AD 780 to 1000 | Event X<br>900 ± 100 yr. | |
| K2<br>Proctor City | | | | | | | Event Z—AD 1812: Sand dikes and sand blow with no soil development | 1812 | Kelson et al. (1996) |
| | | | Post-scarp formation and re-development of graben (event Y) | | | | Event Y—AD 1260 to 1650<br>Poorly constrained; couple hundred years prior to 1812 to erode scarp | Event Y<br>(1450 ± 150 yr.) | |
| | CAMS-13559 | Charcoal | Pre-scarp formation and re-development of graben (event Y) | 660 ± 60 | AD 1260 to 1410 | NA | Event post-dates AD 1260 | | |
| | CAMS-13540 | Charcoal | Post-graben formation (event X) | 960 ± 60 | AD 980 to 1220 | NA | Event X<br>AD 780 to 1000; close minimum | Event X<br>900 ± 100 yr. | |
| | CAMS-13538 | Charcoal | Pre-graben formation (? younger) (event X) | 990 ± 60 | AD 900 to 1210 | NA | | | |

**TABLE 2.1-5**

**SUMMARY OF AGE CONSTRAINTS FOR NEW MADRID SEISMIC ZONE EARTHQUAKES**

Seismic Hazards Report for the ECG ESP Site

| Name of Site | Lab Sample Number[1] | Material | Time Relationship of Sample to Liquefaction | $^{14}C$ Age, years BP ± 1-sigma | Calibrated Age 2-sigma (95% Probability)[2] | Age Estimate Based on Ceramics and Points | Maximum Age Range (published correlation, comments) | Estimated Event Correlation | Reference |
|---|---|---|---|---|---|---|---|---|---|
| K2 (Continued) | CAMS-13537 | Charcoal | Pre-graben formation (event X) | 1110 ± 60 | AD 780 to 1030 | NA | Close maximum | | |
| Kochtitzky Ditch 1 | Beta-97573 | Charcoal | Postliquefaction | 2020 ± 60 | BC 180 to AD 110 (reworked?) | AD 800 to 1670 Mississippian | AD 990 to 1660 Event occurred during occupation of site, probably during Late Mississippian | Event Y (1450 ± 150 yr.) | Tuttle (1999) |
| | Beta-102512 | Charcoal | Postliquefaction | 360 ± 50 | AD 1440 to 1660 | AD 800 to 1670 Mississippian | | | |
| | Beta-97574 Artifacts | Charcoal | Preliquefaction | 960 ± 60 | AD 990 to 1220 | AD 800-1000 Mississippian; elsewhere at site this horizon contains Middle-Mississippian (AD 1000 to 1400) artifacts and Late-Mississippian house floor (AD 1400 to 1670) | | | |
| Lowrance | Beta-133011 | Charcoal 43 cm below sand blow | Preliquefaction | 330 ± 50 | AD 1450 to 1660 | NA | Probably 1811-1812 | 1811-1812 | Tuttle et al. (2000) |
| L1 (Site WY) | Beta-74810 | Charcoal | Postliquefaction | 480 ± 60 | AD 1400 to 1620 | NA | AD 55 to 1620 | Could correlate to event W (AD 300 ± 200 yr.), event X (900 ± 100 yr.), or event Y (1450 ± 150 yr.) | Li et al. (1998) |
| | Beta-92884 (S) | Dispersed carbon | Preliquefaction | 2060 ± 60 | 195 BC to AD 75 | NA | | | |
| | Beta-92883 (C2) | Charcoal | Preliquefaction | 1850 ± 60 | AD 55 to 340 | NA | | | |
| L2 (Site WD) | Beta-71233 (S) | Twig | Preliquefactions (event 2) Postliquefaction (event 1) | 240 ± 60 | AD 1510 to 1950 | NA | Two sand blows, 1811-1812 and 900 ± 100 yr. Lower sand blow exposed at surface ~ 800 ± 100 yr. prior to burial by younger sand blow | 1811-1812 (event 2) Event X 900 ± 100 yr. (event 1) | Li et al. (1998) |
| | Beta-71234 | Soil (dispersed carbon) | Postliquefaction (event 1) | 1140 ± 60 | AD 770 to 1040 | NA | | | |
| Main 8 | GX-17728 | Wood | Preliquefaction | 4930 ± 160 | BC 4035 to 3360 | NA | Three generations of liquefaction features formed since BC 4040 | | Tuttle (1993) |
| New Franklin 3 | Beta-84975 | Charcoal | Postliquefaction | 210 ± 60 | AD 1530 to 1560 AD 1630 to 1950 | NA | 180 BC to AD 990 | Event X 900 ± 100 yr. | Tuttle (1999) |
| | Beta-97577 | Soil | Postliquefaction | 1030 ± 60 | AD 890 to 1170 | NA | | | |
| | Beta-97578 | Soil | Postliquefaction | 1110 ± 50 | AD 860 to 1020 | NA | | | |
| | Beta-86191 | Soil | Postliquefaction | 1200 ± 60 | AD 690 to 990 | NA | | | |
| | Beta-97579 | Soil | Preliquefaction | 2000 ± 70 | 180 BC to AD 150 | NA | | | |
| | Beta-84976 | Soil | Preliquefaction | 2050 ± 60 | 190 BC to AD 90 | NA | | | |

**TABLE 2.1-5**

**SUMMARY OF AGE CONSTRAINTS FOR NEW MADRID SEISMIC ZONE EARTHQUAKES**

Seismic Hazards Report for the ECG ESP Site

| Name of Site | Lab Sample Number[1] | Material | Time Relationship of Sample to Liquefaction | $^{14}C$ Age, years BP ± 1-sigma | Calibrated Age 2-sigma (95% Probability)[2] | Age Estimate Based on Ceramics and Points | Maximum Age Range (published correlation, comments) | Estimated Event Correlation | Reference |
|---|---|---|---|---|---|---|---|---|---|
| Nodena | Beta-133012 (T1-C1) | Charcoal | Preliquefaction (<1 cm below) | 290 ± 50 | AD 1470 to 1670<br>*AD 1780* to *1800* | NA | Two events in the same earthquake sequence<br>AD 1450-1670 | Event Y<br>(1450 ± 150 yr.) | Tuttle et al. (2000) |
| | Beta-133013 (T1-C4) | Charcoal | Preliquefaction (45 cm below) | 280 ± 50 | AD 1480 to 1680<br>*AD 1780* to *1800*<br>*AD 1940* to *1950* | NA | | | |
| | Beta-133014 (T2-C1) | Charcoal (root cast into sand blow) | Postliquefaction | 230 ± 50 | AD 1520 to 1580<br>AD 1630 to 1690<br>AD 1730 to 1810<br>AD 1930 to 1950 | NA | | | |
| | Beta-133015 (T2-C20) | Charcoal | Preliquefaction (9 cm below) | 350 ± 40 | AD 1450 to 1650 | NA | | | |
| | Beta-133016 (T2-C101) | Charcoal | Preliquefaction (3 cm below) | 340 ± 30 | AD 1460 to 1650 | NA | | | |
| | | Ceramics | Postliquefaction | NA | NA | AD 1000 to 1700 | | | |
| | | Artifacts | Preliquefaction | NA | NA | AD 1400 to 1700 | | | |
| Obion 200 | Beta-146738 | Wood W2 collected from silt deposit above sand blow | Postliquefaction | 230 ± 40 | AD 1530 to 1550<br>AD 1640 to 1680<br>*AD 1740 to 1810*<br>*AD 1930 to 1950* | NA | Before AD 1810 and After AD 1300<br>(based on probability distribution) | Event Y<br>(1450 ± 150 yr.) | Tuttle (2001) |
| | Beta-146737 | Wood W1 collected within 1 cm of base of sand blow | Preliquefaction | 590 ± 40 | Close maximum<br>AD 1300 to 1420 | NA | | | |
| Obion 216 | Beta-152008 | Wood (W2 from outer 1 cm of horizontally bedded log buried by sand blow) | Preliquefaction | 800 ± 60 | AD 1060 to 1080<br>AD 1150 to 1290 | NA | Event soon after AD 1300<br>(based on probability distribution) | Event Y<br>(1450 ± 150 yr.) | Tuttle (2001; Tuttle and Wolf (2003) |
| | Beta-152009 | Wood (W4 from outer 1 cm of tree trunk in growth position in clay deposit beneath sand blow. | Preliquefaction | 730 ± 60 | AD 1160 to 1300 | NA | | | |
| RP Haynes | Beta-133009 (C2) | Charcoal | Preliquefaction | 160 ± 40 | AD 1660 to 1950 | NA | Event after AD 1000; possibly after AD 1660 | Possibly 1811-1812 | Tuttle et al. (2000); Barnes (2000) |
| | Beta-133010 (C5) | Charcoal | Preliquefaction | 260 ± 80 | AD 1450 to 1710<br>AD 1720 to 1890<br>AD 1910 to 1950 | NA | | | |

**TABLE 2.1-5**

**SUMMARY OF AGE CONSTRAINTS FOR NEW MADRID SEISMIC ZONE EARTHQUAKES**

Seismic Hazards Report for the ECG ESP Site

| Name of Site | Lab Sample Number[1] | Material | Time Relationship of Sample to Liquefaction | $^{14}C$ Age, years BP ± 1-sigma | Calibrated Age 2-sigma (95% Probability)[2] | Age Estimate Based on Ceramics and Points | Maximum Age Range (published correlation, comments) | Estimated Event Correlation | Reference |
|---|---|---|---|---|---|---|---|---|---|
| RP Haynes (Continued) | Beta-142450 (C100) collected 40 cm below sand blow | Charcoal | Preliquefaction | 970 ± 40 | AD 1000 to 1170 | | | | |
| | | Ceramics from horizon below sand blow | Preliquefaction | NA | NA | AD 800 to 1000<br>Mostly Late Woodland; few Early Mississippian shards | | | |
| Towosaghy (S1) | Beta-36669 | Charcoal | Postliquefaction (event 2) | 520 ± 60 | AD 1414 | | Event 2 probably occurred in the early part of the period AD 539 to 991<br><br>Event 1 estimated to have occurred <100 yr. prior to AD 539 | Event X (?)<br>900 ± 100 yr. (event 2)<br><br>Event 1<br>AD 440 to 540 | Saucier (1991) |
| | Beta-36670 | Charcoal | Post- liquefaction (event 2) | 1050 ± 120 | AD 991 (intercept) | | | | |
| | Beta-36671 | Charcoal | Preliquefaction (event 2)<br>Postliquefaction (event 1) | 1540 ± 110 | AD 539 (intercept) | | | | |
| Towosaghy (re-excavate S1 site) | Dating underway | Artifacts | Preliquefaction (event 3) | NA | NA | Sand dike crosscuts horizon containing artifacts | Event 3; not yet determined | Event 3; Not yet determined | Tuttle and Wolf (2003) |
| | Dating underway | Artifacts | Postliquefaction (event 1) | NA | NA | Late Woodland to Early Mississippian (AD 400 to 1000) above sand blow; few artifacts below sand blow | Evidence for event 1 but not event 2 of Saucier | May correlate to event W<br>AD 300 ± 200 yr. (event 1) | |
| Walker | Artifacts on surface and within plow zone | | | | Presence of Mississippian archeological site | | | | Tuttle et al. (2000); Barnes (2000) |
| | Beta-133017 (T2-C1) | Charcoal | Postliquefaction | **43210** ± 720 (probably reworked) | NA | NA | Trench T2—AD 1420 to 1670 during Late Mississippian<br>Trench T3—Also during the Mississippian, probably during same event as seen in trench T2. Soil lamellae developed in upper 40 cm of sand dikes indicate that they are prehistoric | Event Y<br>(1450 ± 150 yr.)<br>Root cast may have been intruded by sand during subsequent event, 1811-1812 | Tuttle et al. (2000) |
| | Beta-133018 (T2-C2) | Charcoal from cultural horizon < 1 cm below sand blow; artifacts | Preliquefaction | 440 ± 40 | AD 1420 to 1500<br>Close maximum | AD 1400 to 1670—Late Mississippian<br>AD 1000 to 1400—Middle Mississippian (strap handle) | | | |
| | Beta-133019 (T3-C2) | Charcoal from root cast | Preliquefaction (same or later event) | 230 ± 40 | AD 1530 to 1550<br>AD 1640 to 1680<br>AD 1740 to 1810<br>AD 1930 to 1950 | NA | | | |
| | | Artifacts in cultural horizon below sand blow | Preliquefaction | | | Mississippian | | | |

**TABLE 2.1-5**

**SUMMARY OF AGE CONSTRAINTS FOR NEW MADRID SEISMIC ZONE EARTHQUAKES**

Seismic Hazards Report for the ECG ESP Site

| Name of Site | Lab Sample Number[1] | Material | Time Relationship of Sample to Liquefaction | $^{14}C$ Age, years BP ± 1-sigma | Calibrated Age 2-sigma (95% Probability)[2] | Age Estimate Based on Ceramics and Points | Maximum Age Range (published correlation, comments) | Estimated Event Correlation | Reference |
|---|---|---|---|---|---|---|---|---|---|
| Walker (Continued) | Beta-133020 (T3-C3) | Organic material from deposit below cultural horizon | Preliquefaction | 1470 ± 40 | AD 540 to 660 | NA | | | |
| Yarbro 1 | ISGS-2968 | Tree root (large sample from outer ring sent to three labs) | Postliquefaction | 640 ± 70 | NA | NA | AD 1420 to 1670 | Event Y (1450 ± 150 yr.) | Tuttle (1999) |
| | QL-4787 | | Postliquefaction | 181 ± 16 | AD 1668 to 1686<br>AD 1737 to 1788<br>AD 1791 to 1810<br>AD 1928 to 1954 | NA | | | |
| | Beta-80749 | | Postliquefaction | 130 ± 60 | AD 1660 to 1950 | NA | | | |
| | Beta-79237 | Twig | Preliquefaction (close maximum) | 370 ± 80 | AD 1420 to 1670 | NA | | | |
| | Beta-81310 | Soil | Preliquefaction | - | AD 1420 to 1540<br>AD 1550 to 1640 | NA | | | |
| Yarbro 2 | Beta-79350 | Pond nut | Postliquefaction | 160 ± 60 | AD 1650 to 1950 | NA | | 1811-1812 | Tuttle (1999) |
| | Beta-79354 | Wood from top of A horizon | Postliquefaction | 180 ± 70 | AD 1540 to 1550<br>AD 1640 to 1950 | NA | | | |
| | Beta-79355 | Wood from base of A horizon | Postliquefaction | 320 ± 60 | AD 1450 to 1670<br>AD 1780 to 1800<br>AD 1945 to 1950 | NA | | | |
| | Beta-79352 | Large twig collected at the contact of the sand blow and pre-event paleosol | Preliquefaction | 90 ± 60 | AD 1670 to 1950 | NA | | | |
| | Beta-79353 | Wood | Preliquefaction | 80 ± 60 | AD 1670 to 1780<br>AD 1800 to 1950 | NA | | | |
| Yarbro 3 | Beta-84977 | Tree | Preliquefactions | 90 ± 40 | AD 1680 to 1760<br>AD 1810 to 1940 | NA | | 1811-1812 | Tuttle (1999) |
| | Beta-84977 | Tree | Postliquefaction | 90 ± 40 | AD 1680 to 1760<br>AD 1810 to 1940 | NA | Two sand blows are interpreted to have formed during the same event, circa AD 1530 ± 130 yr. | Event Y (1450 ± 150 yr.) | |
| | Beta-108882 | Tree center | Preliquefaction | 330 ± 40 | AD 1445 to 1670<br>Plus 68 rings<br>(AD 1513 to 1738) | NA | | | |

**TABLE 2.1-5**

**SUMMARY OF AGE CONSTRAINTS FOR NEW MADRID SEISMIC ZONE EARTHQUAKES**

Seismic Hazards Report for the ECG ESP Site

**NOTES:**

[1] Beta—Beta Analytic, Inc. (Miami, FL); CAMS—Center for Accelerator Mass Spectrometry (Livermore, CA);G—Krueger Enterprises' Geochron Laboratory; ISGS—Illinois State Geological Survey; QL—Quaternary Isotope Laboratory, University of Washington (Seattle, WA):

2 Intervals that can be eliminated based on stratigraphic or historical evidence are shown in italics.

## TABLE 2.1-6

## SUMMARY OF NEW INFORMATION FOR WABASH VALLEY SEISMIC ZONE (WVSZ)

Seismic Hazards Report for the EGC ESP Site

| AUTHOR(S); YEAR | TITLE | SIGNIFICANCE OF WORK |
|---|---|---|
| **GEOPHYSICAL AND SEISMOLOGIC DATA—WABASH VALLEY SEISMIC ZONE** | | |
| Sexton et al. (1986) | "Seismic-reflection Profiling Studies of a Buried Precambrian Rift beneath the Wabash Valley Fault Zone" | Interprets a graben (the Grayville graben) approximately 1 mile (1.5 km) wide and containing 2 miles (3 km) of fill. This late-Precambrian rift is inferred to be one arm of the New Madrid rift complex. Wabash Valley faults are traced downward into older, large-offset faults, suggesting that the Wabash Valley faults represent a post-Pennsylvanian reactivation of the rift system. |
| Pratt et al. (1989) | "Major Proterozoic Basement Features of the Eastern Midcontinent of North America Revealed by Recent COCORP Profiling" | Identifies a Precambrian (probably Middle-Proterozoic or older) layered assemblage that may be as much as 6.6 miles (11 km) thick beneath southern Illinois, Indiana, and western Ohio.<br>Interpretation of deep seismic-reflection data indicates an absence of a thick section of rift-related sedimentary rocks, suggesting an arm of Reelfoot rift does not extend north of Grayville graben. |
| Bear et al. (1997) | "Seismic Interpretation of the Deep Structure of the Wabash Valley Fault System" | Identifies location, extent, and displacement on individual faults/structures in the Wabash Valley fault system (WVFS). |
| Potter et al. (1997) | "Proterozoic structure, Cambrian rifting, and younger faulting as revealed by a regional seismic reflection network in the southern Illinois Basin" | Based on review of seismic-reflection profiles, extensional fault zones in the WVFS and the Flourspar area fault complex are developed north and south of the Rough Creek fault system, respectively, and are not connected to each other. The WVFS lacks a through-going, basement-cutting "master fault." Only one fault in the WVFS affects the top of Precambrian basement. |
| McBride and Nelson (1999) | "Style and Origin of Mid-Carboniferous Deformation in the Illinois Basin, USA—Ancestral Rockies Deformation?" | Evaluates the style and origin of intra-cratonic deformation based on an integration of outcrop, borehole, and seismic-reflection data from the Illinois basin. Typical structures are high-angle reverse faults in Precambrian basement that propagated upward to monoclines and asymmetrical anticlines in Paleozoic cover. |
| Pavlis et al. (2002) | "Seismicity of the Wabash Valley Seismic Zone Based on a Temporary Seismic Array Experiment" | Lowers earthquake detection threshold to magnitudes of 1.2 to 1.5 based on local array. Excess events in region are related to a cluster of earthquakes near New Harmony, Indiana. However, small-magnitude events in this cluster appear to be artificially induced. Discarding these events produces seismicity rates more consistent with previous data. |

## TABLE 2.1-6

## SUMMARY OF NEW INFORMATION FOR WABASH VALLEY SEISMIC ZONE (WVSZ)

Seismic Hazards Report for the EGC ESP Site

| AUTHOR(S); YEAR | TITLE | SIGNIFICANCE OF WORK |
|---|---|---|
| **GEOPHYSICAL AND SEISMOLOGIC DATA—WABASH VALLEY SEISMIC ZONE** | | |
| McBride et al. (2002a) | "Interpreting the Earthquake Source of the Wabash Valley Seismic Zone (Illinois, Indiana, and Kentucky) from Seismic Reflection, Gravity, and Magnetic Intensity" | Reprocessing of seismic-reflection data provides new images of upper- to middle-crustal structures beneath the WVSZ. A series of moderately dipping crustal reflectors are identified below the western flank of the WVFS and locally following the Commerce geophysical lineament (CGL). Association of dipping crustal reflectors and gently arched Paleozoic strata also hint at a limited degree of Phanerozoic reactivation. The $m_{bLg}$ 5.5 1968 earthquake (focal mechanism—moderately dipping reverse fault) is correlated to reflectors in basement (inferred reactivated thrust in basement). |
| **SEISMOGENIC FAULTS** | | |
| Fuller, Mossbarger, Scott & May Engineers (2001) | "J.T. Myers Locks and Dam Seismological Study, Summary of Deterministic and Probabilistic Seismic Hazard Analyses and Generation of Time Histories Report" | Identifies late Pleistocene displacement on Wabash Island fault within the Wabash Valley fault system. |
| Heigold and Larson (1994) | "Geophysical Investigations of Possible Recent Ground Deformation and Neotectonism in White County, Illinois" | Evaluates escarpment along projection of Herald-Phillipstown fault zone and concludes that it formed as a result of erosion, possibly along the fault zone. Vertical electric soundings, seismic-refraction profiling, resistivity profiling, and boreholes are used to evaluate the depth to Pennsylvanian bedrock. The study finds no evidence to support recent movement along pre-existing or newly formed faults. |
| Nelson et al. (1997) | "Tertiary and Quaternary Tectonic Faulting in Southernmost Illinois" | Documents Tertiary and/or Quaternary tectonic faulting in three areas: the Fluorspar area fault complex (FAFC); the Ste. Genevieve fault zone (SGFZ); and the Commerce fault zone(CFZ). In the FAFC, faults displace Mounds Gravel (late Miocene to early Pleistocene) and locally Metropolis terrace gravel (Pleistocene; pre-Woodfordian). Deformed Quaternary sediments are not observed along the SGFZ. The CFZ displaces Mounds Gravel and units as young as Peoria Silt (Woodfordian) in Missouri. Only the CFZ exhibits slip that conforms to the current stress field. |

## TABLE 2.1-6

## SUMMARY OF NEW INFORMATION FOR WABASH VALLEY SEISMIC ZONE (WVSZ)

Seismic Hazards Report for the EGC ESP Site

| AUTHOR(S); YEAR | TITLE | SIGNIFICANCE OF WORK |
|---|---|---|
| **SEISMOGENIC FAULTS** | | |
| Odum et al. (2002) | "Near-Surface Faulting and Deformation Overlying the Commerce Geophysical Lineament in Southern Illinois" | Structural features interpreted from the Tamms, Illinois, high-resolution seismic-reflection survey and supporting microgravity data correlate with anomalous changes in drainage patterns, strikingly linear topographic bluff-front scarps, and the complex faulting and folding of Paleozoic rock. Several faults are traceable to the Paleozoic/Quaternary interface, and, at one site, deformed Quaternary strata may have been faulted upward 16 to 30 feet. |
| McBride et al. (2002a) | "Interpreting the Earthquake Source of the Wabash Valley Seismic Zone (Illinois, Indiana, and Kentucky) from Seismic Reflection, Gravity, and Magnetic Intensity" | Results suggest that the seismogenic source just north of the New Madrid seismic zone consists, in part, of a pre-existing fabric of thrusts in the basement localized along pre-existing igneous intrusions, locally coincident with the CGL |
| Wheeler et al. (1997) | "Seismotectonic Map Showing Faults, Igneous Rocks, and Geophysical and Neotectonic Features in the Vicinity of the Lower Wabash Valley, Illinois, Indiana, and Kentucky" | Describes neotectonic features (defined as younger than Miocene) in the lower Wabash Valley (see Fraser et al., 1997; and Heigold and Larson, 1994). |
| Fraser et al. (1997) | "Geomorphic Response to Tectonically-Induced Ground Deformation in the Wabash Valley" | Morphometric analysis of the land surface, detailed geologic mapping, and structural analysis of bedrock indicate westward-dipping surfaces in the Wabash Valley region along the western edge of the Commerce deformation zone in the region of the restraining bend. |
| **PALEOLIQUEFACTION STUDIES** | | |
| See Attachment 1 (Table B-1-1) | | |
| **SEISMIC SOURCE CHARACTERIZATION / SOURCE MODELS** | | |
| Frankel et al. (1996) | "National Seismic-Hazard Maps. Documentation June 1996" | 1996 National Ground Motion Hazard Maps use a five-sided, ~ rectangular zone for the Wabash Valley source. Recurrence is based on historical seismicity; $M_{max}$ 7.5. This polygonal zone is based on the spatial association of the Wabash Valley fault system, paleoliquefaction energy centers, and historical seismicity. This zone was assigned the higher $M_{max}$ of 7.5 than assigned to the surrounding craton (M6.5) largely on the basis of the paleoliquefaction evidence. |

## TABLE 2.1-6

## SUMMARY OF NEW INFORMATION FOR WABASH VALLEY SEISMIC ZONE (WVSZ)

Seismic Hazards Report for the EGC ESP Site

| AUTHOR(S); YEAR | TITLE | SIGNIFICANCE OF WORK |
|---|---|---|
| **SEISMIC SOURCE CHARACTERIZATION / SOURCE MODELS** | | |
| Frankel et al. (2002) | "Documentation for the 2002 Update of the National Seismic Hazard Maps" | The 2002 National Ground Motion Hazard Maps use the Tri-State zone for the Wabash Valley source. This zone is an oval larger than the polygonal source zone used for the 1996 maps. This zone is centered on the energy centers of the largest paleoearthquakes. Recurrence is based on historical seismicity; $M_{max}$ 7.5. |
| Wheeler and Cramer (2002) | "Updated Seismic Hazard in the Southern Illinois Basin—Geological and Geophysical Foundations for Use in the 2002 USGS National Seismic-Hazard Maps" | Develops alternative geometries for the Wabash Valley source, including a Tri-State source zone, Commerce geophysical lineament source zone, and Grayville graben. The latter two zones encompass the structures for which they are named. |
| Toro and Silva (2001) | "Scenario Earthquakes for Saint Louis, MO, and Memphis, TN, and Seismic Hazard Maps for the Central United States Region including the Effect of Site Conditions" | Develops alternative geometries for the Wabash Valley source. A large, extended zone is based on the extent of paleoliquefaction and diffuse historical seismicity. |

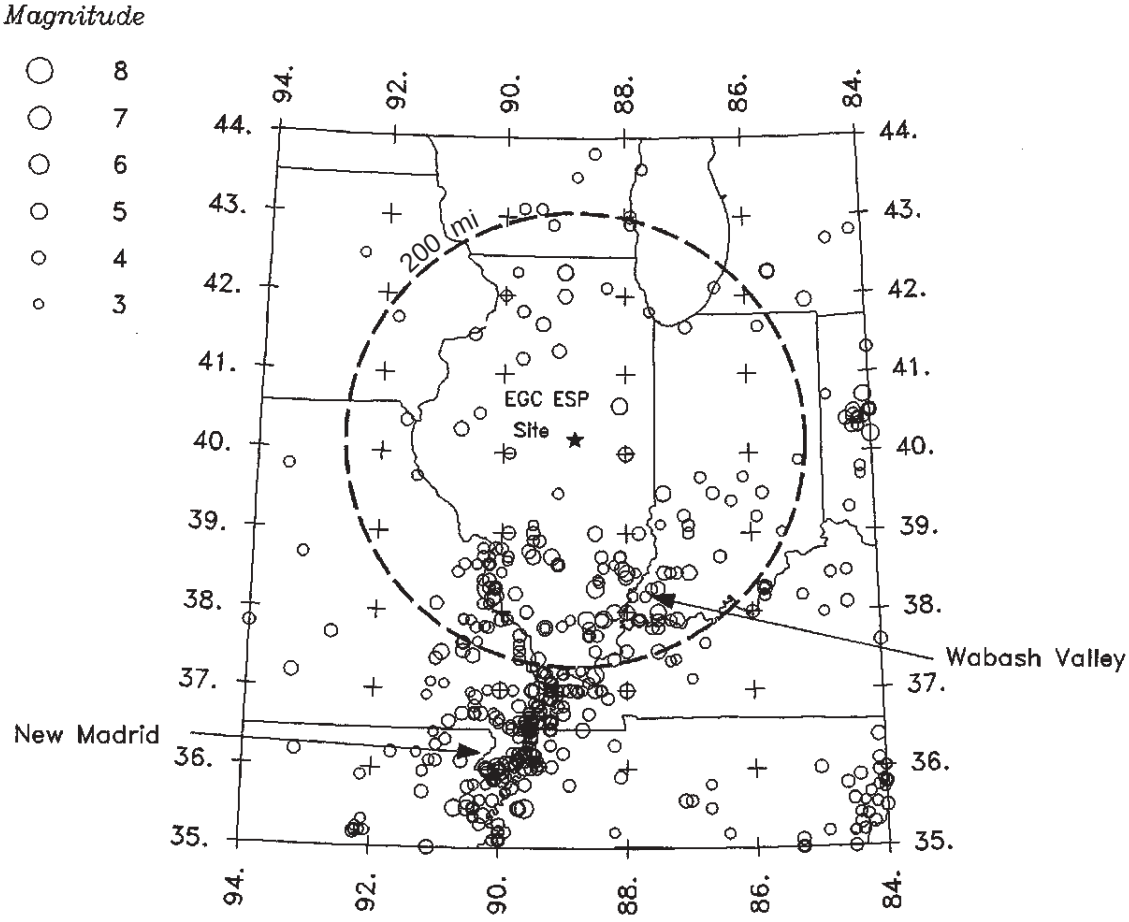


s:\7900\7935\7935.000\03_0109_eesp_fig_2.1-01(22).ai (2003-05-27, 13:51)

**Seismic Hazards Report for the EGC ESP Site**

**Location of the EGC ESP Site and Regional Seismicity**

Figure **2.1-1**

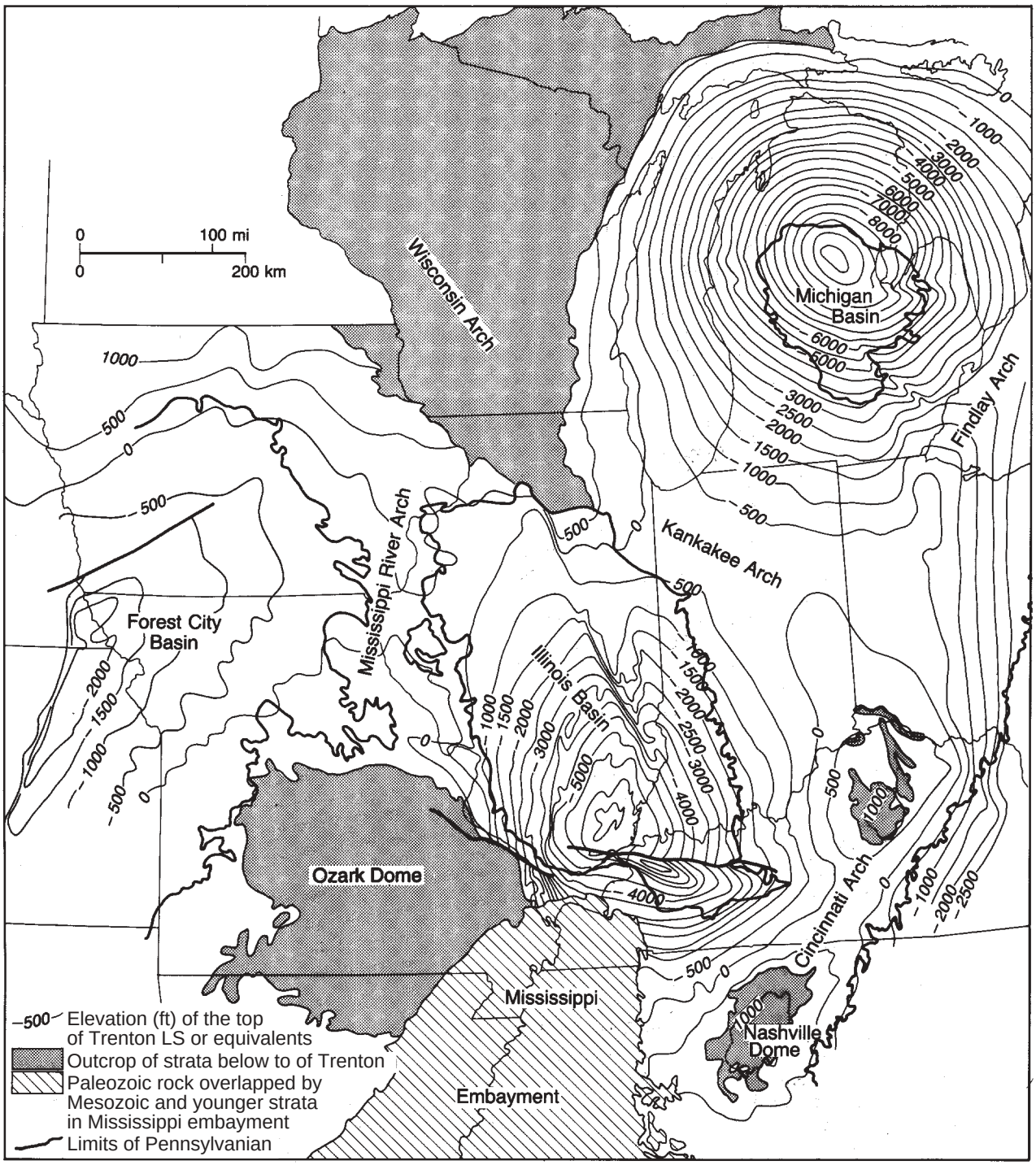


From Nelson (1995)

**Seismic Hazards Report for the EGC ESP Site**

**Regional Structural Setting of Illinois**

Figure **2.1-2**

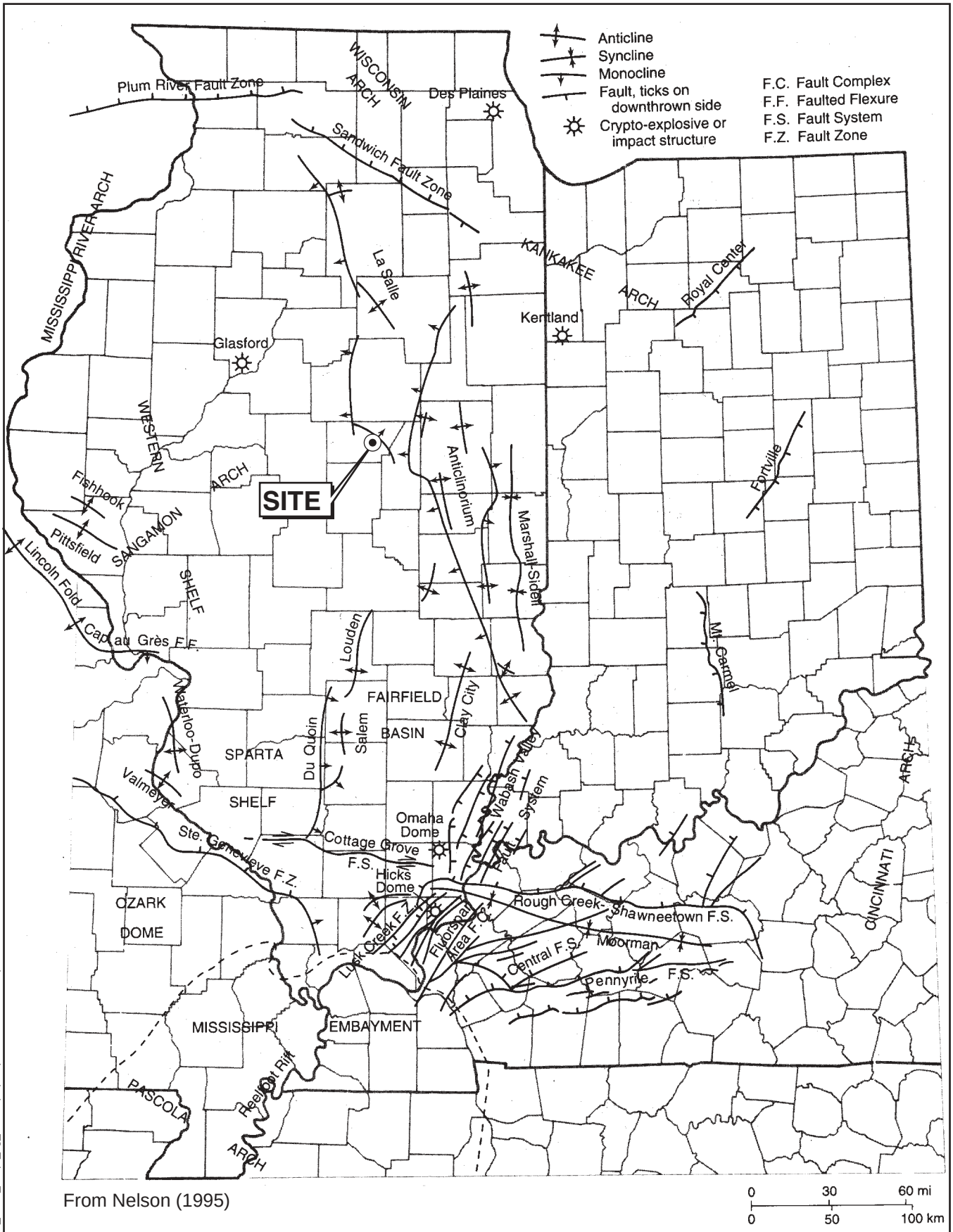


From Nelson (1995)

s:\7900\7935\7935.000\03_0109_eespl_fig_2.1-03(02).ai (2003-05-27, 14:01)

**Seismic Hazards Report for the EGC ESP Site**

**Major Structural Features in Illinois and Neighboring States**

Figure **2.1-3**

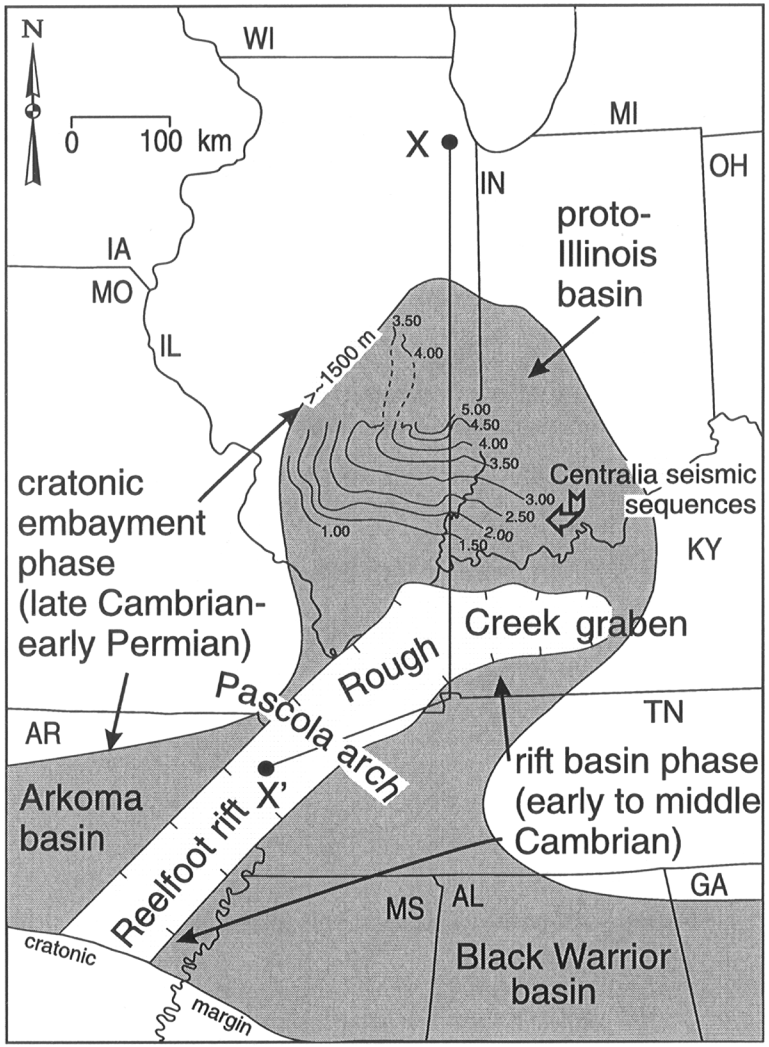


**a)** Map showing development of rift basin and subsequent formation of the proto-Illinois basin centered over the rift junction. Shading indicates Paleozoic strata thicker than ~4900 feet (1500 m). A simplified structural contour map (travel time) for base of Centralia seismic sequence is also shown.

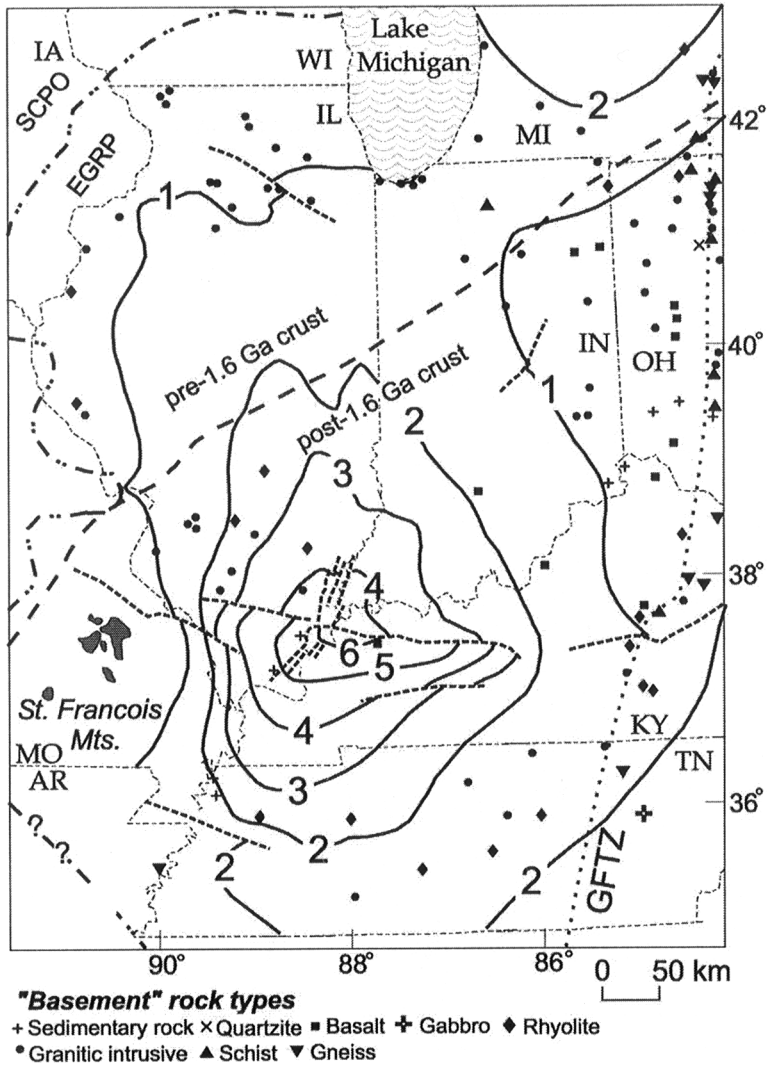


**b)** Compilation of major basement rocks encountered in drill holes and principal basement provinces. SCPO - Southern Central Plains orogen; EGRP - Eastern granite-rhyolite province; GFTZ - Grenville Front tectonic zone. Depth-to-basement contours (contour interval 1 km).

From McBride et al. (2003)

**Seismic Hazards Report for the EGC ESP Site**

**Interpretations of Basement Geology**

Figure **2.1-4**

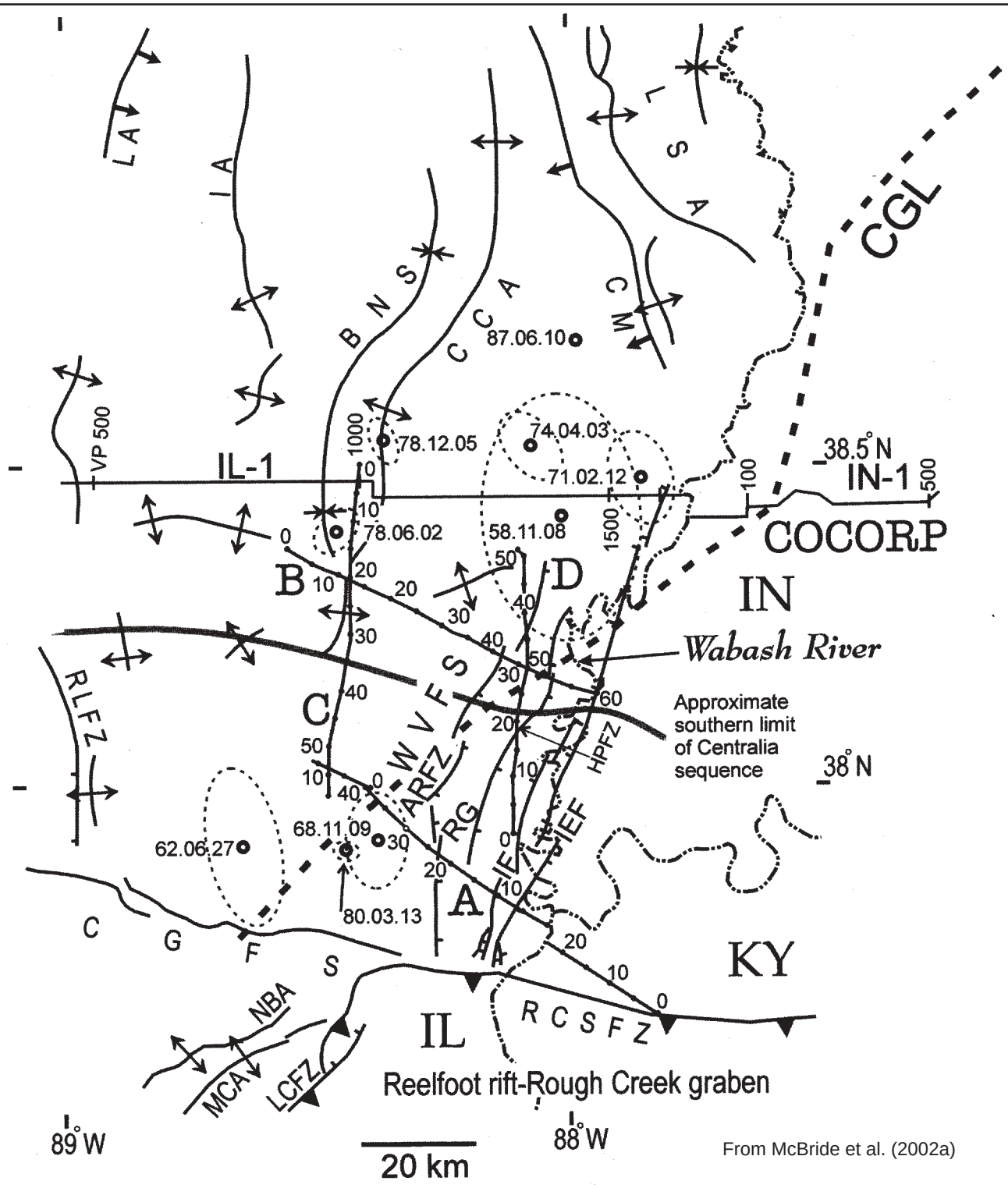


From McBride et al. (2002a)

Map of the south-central Illinois basin and Wabash Valley fault system (WVFS), known fold axes, faults, and other structures (Nelson, 1995), and revised, instrumentally recorded epicenters ($m_{bLg} \geq 3.0$) with nominal 95% confidence ellipses (Gordon, 1988; Langer and Bollinger, 1991). Limit for the Centralia seismic sequence is from McBride and Kolata (1999). A, B, C, and D (with km along the line shown) refer to reflection profiles reprocessed for this study. Also shown is the location of the COCORP deep seismic-reflection profile, Illinois Line 1 and Indiana Line 1 (VP is vibrator point). The Commerce geophysical lineament (CGL) is shown as a dashed line. RCSFZ: Rough Creek-Shawneetown fault zone; LCFZ: Lusk Creek fault zone; MCA: McCormick anticline; NBA: New Burnside anticline; CGFS: Cottage Grove fault system; RLFZ: Rend Lake fault zone; BRS: Bogata-Rinard syncline; CCA: Clay City anticline; CM: Charleston monocline; ARFZ: Albion-Ridgway fault zone; RG: Ridgway graben; IF: Inman fault; IEF: Inman East fault; HPFZ: Herald-Phillipstown fault; LSA: LaSalle anticlinorium; LA: Louden anticline; IA: Iola anticline.

**Seismic Hazards Report for the EGC ESP Site**

**Map Showing Locations of Deep Seismic Profiles Used to Evaluate Structures in the Southern Illinois Basin**

Figure **2.1-5**

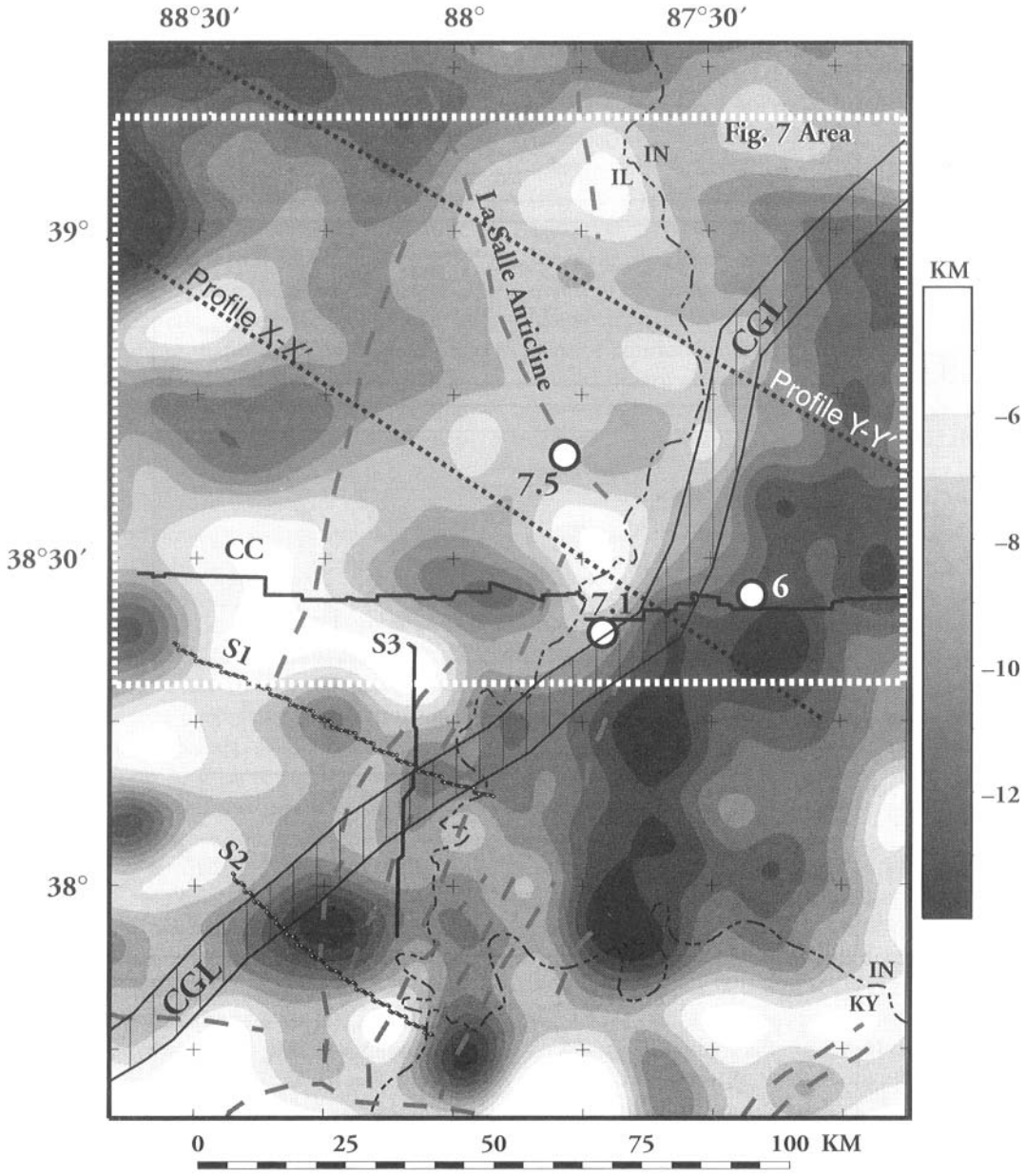


Calculated elevations of the top of a proposed dense igneous source (center) (with respect to sea level) based on inverted gravity data. The inversion results indicate that the igneous center lies near or at the Precambrian surface. Vertical line pattern shows the CGL, interpreted as a 3- to 6-mile-wide deformation zone bounding the igneous center on the southeast. Lines CC, S1, S2, and S3 are profiles analyzed by McBride et al. (2002) to characterize this source of the CGL using seismic-reflection, gravity, and magnetic data. Dashed gray lines depict faults (one follow the La Salle anticline as labeled). Three white dots are the approximate locations of inferred epicenters of large prehistoric earthquakes (interpreted moment magnitudes of ~6, 7.1, and 7.5; McNulty and Obermeier, 1999).

From Hildenbrand et al. (2002)

**Seismic Hazards Report for the EGC ESP Site**

**Map Showing Inverted Gravity Data Along the Commerce Geophysical Lineament (CGL)**

Figure **2.1-6**

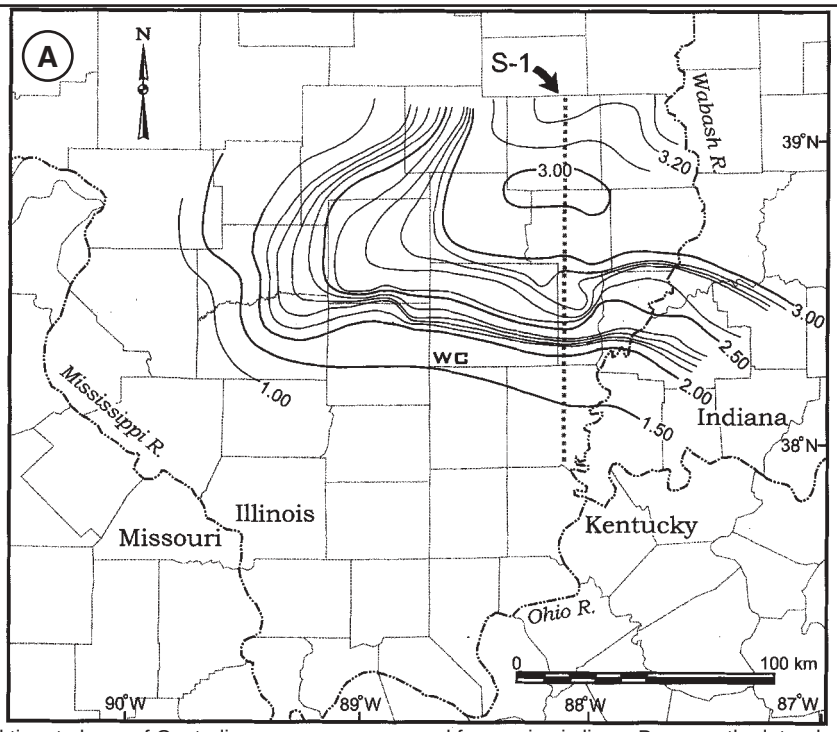


A.) Two-way isotravel time to base of Centralia sequence as mapped from seismic lines. Because the lateral change in seismic velocity for the Paleozoic section across the Illinois basin and the vertical change in velocity between the Paleozoic section and Precambrian basement are relatively small, little appreciable traveltime distortion of depth relations is expected. Contour interval is 100 ms (or 300 m at 6.0 km $s^{-1}$). For traveltimes less then 2 s, the contour interval is 500 ms.

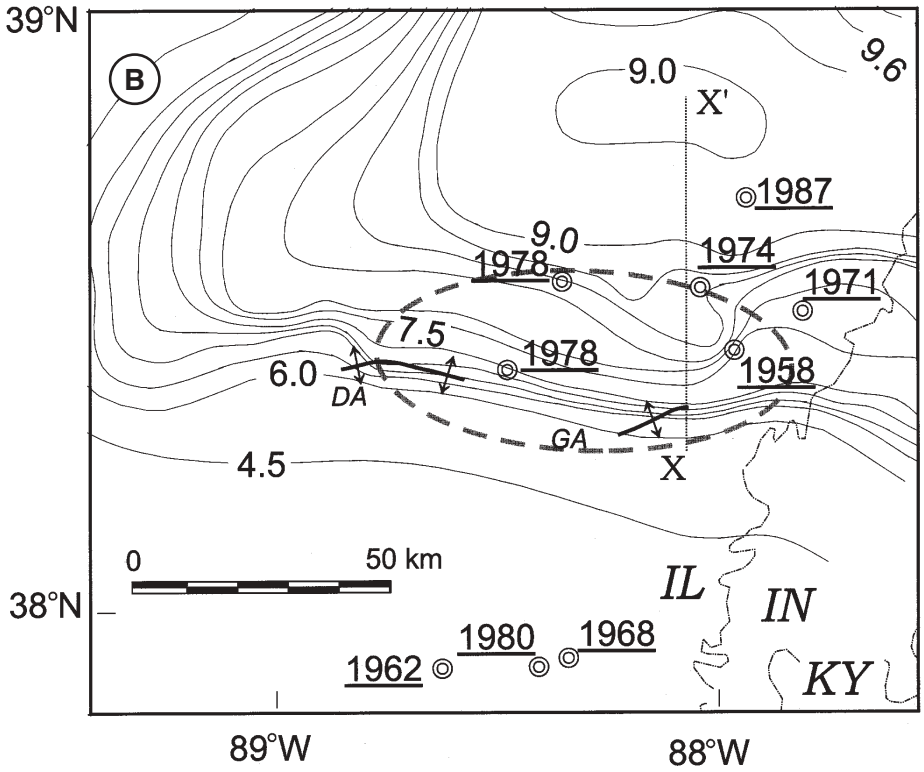


B.) Epicenters of significant ($m_{bLg} \geq 3.0$) magnitude earthquakes in the southern part of the Illinois basin in Illinois, Indiana, and Kentucky (from Gordon, 1988; Langer and Bollinger, 1991). Contours are depth (converted from traveltime contours in A using a simple conversion velocity of 6.0 km $s^{-1}$) to base of the Centralia sequence marked by inward-dipping and disrupted reflectors. DA-Divide anticline; GA-Goldengate anticline.

From McBride and Kolata (1999)

**Seismic Hazards Report for the EGC ESP Site**

**Maps Showing Correlation of Deformed Region of Precambrian Basement and Historical Earthquakes in the Southern Illinois Basin**

Figure **2.1-7**

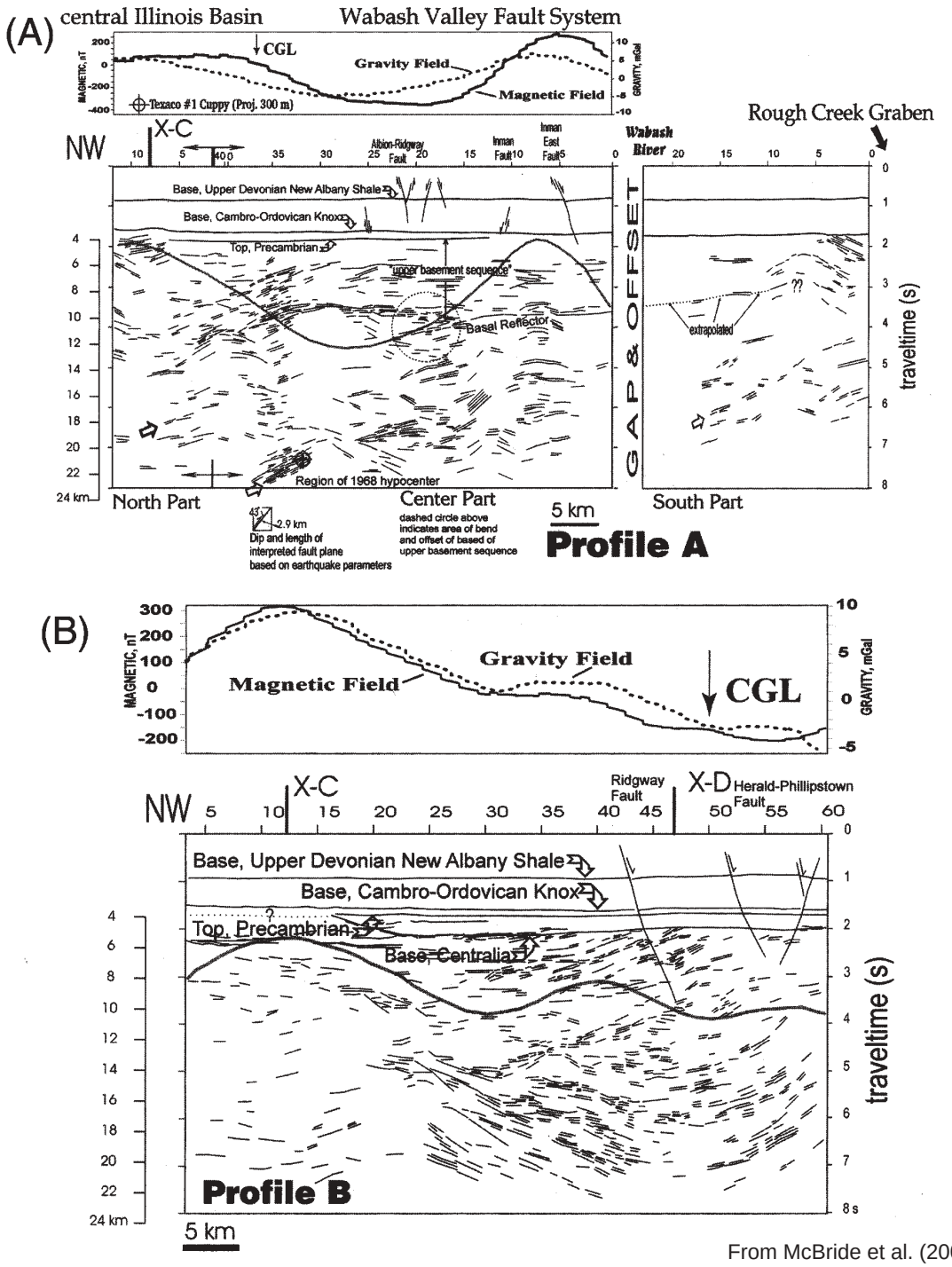


From McBride et al. (2002a)

Vertically exaggerated interpretive line drawings of profiles A, B, C, and D (based on reprocessed seismic reflection data. Only the principal stratigraphic markers are shown simplified for the mostly horizontal Illinois basin sequence. Cross sections of gravity and magnetic data are also shown, as well as the model density boundary superimposed on the reflection line drawing as a gray line. Small box for A shows apparent dip of west-dipping nodal plane for the 1968 event (interpreted as the fault plane) and its modeled rupture length. Position of $m_b$ 5.5 1968 hypocenter is shown (Gordon, 1988); depth uncertainty is ± 5.4 km or ~-5.4-8.9s based on Gordon's (1988) estimate. Stratigraphic identifications from McBride et al. (1997). WVFS is Wabash Valley fault system.

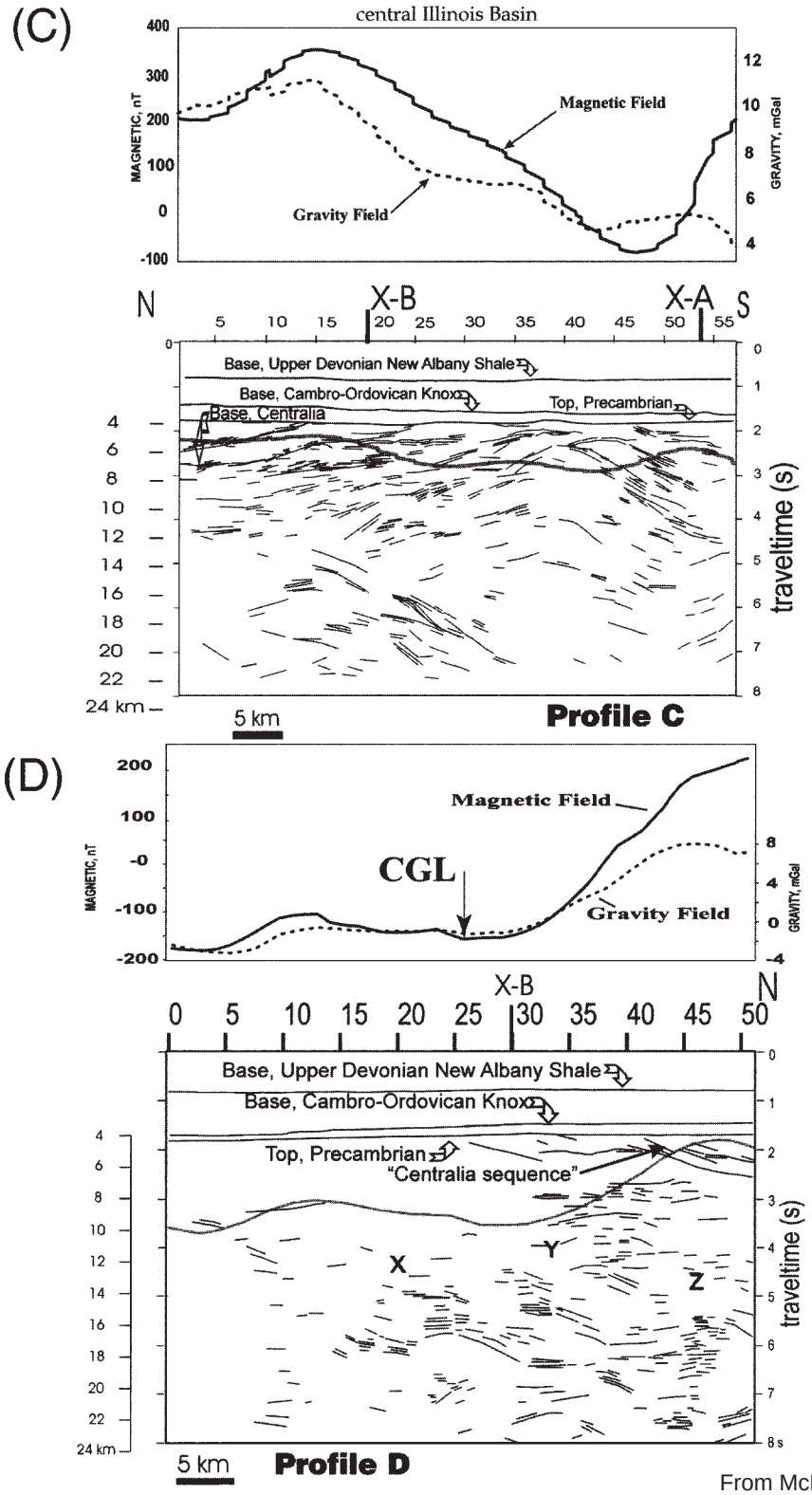


From McBride et al. (2002a)

Vertically exaggerated interpretive line drawings of profiles A, B, C, and D (based on reprocessed seismic reflection data). Only the principal stratigraphic markers are shown simplified for the mostly horizontal Illinois basin sequence. Cross sections of gravity and magnetic data are also shown, as well as the model density boundary superimposed on the reflection line drawing as a gray line. Small box for A shows apparent dip of west-dipping nodal plane for the 1968 event (interpreted as the fault plane) and its modeled rupture length. Position of $m_b$ 5.5 1968 hypocenter is shown (Gordon, 1988); depth uncertainty is ± 5.4 km or ~-5.4-8.9s based on Gordon's (1988) estimate. Stratigraphic identifications from McBride et al. (1997). WVFS is Wabash Valley fault system.

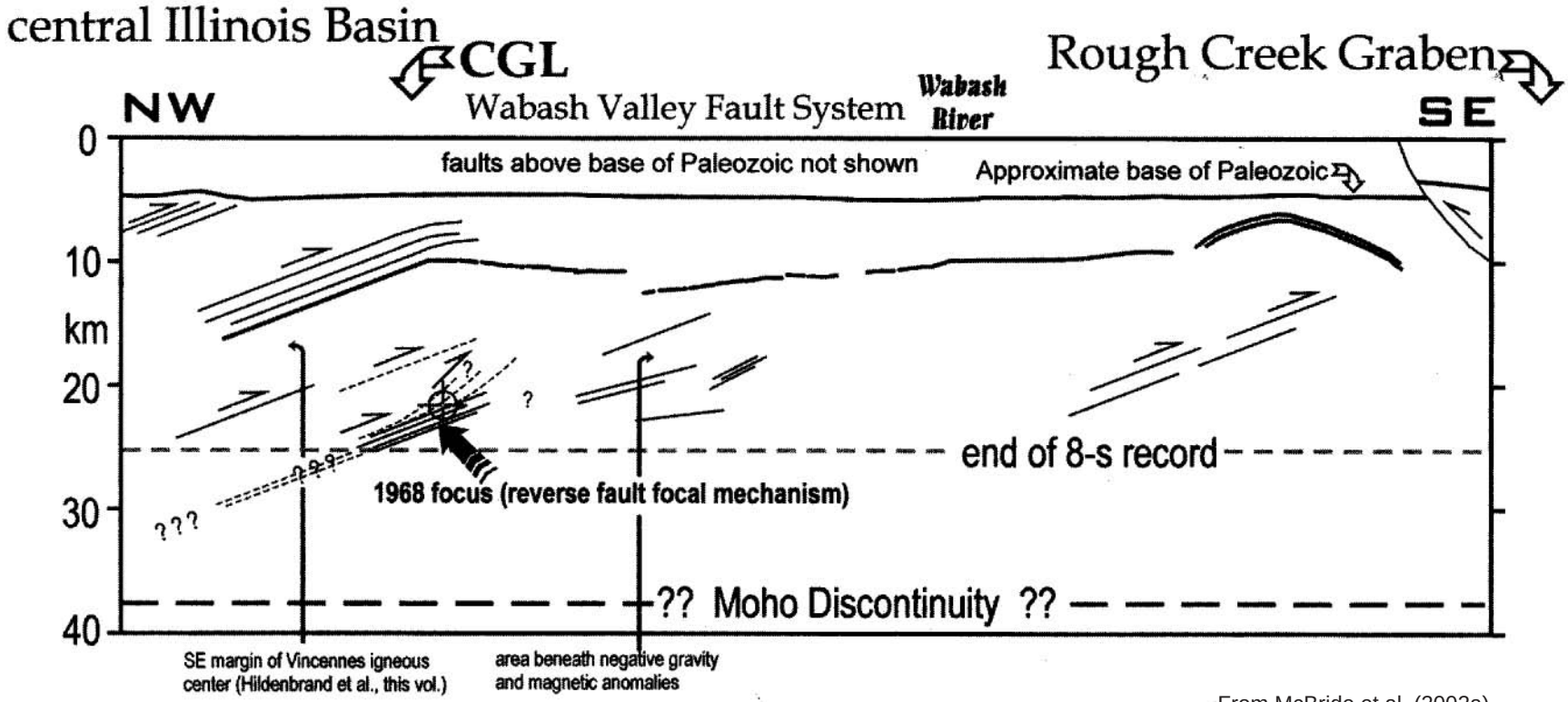


From McBride et al. (2002a)

Interpretive model corresponding to area of Figure 2.1-27A. Dashed lines are speculative. No Vertical exaggeration implied.

**Seismic Hazards Report for the EGC ESP Site**

**Profile Showing Correlation of 1968 Earthquake Hypocenter to Postulated Reverse Fault in Precambrian Basement**

Figure **2.1-9**

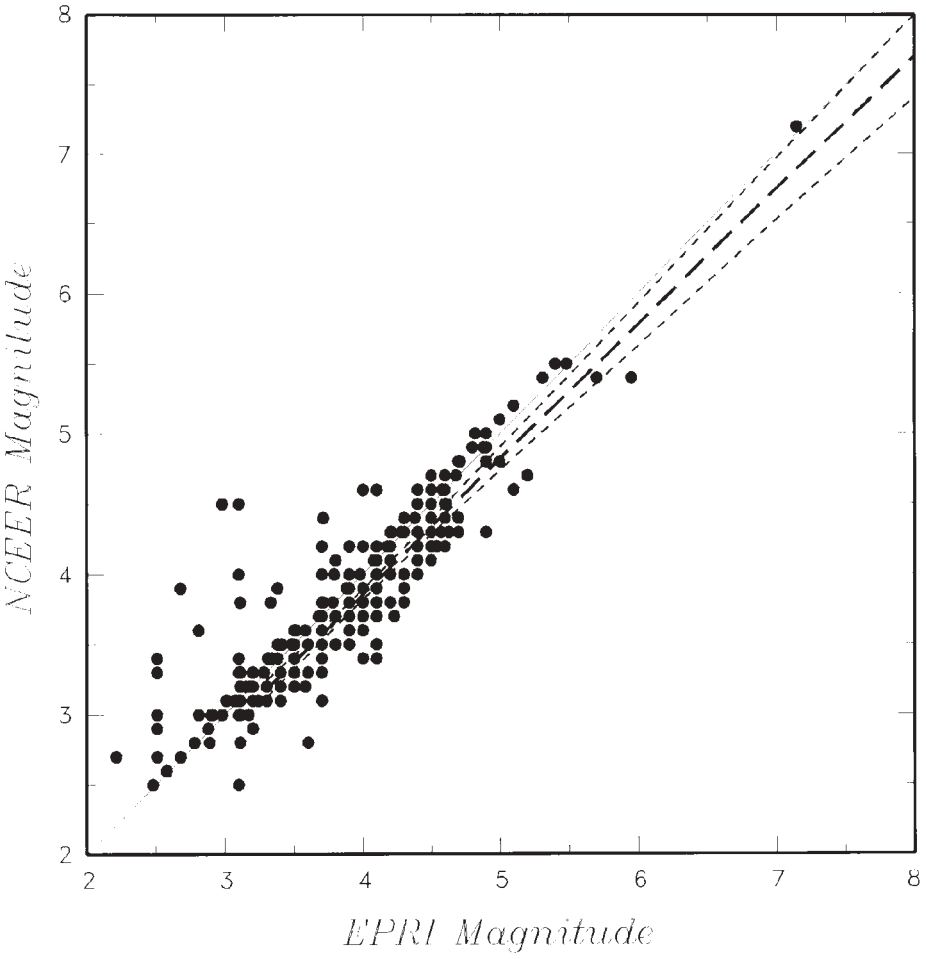


**Seismic Hazards Report for the EGC ESP Site**

**Comparison of Magnitudes in EPRI and NCEER Catalogs**

Figure **2.1-10**

EPRI 1777-1985

USGS 1985-1995
CNSS 1995-2002

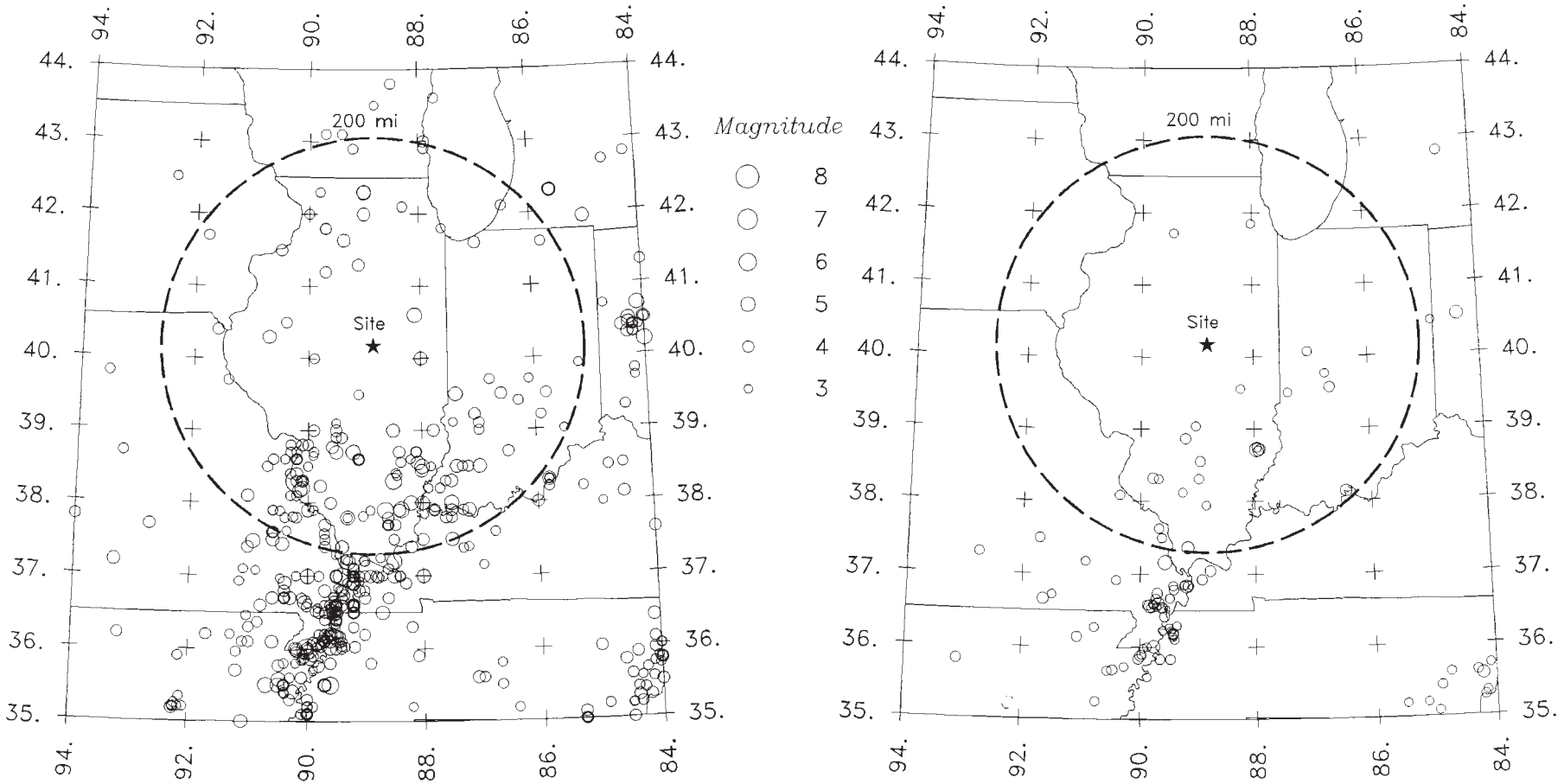


**Seismic Hazards Report for the EGC ESP Site**
**Updates to Seismicity Catalog**

Figure
**2.1-11**

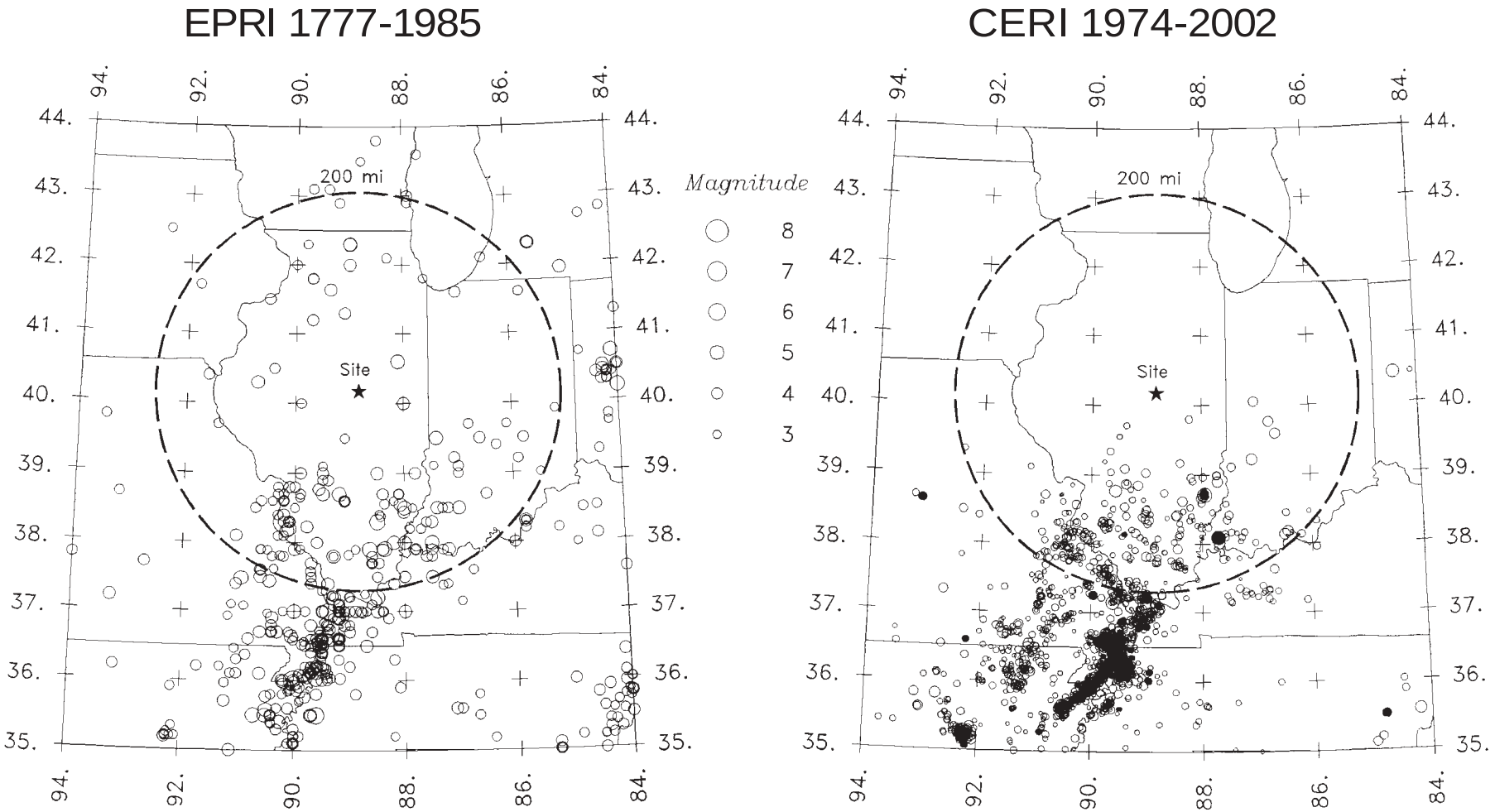


**Seismic Hazards Report for the EGC ESP Site**

**Comparison of EPRI-SOG Catalog to CERI (1974-2002) Catalog**

Figure **2.1-12**

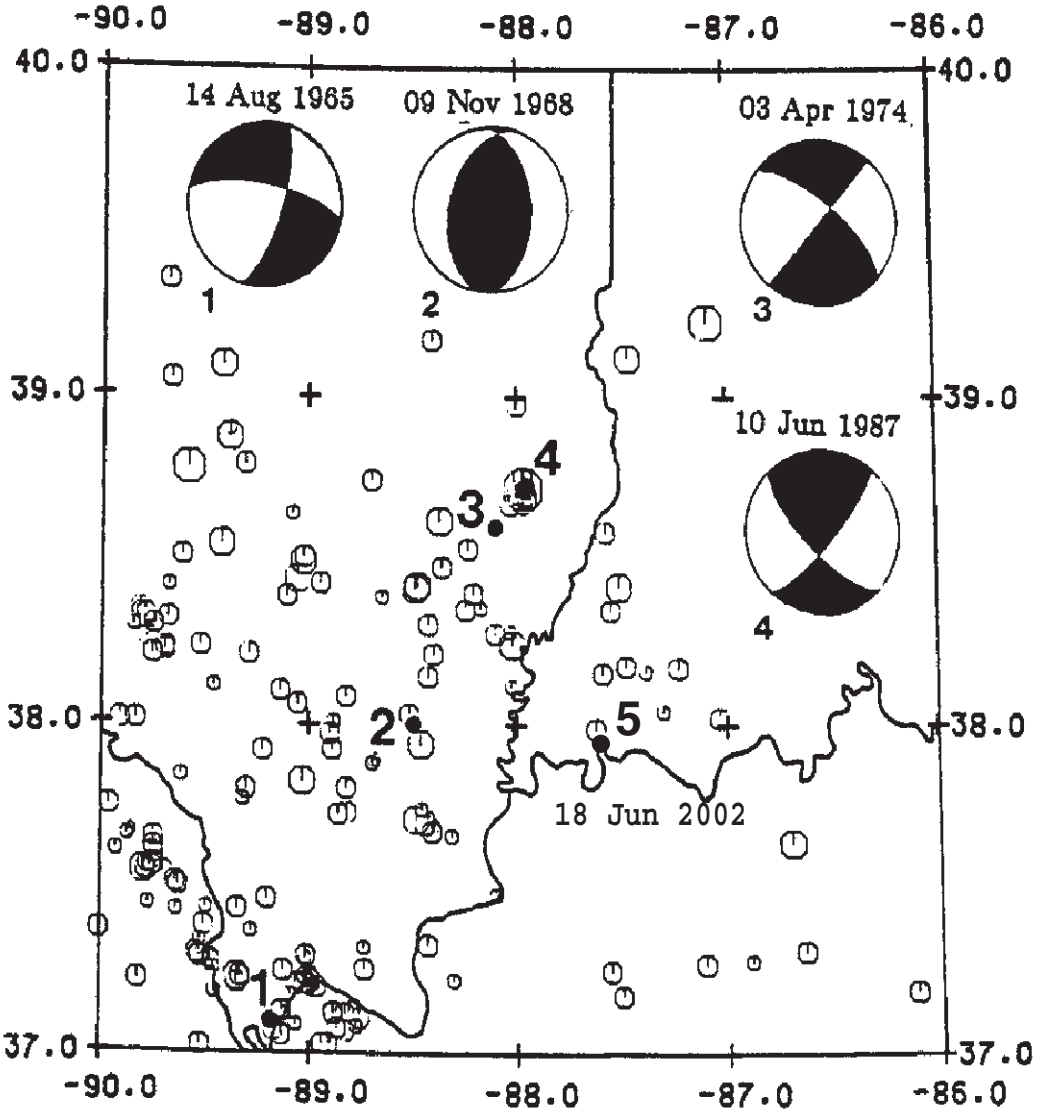


Instrumentally located seismicity for period 1974 to 1987. Map Symbol sizes are proportional to magnitude. Compressional quadrants in the focal mechanisms are shaded.

| | Event | Magnitude | Depth |
|---|---|---|---|
| 1. | 14 August 1965 | --- | 2 km |
| 2. | 09 November 1968 | **M** 5.4 | 22 km |
| 3. | 03 April 1974 | **M** 4.3 | 15 km |
| 4. | 10 June 1987 | **M** 5.0 | 7-12 km |
| 5. | 18 June 2002 | **M** 4.45 | 19 km |

Modified from Taylor et al. (1989)

**Seismic Hazards Report for the EGC ESP Site**

**Location and Surface-Wave Mechanisms for Larger Events in Southern Illinois**

Figure **2.1-13**

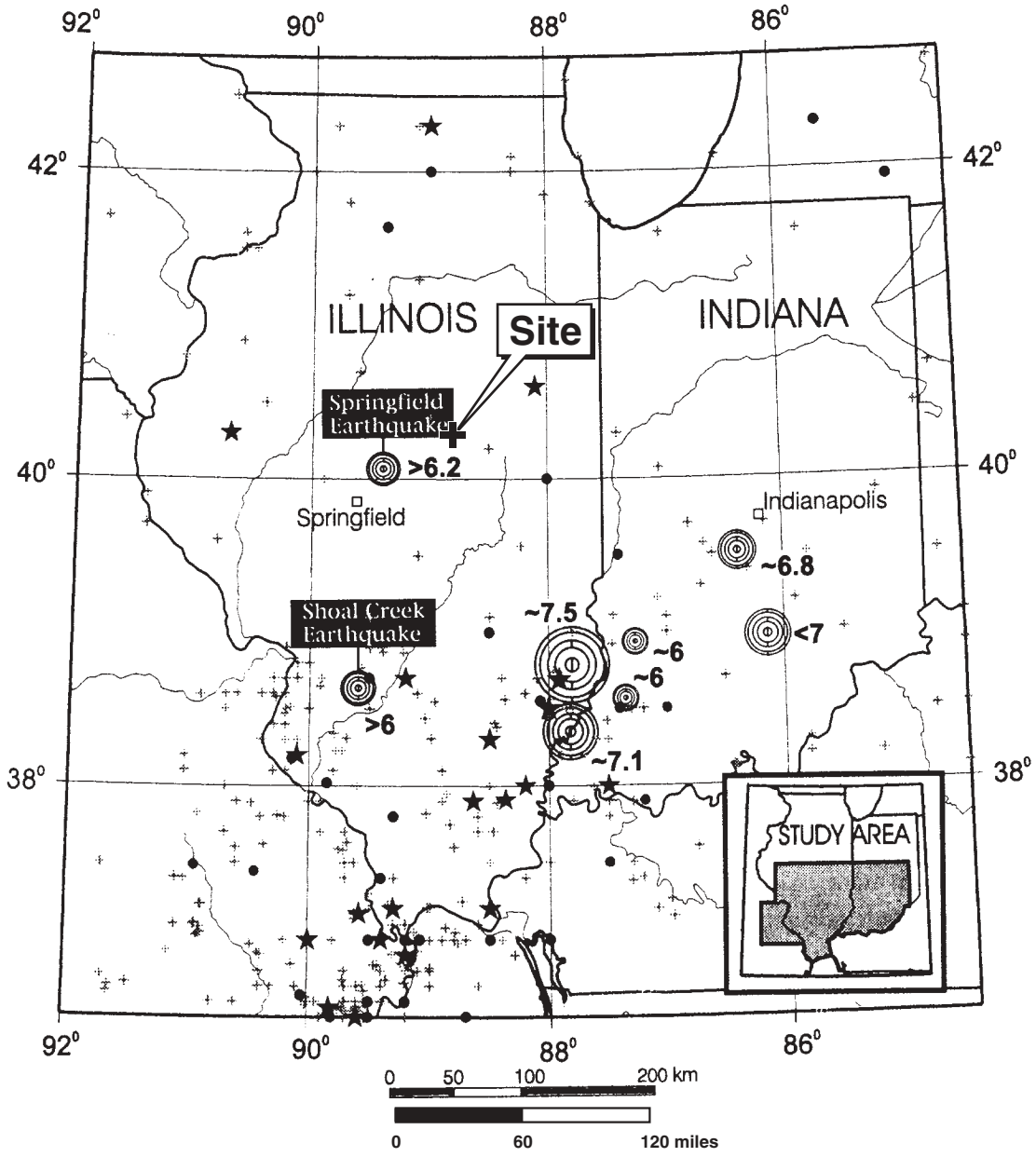


A star represents a magnitude of 5 or higher. A solid circle represents a magnitude between 4.5 and 5. A plus sign represents a magnitude between about 2.3 and 4.5. Historical earthquake data are from USGS/NEIC Global Hypocenter Data Base CD-ROM (Version 3.0). Concentric circles show estimated energy centers of large prehistoric earthquakes. The estimated moment magnitude, M, for a prehistoric earthquake is located near the circle.

Note:
Epicenters of historical earthquakes are shown for the time period 1804-1992

From McNulty and Obermeier (1999)

**Seismic Hazards Report for the EGC ESP Site**

**Historical Seismicity and Estimated Centers of Large Prehistoric Earthquakes in Site Region**

Figure **2.1-14**

S:\7900\7935\7935.000\03_0109_eesp_fig_2.1-10(02).ai

s:\7900\7935\7935.000\03_0109_eesp_fig_2.1-11(29).ai (2003-05-29, 11:48)

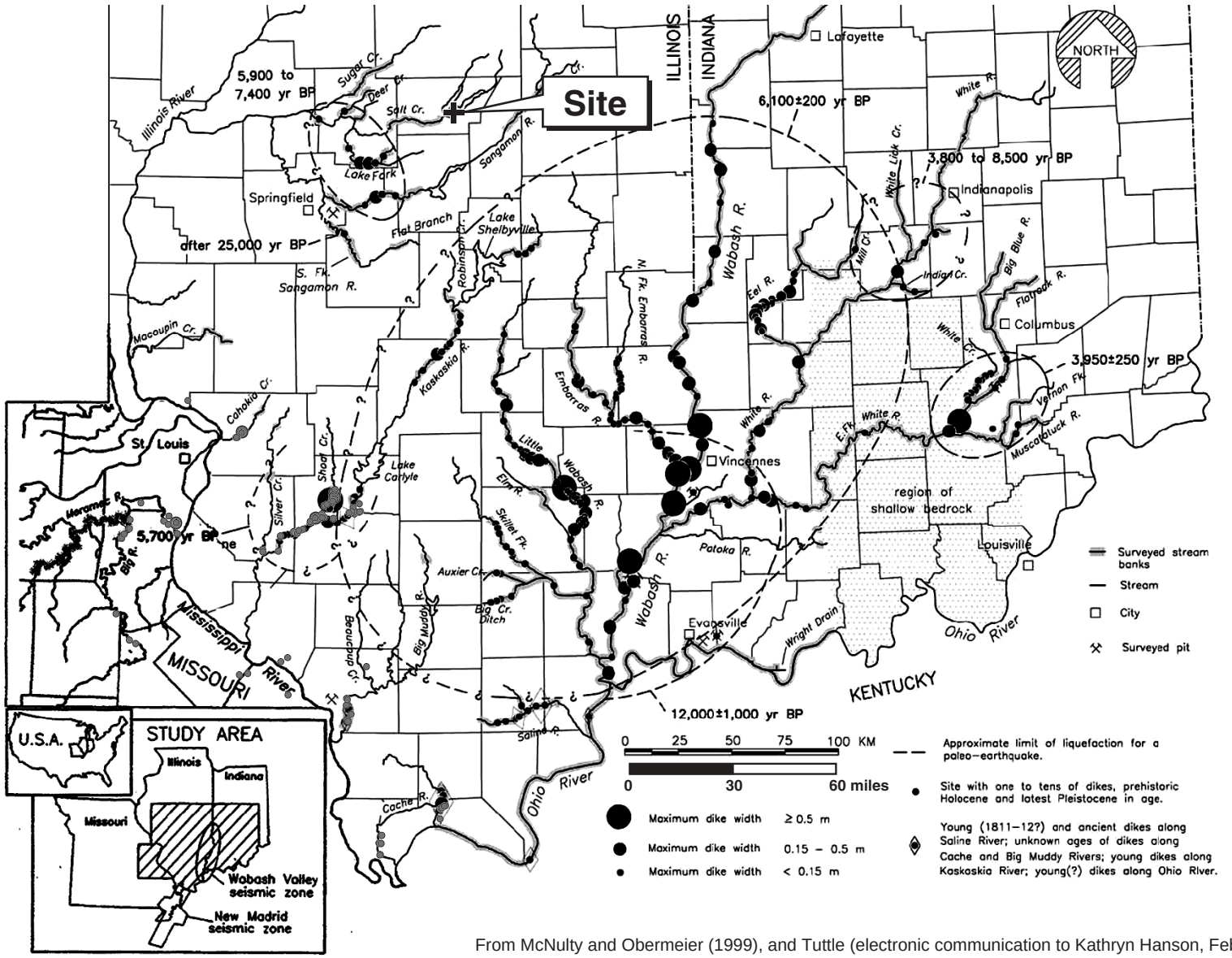


From McNulty and Obermeier (1999), and Tuttle (electronic communication to Kathryn Hanson, February 11, 2003)

**Seismic Hazards Report for the EGC ESP Site**

**Locations of Paleoliquefaction Sites in Southern Indiana and Illinois**

Figure **2.1-15**

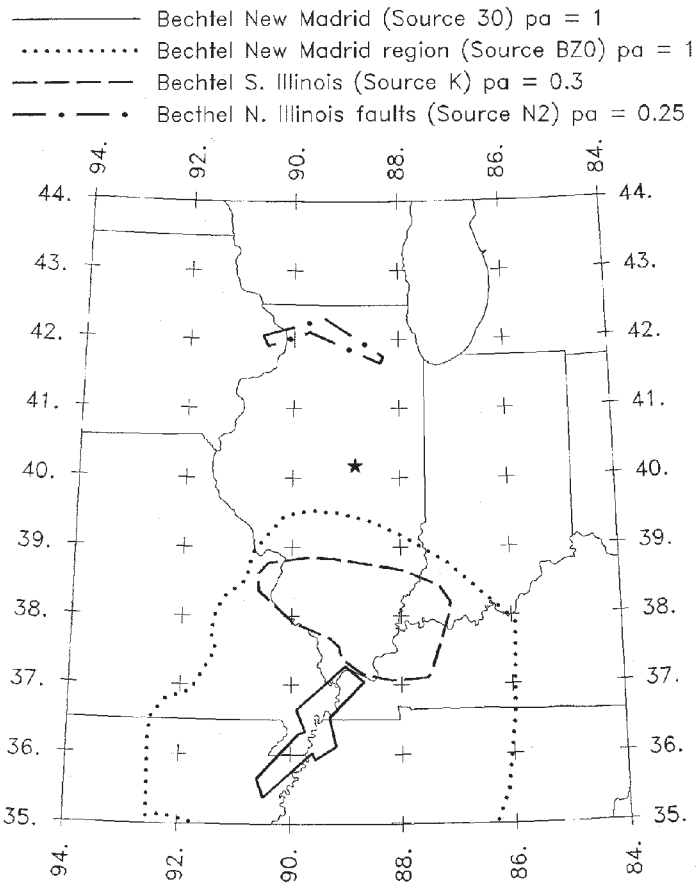


Background Source Included
Bechtel Team

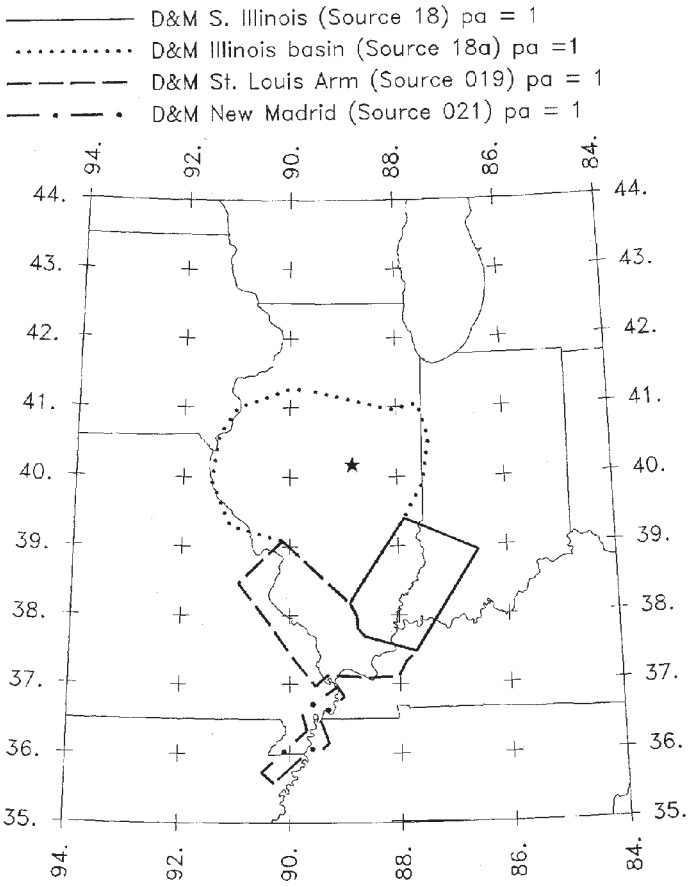


Dames & Moore Team

**Seismic Hazards Report for the EGC ESP Site**

**Controlling EPRI-SOG Seismic Sources - Bechtel/Dames & Moore Teams**

Figure
**2.1-16**

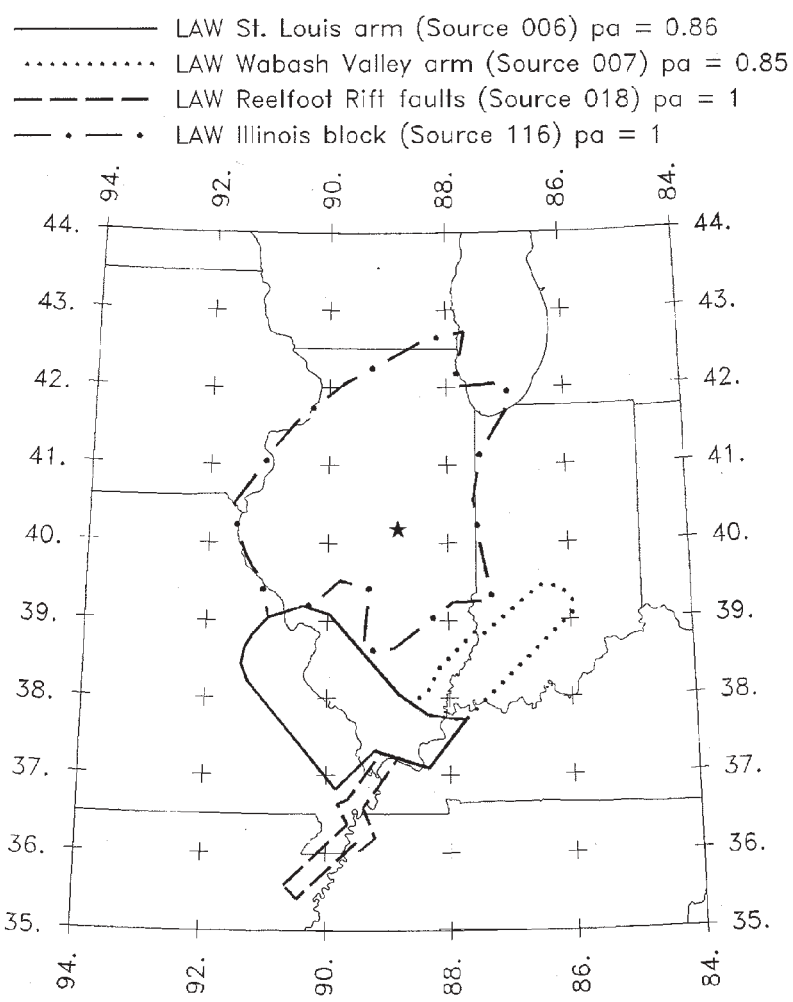


Law Team

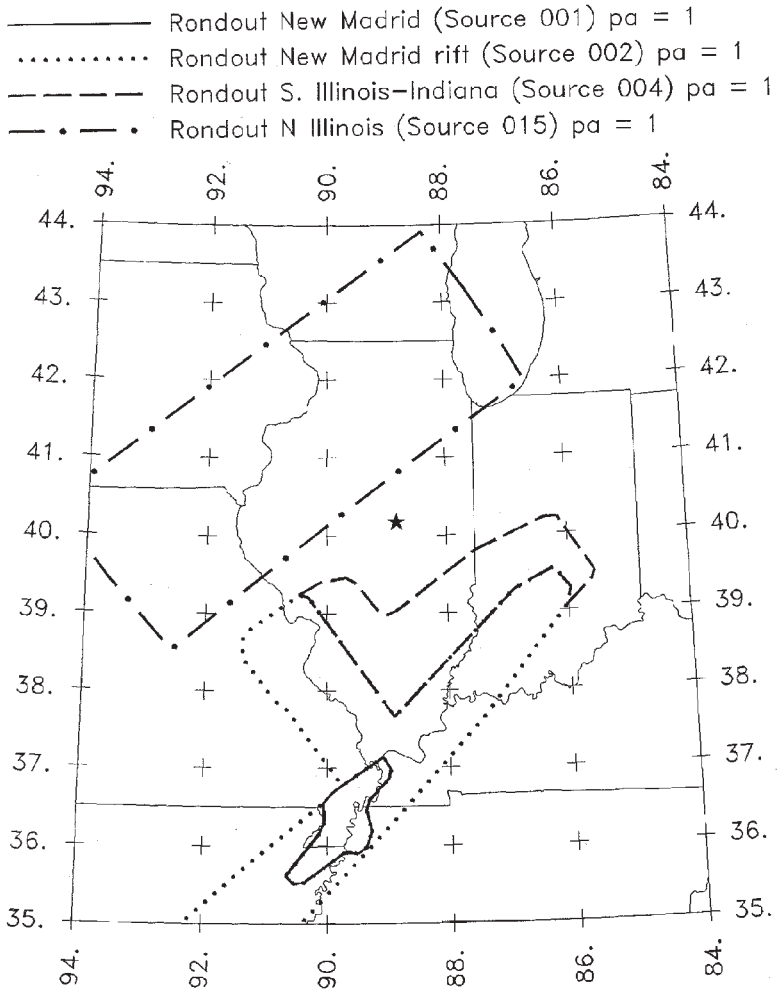


Background Source Included
Rondout Team

**Seismic Hazards Report for the EGC ESP Site**

**Controlling EPRI-SOG Seismic Sources - Law/Rondout Teams**

Figure
**2.1-17**

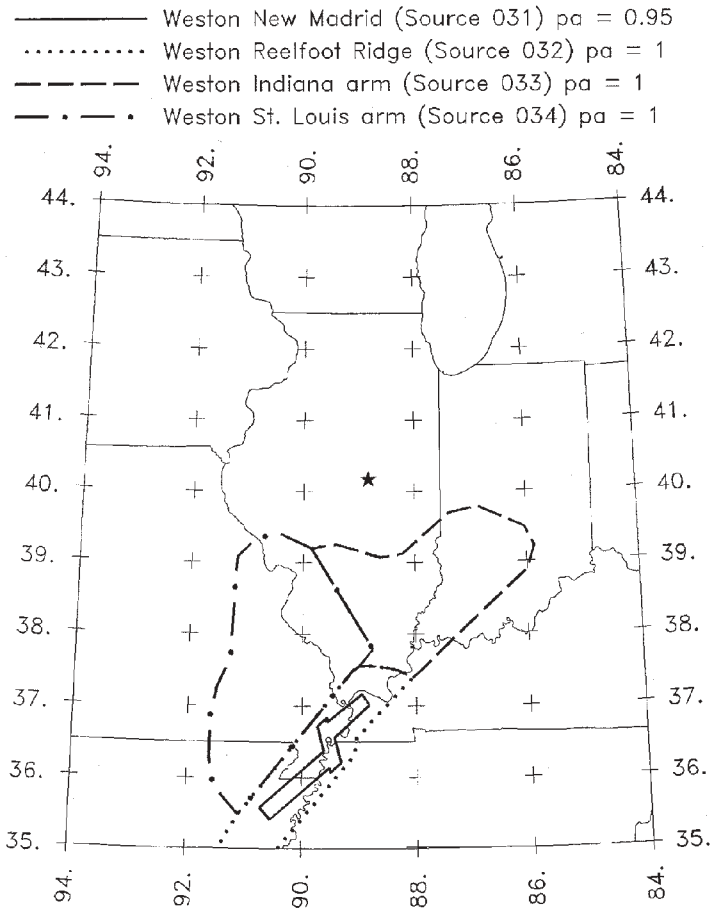


Weston Team

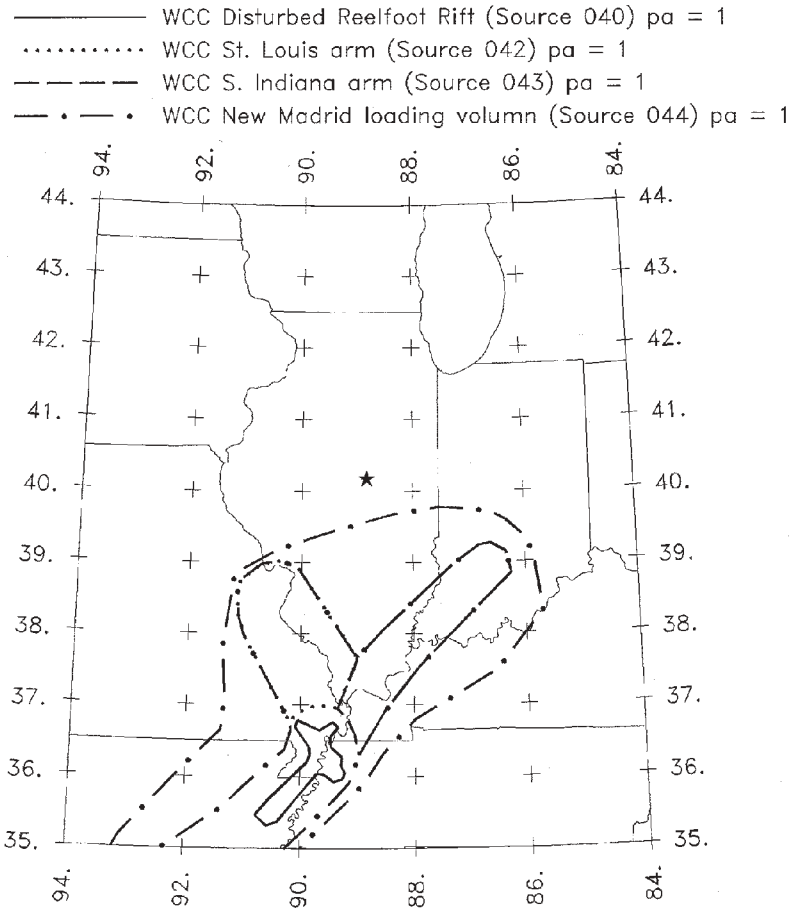


Background Source Included
Woodward-Clyde Team

**Seismic Hazards Report for the EGC ESP Site**

**Controlling EPRI-SOG Seismic Sources - Weston/Woodward-Clyde Teams**

Figure **2.1-18**

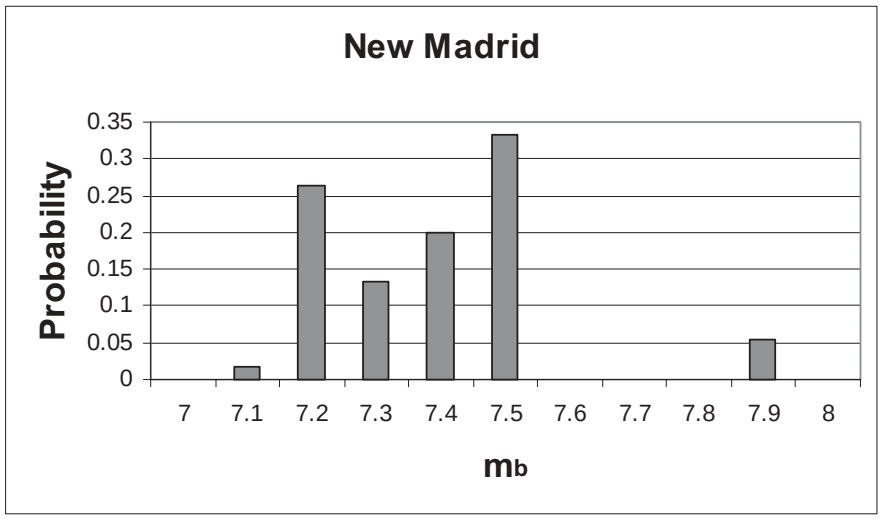


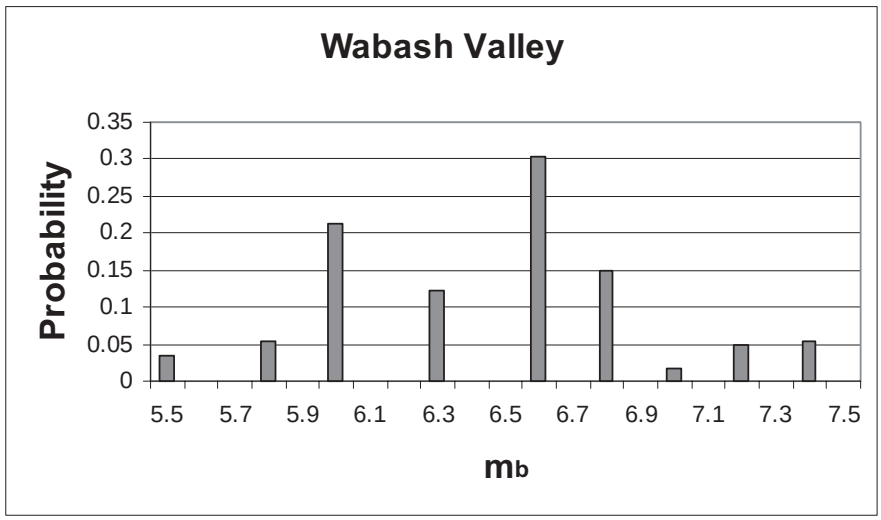


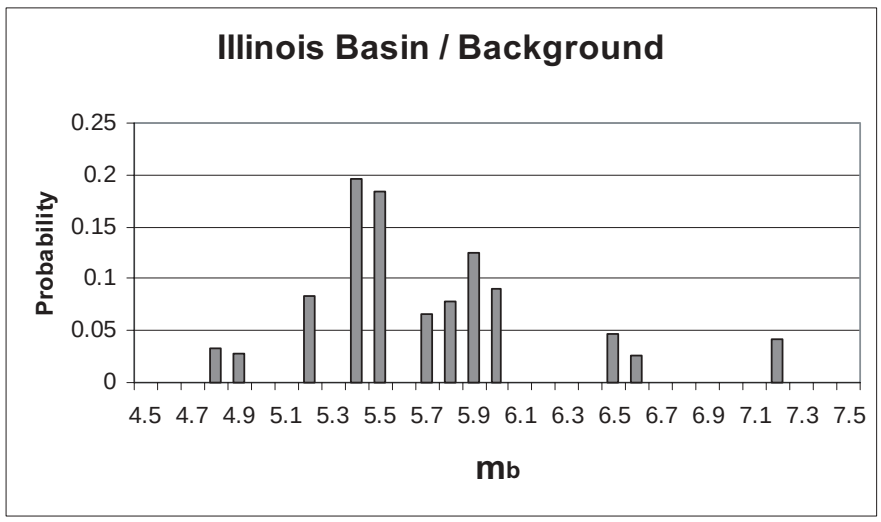


s:\7900\7935\7935.000\03_0109_eesp_fig_2.1-15.ai (2003-05-28, 09:37)

**Seismic Hazards Report for the EGC ESP Site**

**Composite EPRI-SOG Maximum Magnitude Distributions**

Figure **2.1-19**